Engineering and Urology Society

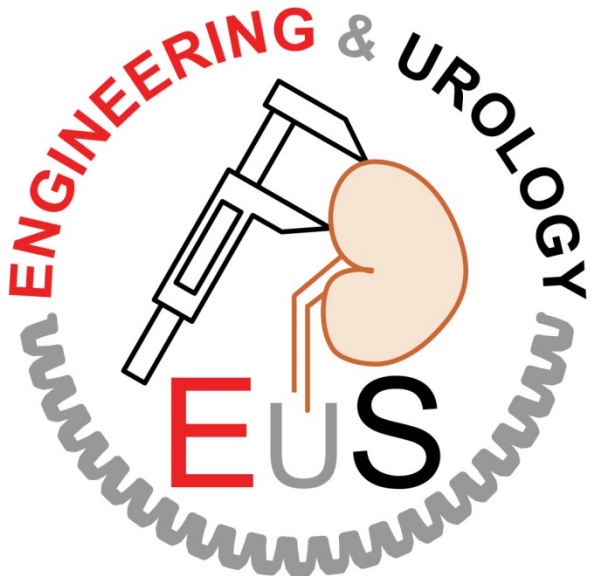

28th Annual Meeting

Saturday May 4th, 2013

San Diego Marriott Marquis
San Diego, CA

http://engineering-urology.org/

The Engineering and Urology society stands at the crossroads of clinical care and technological development, and strives to promote the latest advances in urological technology from lab workbench to the operating room. As such, we are very pleased to be able to once again hold our Annual meeting in conjunction with the American Urological Association congress, thus offering colleagues an unique opportunity to get acquainted with the cutting edge applications of uro-technology.

This year's meeting will take place on May 4th, and has been organized by program chairmen Raymond Leveillee and Nelson Salas. The morning sessions will begin with a thought-provoking discussion on the intersection of entrepreneurship and urology. Following that, the spotlight is turned to advances in imaging and treatment of benign and malignant prostate disorders. Next, colleagues from the European Association of Urology (EAU), Uro-Technology section (ESUT) will present developments in robotic technology from several countries and novel guidance techniques for percutaneous puncture techniques. After the lunch break, imaging and treatment of the renal conditions and urolithiasis will be highlighted. The current and future state of LESS and NOTES will be then discussed, with experts examining the possible directions into which minimal invasive surgery will expand. The sixth session will be dedicated to stent technology and the evolution of their design and composition. The final session will review image guided interventions, focusing on the management of diagnosis and treatment of renal masses and upper tract urothelial carcinoma.

Four poster session during the afternoon will provide a forum for uro-technology researchers to present and discuss their latest findings. The review of the abstracts for the poster sessions was performed online by a group of 64 reviewers from around the world. Each paper received between 19 and 22 reviews. We would like to thank the reviewers, listed at the end of this program book, for their essential contribution to the quality of the meeting and their constructive comments that they made for the research.

Based on the peers review, the Best Paper Award goes to Drs. Hyung-joo Kim , Hyun-do Choi, Jun-Won Jang, and Jong-hwa Won from the Samsung Advanced Institute of Technology, Korea for their abstract "A Novel Compact Single Incision Surgical Robot with Conical Remote Center-of-Motion Mechanism and Rod Elbow Joint". Top 10 abstracts have also been nominated and are listed in this program. Their authors are invited to submit full articles to the Journal of Endourology on the respective topics.

We gratefully thank all reviewers for their hard work, objective scoring, and contribution to the success of the meeting. The society also presents Best Reviewer Awards based on the grading performance and the number of reviews performed. The Best Reviewer Awards are presented to Drs. Ernesto III Arada, Haixin Chen, Mahesh Desai, Mohamed Elkoushy, Oscar Fugita, Louis Kavoussi, Sutchin Patel, Koon Ho Rha, Mathew Sorensen, and Hessel Wijkstra.

We congratulate all award winners and welcome all urologists, engineers, and scientists to join us for this unique multi and interdisciplinary experience. As always, we are grateful to Dr. George Nagamatsu, the founder and first president of the society for setting the foundations based upon which we meet.

Please visit the website http://engineering-urology.org for a complete version of this program including the abstracts presented.

Thank you for your continued scientific support,

Evangelos Liatsikos
Frank Keeley
Dan Stoianovici

CONTINUING MEDICAL EDUCATION

Accreditation: The American Urological Association Education & Research, Inc. (AUAER) is accredited by the Accreditation Council for Continuing Medical Education (ACCME) to provide continuing medical education for physicians.

Credit Designation: The American Urological Association Education & Research, Inc. designates this live activity for a maximum of 8.25 AMA *PRA Category 1 Credit(s)™*. Physicians should claim only the credit commensurate with the extent of their participation in the activity.

The AUAER takes responsibility for the content, quality, and scientific integrity of this CME activity.

AUAER Disclosure Policy: As a provider accredited by the ACCME, the AUAER must ensure balance, independence, objectivity and scientific rigor in all its activities.

All faculty and program planners participating in an educational activity provided by the AUAER are required to disclose to the provider any relevant financial relationships with any commercial interest. The AUAER must determine if the faculty's relationships may influence the educational content with regard to exposition or conclusion and resolve any conflicts of interest prior to the commencement of the educational activity. The intent of this disclosure is not to prevent faculty with relevant financial relationships from serving as faculty, but rather to provide members of the audience with information on which they can make their own judgments.

Off-label or Unapproved Use of Drugs or Devices: It is the policy of the AUAER to require the disclosure of all references to off-label or unapproved uses of drugs or devices prior to the presentation of educational content. The audience is advised that this continuing medical education activity may contain reference(s) to off-label or unapproved uses of drugs or devices. Please consult the prescribing information for full disclosure of approved uses.

Disclaimer: The opinions and recommendations expressed by faculty, authors, and other experts whose input is included in this program are their own and do not necessarily represent the viewpoint of the AUAER.

Evidence Based Content: As a provider of continuing medical education accredited by the ACCME, it is the policy of the AUAER to review and certify that the content contained in this CME activity is valid, fair, balanced, scientifically rigorous, and free of commercial bias.

Special Assistance/Dietary Needs
The American Urological Association Education & Research, Inc. (AUAER), an organization accredited for Continuing Medical Education (CME), complies with the Americans with Disabilities Act §12112(a). If any participant is in need of special assistance or has any dietary restrictions, a written request should be submitted at least one month in advance. For additional assistance with your request please call 800-908-9414.

CONTINUING MEDICAL EDUCATION

FACULTY DISCLOSURES:

Albala, David M.: Titan Medical, Consultant or Advisor
Best, Sara L.: Nothing to disclose
Borin, James F: Cook Medical, Consultant or Advisor
Cadeddu, Jeffrey A.: Nothing to disclose
Chaussy, Christian G.: EDAP TMS, Consultant or Advisor, Meeting Participant or Lecturer, Scientific Study or Trial
Chew, Ben: Boston Scientific Corporation, Consultant or Advisor
Desai, Mihir: Hansen Medical, Investment Interest
Dixon, Christopher: NxThera, Consultant or Advisor, Meeting Participant or Lecturer, Scientific Study or Trial
Gustafson, David: Nothing to disclose
S. Duke Herrell, III: Investment Interest
Hoey, Michael: NxThera Inc., Owner, Produce Development, Employee
Irwin, Brian H.: Nothing to disclose
Jaspers, Joris: UMC Utrect, Owner Product Development
Kaouk, Jihad H.: Endocare, Meeting Participant or Lecturer
Kulkarni, Ravindra: Nothing to disclose
Laguna, Pilar M.: Nothing to disclose
Lamb, Bill: iSYS, Leadership Position
Lange, Dirk: Boston Scientific, Consultant or Advisor
Leveillee, Raymond J.: Intuitive, Meeting Participant
Rodrigues Lima, Estevao Augusto: Nothing to disclose.
Marberger, Michael: GP Pharm, Consultant or Advisor, Meeting Participant or Lecturer, Scientific Study or Trial
Monga, Manoj: US Endoscopy, Consultant or Advisor
Muschter, Rolf:
Nakada, Stephen Y.: Endourology Society, Leadership Position
Nields, Morgan: INTIO Inc, Leadership Position, Investment Interest
Perry, Kent T Jr.: Nothing to disclose
Petrut, Bogdan: Nothing to disclose
Pinto, Peter A: Nothing to disclose
Rane, Abhay: Nothing to disclose
Rassweiler, Jens: Karl Storz Germany, Other
Rassweiler, Marie-Claire: Nothing to disclose
Rastinehad, Art: Philips, Inc., Scientific Study or Trial
Richstone, Lee: Nothing to disclose
Ryan, Walter N: Cook Incorporated, Leadership Position, Employee
Saglam, Remzi: ELMED Lithotripsy Systems, Consultant or Advisor, Scientific Study or Trial, Owner, Product Dev.
Salas, Nelson: MedWaves, Inc., Scientific Study or Trial
Seibold, Ulrich: German Aerospace Center (DLR) Employee
Shalhav, Arieh Leib: Nothing to disclose
Stark, Michael: SOFAR, S.p.A. Milan, Consultant or Advisor, Other
Stifelman, Michael, Intuitive Surgical, Meeting Participant or Lecturer
Stoianovici, Dan: Nothing to disclose
Teber, Dogu: Nothing to disclose
Traxer, Olivier: Cook Medical, Meeting Participant or Lecturer
Ukimura, Osamu: Nothing to disclose
Van Velthoven, Roland F.P.: Nothing to disclose
White, Wesley: Nothing to disclose

CONTINUING MEDICAL EDUCATION

SPONSORS

The Engineering and Urology Society thanks the following company for their support of this course:

Olympus America, Inc.

Olympus, which incorporates surgical market leader Gyrus ACMI, is transforming the future of healthcare to help Urologists improve outcomes and enhance quality of life for their patients by enabling less invasive procedures with innovative diagnostic and therapeutic solutions. We offer advanced HD visualization with Narrow Band Imaging (NBI), best-in-class, advanced bipolar energy tissue treatment and comprehensive stone management solutions including laser and ultrasonic technologies with a broad line of access, retrieval and drainage single-use devices. Our Laparo-Endoscopic Single-Site (LESS) surgery platform of products includes single-port access devices, deflectable tip scopes with HD visualization and versatile bipolar and ultrasonic energy.

EXHIBITORS

Boston Scientific – Urology

Boston Scientific is a leading developer of less-invasive medical technologies. Products for the Urology/Women's Health division include devices for the diagnosis and treatment of kidney stones, BPH, female urinary incontinence, and pelvic floor reconstruction. Please visit our exhibit to learn about our newest technologies and our commitment to physician education.

Cook Medical

Cook Medical has been a leading supplier of medical devices for urologists for over 35 years. Offering interventional and Biodesign® technologies that support diagnostic and therapeutic procedures in adult and pediatric urology, Cook has placed particular emphasis on stone management as well as both male and female pelvic health.

PROGRAM

28th Annual Meeting
Saturday, May 4, 2013
San Diego Marriott Marquis
Room: Marina Ballroom E
San Diego, CA

Program Chairmen: Raymond Leveillee, Arieh Shalhav, Nelson Salas, Kyle Richards

7:15 – 7:30	**Registration**	
7:30 –9:15	**SESSION 1: ENTREPRENEURSHIP IN UROLOGY AND ENGINEERING**	**Raymond Leveillee** **Arieh Shalhav**
7:30 AM	"Publish or Perish" vs. "Publish and Perish" – The Entrepreneur's Dilemma	Michael Hoey
7:50 AM	Innovation and Surgeon/Corporate Interaction: Where have we gone? Where are we going?	Carlos Babini
8:10 AM	Key Steps Toward Entrepreneurial Success in the Medical Industry	Morgan Nields
8:30 AM	How to Work with Industry to Commercialize your IDA	Walter Ryan
8:40 AM	Maximizing Industry Relations – How to be Innovative and Maintain Objectivity	David Albala
8:50 AM	Questions and Answers	
9:00 – 10:15	**SESSION 2: ADVANCES IN IMAGING AND TREATMENT: PROSTATE**	**David Albala** **Nelson Salas**
9:00 AM	Evolution and Outcomes of 3MHz High Intensity Focused Ultrasound Therapy for Localized Prostate Cancer over 15 years	Christian Chaussy
9:15 AM	MRI and Ultrasound Fusion Guidance for Prostate Biopsy and Treatment Interventions	Peter Pinto
9:30 AM	Utilization of Vapor as Source of Energy for the Hyperthermic Treatment of BPH	Christopher Dixon
9:45 AM	Robotically-Manipulated TRUS Device (ViKY System) During Robotic Assisted Prostatectomy	Osamu Ukimura
10:00 AM	Questions and Answers	
10:15 – 10:30	**AWARDS PRESENTATIONS**	**Dan Stoianovici**
10:25 AM	Best Paper Award: A Novel Compact Single Incision Surgical Robot with Conical Remote Center-of-Motion Mechanism and Rod Elbow Joint	Hyung-joo Kim

10:30–12:00	**SESSION 3: ESUT SESSION**	**Roland van Velthoven** **M. P. Laguna** **Rolf Muschter**
10:30 AM	The German Robot	Ulrich Seibold
10:40 AM	The Italian Robot	Michael Stark
10:50 AM	The Dutch Robotic Device	Joris Jaspers
11:00 AM	Motorized DOF-Instruments from France	Andreas Blana
11:10 AM	The Turkish Robot	Remzi Saglam Jens Rassweiler
11:20 AM	Percutaneous Puncture of Renal Tumours Using Attitude Measuring	Bogdan Petrut
11:30 AM	Percutaneous Access to Collecting System using IPAD	Marie Claire Rassweiler Dogu Teber
11:40 AM	Percutaneous Access to Collecting System Only by Electromagnetic Tracking	Estevao Lima
11:50 AM	Questions and Answers	

12:00–1:00 LUNCH BREAK

1:00-2:00	**SESSION 4: ADVANCES IN IMAGING AND TREATMENT: KIDNEY/KIDNEY STONES**	**Stephen Nakada** **Sara Best**
1:00 PM	CT Guided Robotic Interventional Procedures. Maxio™ For Precision Planning and Needle Placement	David E. Gustafson
1:10 PM	A Novel Magnetic Tool for Retrieval of paramagnetic Rendered Stone Fragments	Jeffrey Cadeddu
1:20 PM	Current Technologies for Prevention of Stone Migration During Lithotripsy	Manoj Monga
1:30 PM	3-D Image-Guided Robotic Abdominal Surgery	Duke Herrell
1:40 PM	Isocentric Tool Positioning with the Gantry: iSYS 1 Needle Guidance Platform	Bill Lamb
1:50 PM	Questions and Answers	

2:00-3:00	**SESSION 5: NOTES AND LESS**		**Abhay Rane**
2:00 PM	Finger on the Pulse of LESS: What is Being Done Routinely Today		Lee Richstone
2:10 PM	Do we have Evidence we Seeing Benefits of Less?	Yes	Wesley White
		No	Arieh Shalhav
2:30 PM	Another Year of LESS and NOTES		Brian Irwin
2:35 PM	What Can We Expect in the Next 5 Years – LESS		Mihir Desai
2:40 PM	What Can we Expect in the Next 5 Years - NOTES		Jihad Kaouk
2:45 PM	Questions and Answers		

3:00-4:00	**SESSION 6: STENT WORKING GROUP**	**Abhay Rane**
	Anti-Infective Measures for Stents	Dirk Lange
	Evolution of Stent Material: Polyurethanes and Bio-Degradable	Ben Chew
	Metals and Segmental Stents	Ravi Kulkarni

4:00-5:00	**SESSION 7: IMAGE GUIDED WORKING GROUP**	**James Borin**
4:00 PM	Critical Assessment of Small Renal Mass Guidelines	James Borin
4:05 PM	Active Surveillance of the Small Renal Mass	Michael Marberger
4:13 PM	Renal Mass Biopsy – What is the Evidence?	Pilar Laguna
4:21 PM	Renal Mass Biopsy – How I do It	Ardeshir Rastinehad
4:29 PM	Renal Cryoablation – Troubleshooting and Trajectory Image Guidance	Kent Perry
4:37 PM	GPS Guidance for Percutaneous Renal Ablation	Osamu Ukimura
4:45 PM	Robot Assisted Partial Nephrectomy Facilitated by Intraoperative Ultrasound and Fluorescence Imaging	Michael Stifelman
4:53 PM	Advances in Ureteroscopic Visualization and Treatment of Upper Tract Urothelial Carcinoma	Olivier Traxer

POSTER SESSIONS:

1:00–2:30PM	**Poster Session 1**	Session 1A Room: Misson Hills	Duke Herrell Mathew Sorensen
		Session 1B Room: Balboa	Louis Kavoussi Dan Stoianovici
3:00–4:30PM	**Poster Session 2**	Session 2A Room: Misson Hills	Oscar Fugita Govindarajan Srimathveeravalli
		Session 2B Room: Balboa	Hessel Wijkstra Koon Ho Rha

POSTER SESSION 1A
1:00 PM – 2:30 PM

Moderators
Duke Herrell
Mathew Sorensen

No.	Title	Presenting Author
1	IN VIVO AND EX VIVO COMPARISON OF OPTICS AND PERFORMANCE OF A NOVEL DUAL CHANNEL FIBEROPTIC URETEROSCOPE	Achim Lusch
2	USE OF IMAGE PROCESSING SOFTWARE TO MORE RELIABLY ESTIMATE TUMOR VOLUME FROM RADICAL PROSTATECTOMY SPECIMENS	Aria A. Razmaria
3	HOME-MADE ANGLE TRAINER FOR PRACTICE IN LAPAROSCOPIC SUTURING AND KNOT-TYING BEFORE LAPAROENDOSCOPIC SINGLE SITE SURGERIES	Ernesto III Arada
4	A SINGLE CENTRE PROSPECTIVE 5 YEAR CLINICAL EXPERIENCE WITH ROBOTIC-ASSISTED TRANSPERINEAL PROSTATE BIOPSY IN PATIENTS WITH PREVIOUS NEGATIVE BIOPSY	Law Zhi Wei
5	COMPREHENSIVE ANATOMIC DESCRIPTION OF RENAL INNERVATION USING 3D COMPUTER ASSISTED MODELING	Andrew Heidari
6	EVALUATION OF DIFFERENT REGION OF INTEREST (ROI) STRATEGIES FOR CHARACTERIZATION OF UPPER URINARY TRACT STONES DETECTED ON COMPUTERIZED TOMOGRAPHY	Vikram Narayan
7	EVALUATION OF DURABILITY AND COST EFFECTIVENESS OF THREE SURGICAL SIMULATORS: MIMIC DV-TRAINER™, ROSS ROBOTIC SURGICAL SIMULATOR™, AND THE SIMULAB EDGE SYSTEM™	Michael Del Junco
8	INDENTER STUDY: HIGHER ELASTICITY OF PROSTATE IS ASSOCIATED WITH LOWER URINARY TRACT SYMPTOMS	Koon Ho Rha
9	A NOVEL COMPACT SINGLE INCISION SURGICAL ROBOT WITH CONICAL REMOTE CENTER-OF-MOTION MECHANISM AND ROD ELBOW JOINT **BEST PAPER AWARD**	Hyung-Joo Kim
10	COLLECTING SYSTEM PERCUTANEOUS ACCESS USING 3D REAL-TIME TRACKING SENSORS: FIRST PIG MODEL IN VIVO EXPERIENCE	Estevao Lima
11	BIOMECHANICAL PROPERTIES OF THE URETER: PRELIMINARY RESULTS	Yaniv Shilo

12	PRE-CLINICAL EVALUATION OF A MRI-SAFE ROBOT FOR ENDORECTAL PROSTATE BIOPSY **TOP 10 ABSTRACT**	Govindarajan Srimathveeravalli
13	MICRO-CRYOABLATION OF ILIOINGUINAL AND GENITOFEMORAL NERVE FIBERS FOR PATIENTS WITH PERSISTENT OR RECURRENT CHRONIC GROIN OR SCROTAL CONTENT PAIN	Ahmet Gudeloglu
14	A NEW TOTALLY POSTERIOR APPROACH TO ROBOT-ASSISTED LAPAROSCOPIC PROSTATECTOMY IMPROVES EARLY CONTINENCE RATES	Koon Ho Rha
15	PROSPECTIVE RANDOMIZED COMPARISON BETWEEN MICROPERC AND RETROGRADE INTRA-RENAL SURGERY OF RENAL CALCULI LESS THAN 1.5 CM.	Shashikant Mishra
16	NOVEL LAPAROSCOPE DEFOGGING AND CLEANING DEVICE FOR ROBOT-ASSISTED LAPAROSCOPIC PROSTATECTOMY (RALP)	Carson Wong
17	IRREVERSIBLE ELECTROPORATION: OUTCOMES IN A MINIMALLY-INVASIVE APPROACH TO RENAL TUMORS **TOP 10 ABSTRACT**	Jonathan Melquist
18	LONG-TERM OUTCOMES OF THE RESONANCE METALLIC URETERAL STENT FOR MALIGNANT AND CHRONIC BENIGN URETERAL OBSTRUCTION	Bailey Zampella
19	CRITICAL EVALUATION OF MRI-TARGETED TRUS-GUIDED TRANSPERINEAL FUSION BIOPSY FOR DETECTION OF PROSTATE CANCER	Timur H. Kuru
20	IN VITRO COMPARISON OF A STANDARD AND NOVEL ECHOGENIC NEEDLE FOR ULTRASOUND-GUIDED PERCUTANEOUS RENAL BIOPSY	Ashleigh Menhadji

POSTER SESSION 1B
1:00 PM – 2:30 PM

Moderators
Louis Kavoussi
Dan Stoianovici

21	BEVELED NEEDLE TRAJECTORY CORRECTION **TOP 10 ABSTRACT**	Changhan Jun
22	WIRELESS TISSUE PALPATION TO LOCALIZE RENAL MASSES: PRELIMINARY ASSESSMENT ON LAPAROSCOPIC TRAINER MODEL	Aaron Benson
23	ENDOSCOPIC FORCEPS FOR URETEROSCOPY: A COMPARATIVE IN VITRO ANALYSIS	Giovanni Marchini
24	INITIAL INVESTIGATION OF A 2450 MHZ MICROWAVE SYSTEM FOR ABLATION OF RENAL TISSUES	Karli Pease
25	ANTHROPOMETRIC RENAL ANATOMIC ALTERATIONS BETWEEN SUPINE AND PRONE POSITIONS IN PERCUTANEOUS RENAL ABLATION FOR RENAL CORTICAL NEOPLASMS	Achim Lusch
26	TRANSPERINEAL OPTIMIZED PROSTATE (TOP) BIOPSY	Georgios Sakas
27	NEW PROTOTYPE CHIP ON THE TIP DIGITAL FLEXIBLE URETEROSCOPE: FIRST CLINICAL FEASIBILITY STUDY.	Shashikant Mishra
28	ROBOT-ASSISTED LAPAROSCOPIC SACROCOLPOPEXY IN PATIENTS WITH PRIOR TRANSVAGINAL REPAIR OF PELVIC ORGAN PROLAPSE	Farshid Hajimirzaee
29	EVALUATION OF A NOVEL DISPOSABLE DIGITAL CYSTOSCOPE	Joseph V Ditrolio
30	EXTRACORPOREAL SHOCK WAVE LITHOTRIPSY (ESWL) COMPLICATIONS DEPENDING ON THE SHOCK WAVE RATE AND NUMBER	Catalin Maria
31	A NERVE COMPRESSION DEVICE AND ELECTROPHYSIOLOGICAL RECORDING OF NERVE RESPONSE TO PRESSURE COMPRESSIONS	Gerald Timm

32	GREENLIGHT HPS-120W VS GREENLIGHT XPS-180W LASER VAPORIZATION OF THE PROSTATE FOR BENIGN PROSTATIC HYPERPLASIA: A GLOBAL, MULTI-CENTER, AND PROSPECTIVE COMPARATIVE ANALYSIS OF OPERATIVE PERFORMANCE	Pierre-Alain Hueber
33	LASER ACTIVATED NANOSHELL ABLATION OF PROSTATE CANCER: A PILOT STUDY IN HUMANS	Joshua Stern
34	A NOVEL SYSTEM TO MEASURE FORCE ON PERINEAL ARTERIES DURING BICYCLING	Sujeeth Parthiban
35	EVALUATION OF ACCEPTABILITY OF PHYSICAL SIMULATION MODEL FOR TRAINING OF LAPAROSCOPIC PYELOPLASTY **TOP 10 ABSTRACT**	Lauren Poniatowski
36	ROBOTIC TRANSPERINEAL SATURATION BIOPSY APPROXIMATES THE “TRUTH” IN DEFINING LOW-RISK PROSTATE CANCER	Kae Jack Tay
37	CONTINUOUS VERSUS CONVENTIONAL BIPOLAR PLASMA VAPORIZATION OF THE PROSTATE AND STANDARD MONOPOLAR RESECTION - A RANDOMIZED COMPARISON OF A NEW TECHNOLOGICAL ADVANCEMENT	Bogdan Geavlete
38	THE CHARACTERISTICS OF MICROCIRCULATION IN RENAL CELL CARCINOMA BY CONTRAST-ENHANCED ULTRASOUND (CEUS)	Maeda Motohiro
39	A PROSPECTIVE COMPARISON BETWEEN NBI AND STANDARD WHITE LIGHT CYSTOSCOPY IN CASES OF NON-MUSCLE INVASIVE BLADDER CANCER	Bogdan Geavlete
40	IN VITRO COMPARISON OF A NOVEL FACILITATED ULTRASOUND TECHNOLOGY AND STANDARD ULTRASOUND FOR PERCUTANEOUS RENAL BIOPSY **TOP 10 ABSTRACT**	Ashleigh Menhadji

POSTER SESSION 2A
3:00 PM – 4:30 PM

Moderators
Oscar Fugita
Govindarajan Srimathveeravalli

41	COMPARISON OF RENAL PARENCHYMAL CLOSING PRESSURE DURING OPEN, LAPAROSCOPIC AND ROBOTIC-ASSISTED RENAL RECONSTRUCTION	Ramtin Khanipour
42	HISTOTRIPSY ACCURACY: CHARACTERIZATION WITH A NOVEL RED BLOOD CELL PHANTOM	Jon Cannata
43	LASER POWER SETTINGS AND STONE CAPTURE IN A PERCUTANEOUS LITHOPAXY MODEL	Giovanni Marchini
44	MAGNETIC RESONANCE IMAGING/ULTRASOUND (MR/US) FUSION-GUIDED PROSTATE BIOPSIES: AN INITIAL REPORT	Simpa Salami
45	VALIDATION OF A SIMULATION TOOL TO SUPPORT ROBOTIC-ASSISTED SURGICAL TRAINING	Lee White
46	COMPARISON OF OPTICS AND PERFORMANCE OF DISTAL SENSOR HIGH DEFINITION, DISTAL SENSOR STANDARD DEFINITION, AND FIBEROPTIC CYSTOSCOPES	Achim Lusch
47	LAPAROSCOPIC VERSUS PERCUTANEOUS CRYOABLATION FOR THE SMALL RENAL MASS: LONG-TERM ONCOLOGIC AND FUNCTIONAL OUTCOMES	Dinesh Samarasekera
48	MICROWAVE ABLATIONS AT 915 MHZ IN EX-VIVO AND IN-VIVO PORCINE KIDNEYS	Karli Pease
49	ZERO ISCHEMIA ROBOTIC PARTIAL NEPHRECTOMY: SEQUENTIAL PRE-PLACED SUTURE RENORRHAPHY TECHNIQUE	Emad Rizkala
50	DEVELOPMENT OF DEDICATED STONE DETECTION PROTOCOLS USING A RESEARCH-BASED ULTRASOUND IMAGER	Ryan Hsi
51	DYNAMIC CONTRAST ENHANCED AND DIFFUSION WEIGHTED MRI CORRELATE WITH HIGHER GRADE PROSTATE CANCER WITH EXTRACAPSULAR EXTENSION	Kae Jack Tay

52	COMPARISON OF CURRENT URINARY DIAGNOSTIC TECHNIQUES FOR BIOPSY PROVEN TRANSITIONAL CELL EPITHELIAL CANCER AGAINST A MULTI-GENE URINARY DETECTION TEST	Joseph V Ditrolio
53	TRANSRECTAL HIGH INTENSIVE FOCUSED ULTRASOUND THERAPY BY ABLATHERM® IN LOCALIZED PROSTATE CANCER - EXPERIENCES OF 15 YEARS	Stefan Thueroff
54	PROSPECTIVE CONTROL TRIAL: FLEXIBLE FIBER-OPTIC CO2 LASER VS. MONOPOLAR CAUTERY FOR ROBOTIC MICROSURGICAL DENERVATION OF THE SPERMARIC CORD	Jamin Brahmbhatt
55	FINE TILT TUNING OF A LAPAROSCOPIC CAMERA BY LOCAL MAGNETIC ACTUATION: TWO-PORT LAPAROSCOPIC NEPHRECTOMY EXPERIENCE ON HUMAN CADAVERS **TOP 10 ABSTRACT**	Ryan Pickens
56	SUCCESS OF PERCUTANEOUS ABLATION FOR RCC IS DEPENDENT ON TUMOR SIZE: A MULTI-INSTITUTIONAL STUDY	Sara Best
57	SILHOUETTE METALLIC COIL REINFORCED STENTS: PARAMOUNT IN TREATMENT OF MALIGNANT URETERAL OBSTRUCTION	Andrew Leone
58	A NOVEL PARABOLOID INTRACORPOREAL LITHOTRIPTOR: CAD ANALYSIS AND IN VITRO COMPARISON WITH HOLMIUM LASER **TOP 10 ABSTRACT**	Ashish Rawandale
59	LASER LITHOTRIPSY RETROPULSION VARIES WITH STONE MASS	Michael Robinson
60	ADVERSE EVENTS RESULTING FROM LASERS USED IN UROLOGY	Abdulaziz Althunayan

POSTER SESSION 2B
3:00 PM – 4:30 PM

Moderators
Hessel Wijkstra
Koon Ho Rha

61	THE SURGICAL SPECTACLE: A SURVEY OF UROLOGISTS VIEWING LIVE CASE DEMONSTRATIONS	Sammy Elsamra
62	ACTIVE REMOVAL OF BUBBLE SHIELDING IN SWL: AN IN-VITRO STUDY **TOP 10 ABSTRACT**	Alexander P Duryea
63	DESIGN OF STEERING MECHANISM AND SURFACE MOSAICS SOFTWARE FOR AUTOMATED BLADDER SURVEILLANCE **TOP 10 ABSTRACT**	Xianming Ye
64	EVALUATION OF A NOVEL CORDLESS ENDOSCOPIC LIGHT SOURCE FOR OPTICAL QUALITY AND PERFORMANCE DURING FLEXIBLE CYSTOSCOPY	Achim Lusch
65	A BASIC NOVEL CONCEPT: PROSTATE-SPECIFIC COORDINATE SYSTEM	Doyoung Chang
66	EVALUATION OF THE IMPACT OF THREE-DIMENSIONAL VISION ON LAPAROSCOPIC PERFORMANCE	Philip Bucur
67	CORRELATION BETWEEN THE PROSTATE SIZE AND LOCATION OF THE NEUROVASCULAR BUNDLES	Haixin Chen
68	COMPARISON OF THE ITRAINER AND STANDARD LAPAROSCOPIC TRAINER FOR BASIC LAPAROSCOPIC TASKS	Renai Yoon
69	TRANSVAGINAL HYBRID NOTES ROBOTIC DONOR NEPHRECTOMY	Ali Khalifeh
70	AUTOMATIC KIDNEY DETECTION AND SEGMENTATION FROM 3D ULTRASOUND IMAGE USING GRAPH SEARCHING AND LEVEL SET	Xin Li
71	PULSED FOCUSED ULTRASOUND AS A METHOD FOR NONINVASIVE TREATMENT OF URETEROCELES	Adam Maxwell

72	FOCUSED ULTRASOUND REPOSITIONS DE NOVO CALCULI IN AN ESTABLISHED STONE-FORMING PORCINE MODEL	Ryan Hsi
73	CONTRAST ULTRASOUND DISPERSION IMAGING IN PROSTATE CANCER DIAGNOSTICS	Massimo Mischi
74	TWO-CENTER EVALUATION STUDY USING THE XENXTM TO PREVENT STONE MIGRATION DURING LASER LITHOTRIPSY	Eugene Kramolowsky
75	THERAPY OF INCIDENTAL PROSTATE CANCER BY HIGH INTENSITY FOCUSED ULTRASOUND: PROSPECTIVE LONG-TERM DATA	Christian Chaussy
76	- THE " CUTAENOUS – PYELO- URETERAL STENT " (C-PU) FOR ROBOTIC ASSISTED LAPAROSCOPIC PYELOPLASTY (RAL-P)	Pankaj Dangle
77	CT CHARACTERIZATION OF DIETARY HYDROXYPROLINE-INDUCED NEPHROLITHIASIS: FURTHER ELUCIDATION OF A PORCINE MODEL OF UROLITHIASIS	Sri Sivalingam
78	RENAL HEMATOMA AFTER ESWL: INCIDENCE AND RISK FACTORS OF AFTER 2500 TREATMENTS	Hans-Martin Fritsche
79	A SCIENTIFIC CORRELATION BETWEEN ROBOTIC PROSTATE BIOPSY RESULTS WITH POST-RADICAL PROSTATECTOMY WHOLE-MOUNT PATHOLOGY SLIDES	Law Zhi Wei
80	"5-PANG SYSTEM"-VERSION 2: A MULTIUTILITY SYSTEM FOR PERCUTANEOUS RENAL ACCESS	Ashish Rawandale

ABSTRACT 1

IN VIVO AND *EX VIVO* COMPARISON OF OPTICS AND PERFORMANCE OF A NOVEL DUAL CHANNEL FIBEROPTIC URETEROSCOPE

Lusch A, Okhunov Z, Khanipour R, Del Junco M, Menhadji A, Yoon R, Landman J
Department of Urology, University of California, Irvine

Introduction: Vision during ureteroscopic laser ablations of large kidney stones or upper tract transitional cell carcinomas can be challenging due to the diminished flow during the procedure. Hence we evaluated and compared characteristics of a novel dual working channel fiber optic ureteroscope [Cobra] [Wolf Cobra, Richard Wolf, Knittlingen, Germany] to two single channel fiber optic ureteroscopes [Viper], [X2] [Wolf Viper, Richard Wolf, Knittlingen, Germany and Storz X2, Karl Storz, Tuttlingen, Germany] and to a single channel distal standard definition sensor digital ureteroscope URF-V [SD-DS] [Olympus America Inc., Center Valley, USA].

Methods: Four new ureteroscopes (Cobra, Viper, X2, SD-DS) were compared for active deflection, irrigation flow and optical characteristics. Each ureteroscope was evaluated with an empty working channel and with various accessories. Optical characteristics (resolution, grayscale imaging, color representation, depth of field and image brightness) were measured using USAF/Edmund optics test targets and illumination meter. We performed a porcine ureteroscopy and measured the time for cleaning the middle calyx after injection of 10 cc's of a standardized bloody solution.

Results: The SD-DS showed a higher resolution [7.42 lines/mm][p=0.0001] compared to the fiber optic ureteroscopes; among the fiber optic ureteroscopes the Cobra had the highest resolution compared to Viper and X2 [4,86 vs. 4.33 vs. 3.56 lines/mm, p<0.0001]. The Wolf Cobra also showed a significant superior illumination at all distances [p<0.0001]. Grayscale distribution and color representation was identical for the fiber optic ureteroscopes, whereas the SD-DS provided a superior color representation and a significant higher depth of field. [Table] The dual channel ureteroscope provided superior flow with empty working channel [86cc/min vs. 68cc/min [Viper] vs. 62,5cc/min [X2] vs. 62cc/min [SD-DS], p=0.0001] and with various accessories in the working channel [p<0.0001]. With regards to deflection the Storz X2 and the Cobra provided superior deflection up and down with empty working channel and several accessories [p<0.0001], except for downward deflection with a guide wire and 3.2 F delta wire grasper, where the SD-DS showed superior results. When evacuating a standardized bloody field, the Cobra provided significant shorter evacuation times compared to Viper, X2 and SD-DS [36.6 sec. vs. 72 sec. vs. 65.6 sec. vs. 72.6 sec, p=0.0001].

Conclusion: In this *in vitro* and porcine evaluation the dual channel ureteroscope Cobra provides superior flow without and with various accessories. The additional working channel may improve vision and performance during challenging ureteroscopic cases by providing an increased flow. The enhanced capabilities of the Cobra have to be bounced with a slightly larger diameter of this ureteroscope.

Resolution (lines/mm)	Cobra	SD-DS	X2	Viper		F-test	Tukey method for adjustment for multiple comparisons				
					p-value	C v SD-DS	C v X2	C v V	SD-DS v X2	SD-DS v V	X2 v V
10 mm	4,86	7,42	3,56	4,33	<0.0001	0,0001	0,0057	0,2736	<0.0001	<0.0001	0,0818
20 mm	2,33	3,43	1,72	2,33	<0.0001	0,0002	0,0092	1	<0.0001	0,0002	0,0092
Deph of field											
5LP	4	9,67	0,33	3,67	<0.0001	0,0001	0,001	0,9361	<0.0001	<0.0001	0,0019
Illumination(Lux)											
10mm	20533,33	3893,33	18943,33	16036,67	<0.0001	<0.0001	<0.0001	<0.0001	<0.0001	<0.0001	<0.0001
20mm	10563,33	1771,33	9226,67	7813,33	<0.0001	<0.0001	<0.0001	<0.0001	<0.0001	<0.0001	<0.0001
50mm	2593,33	461,67	2400,00	2010,00	<0.0001	<0.0001	<0.0001	<0.0001	<0.0001	<0.0001	<0.0001
100mm	801,67	143,33	708,00	623,67	<0.0001	<0.0001	<0.0001	<0.0001	<0.0001	<0.0001	<0.0001

Table: Resolution, Depth of field and illumination

ABSTRACT 2

USE OF IMAGE PROCESSING SOFTWARE TO MORE RELIABLY ESTIMATE TUMOR VOLUME FROM RADICAL PROSTECTOMY SPECIMENS

Aria A. Razmaria[1], Vytas Bindokas[2], Arieh L. Shalhav[1], Aytekin Oto[3]

[1] *University of Chicago Medical Center, Urology*
[2] *University of Chicago, Light Microscopy Core Facility*
[3] *University of Chicago, Radiology*

Introduction: There is no standardized way of tumor volume reporting on pathological radical prostatectomy specimens. The estimates are based on the visual assessment by the pathologist and can vary from one reviewer to the other. This project aims at development of an imaging algorithm based on the reviewed pathologic slides to more reproducibly estimate tumor volume.

Methods: Seven pathologic specimens after radical prostatectomy with good quality whole mount slides build the basis of this exploratory study. These are reviewed by an uropathologist and the tumors outlined on the pathological slides according to a routine protocol. The number of whole mount slides range from 11-15. The slides are subsequently scanned at low resolution to allow for timely image processing. The Imaris ™ software is used for image stacking and 3D reconstruction. The marked outlines on the slides are used as tumor boundaries. Different iterations of image smoothening were applied to achieve best volume rendering.

Results: After scanning of the slides that takes about 10-15 minutes, the image processing time needed is between 15-20 minutes. This can be streamlined to allow for an overall process time between 15-20 minutes. Figures 1A, 1B, and 1C demonstrate the different steps of the image processing algorithm.

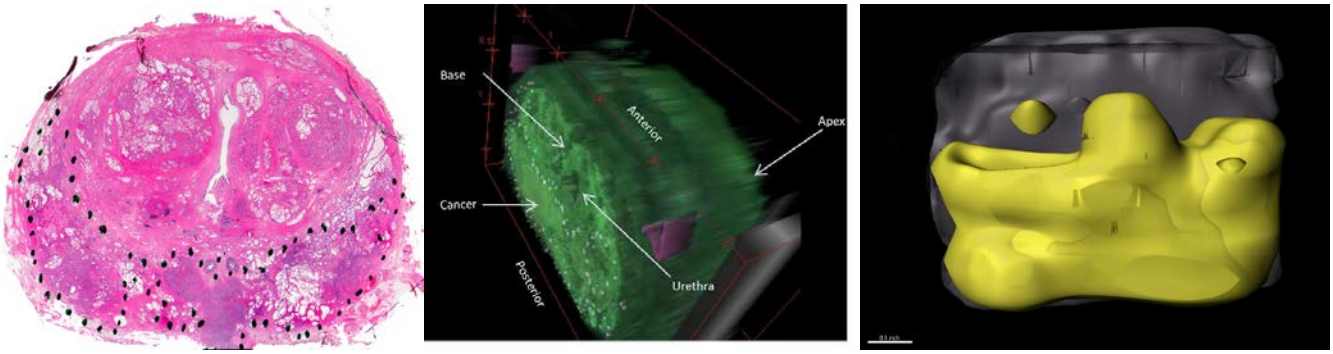

Figure: a) Whole mount pathological radical prostatectomy slide with outlined tumor, b) 3D reconstruction of scanned and stacked images, c) Volume rendering of 3D reconstructed smoothened tumor area

Conclusion: This exploratory study shows the feasibility of a time and resource efficient image processing application for pathological evaluation of radical prostatectomy specimens. This can help to standardize the reporting on tumor volume. The ease of its incorporation into routine pathological practice needs to be further evaluated.

ABSTRACT 3

HOME-MADE ANGLE TRAINER FOR PRACTICE IN LAPAROSCOPIC SUTURING AND KNOT-TYING BEFORE LAPAROENDOSCOPIC SINGLE SITE SURGERIES

Ernesto V. Arada III MD, Ceasar Ballesteros, MD
Quirino Memorial Medical Center, Quezon City, Philippines

Introduction: Laparoscopic trainers for suturing and knot tying generally use needle holders and graspers at an optimum angle of 45 degrees between instruments during multi-port laparoscopic surgeries. Because laparoendoscopic single site (L.E.S.S.) surgeries are done at approximate angles of 12.5 degrees and 17.5 degrees, it helps to practice laparoscopic suturing and knot-tying at more acute angles of 25 degrees and 15 degrees in a Home-made Angle Trainer. This Angle Trainer is so called because practice is done respectively at different angles of 45 degrees, 25 degrees and 15 degrees between instruments.

Methods: An ordinary cardboard box and art materials were used in making a Home-made Angle Trainer (Figure 1). Holes are perforated at one end of the box for inserting needle holder and grasper at angles of 45 degrees, 25 degrees and 15 degrees (Figure 2). The holes are 15.0 cm apart at 45 degrees angle, 8.0 cm apart at 25 degrees angle and 4.5 cm apart at 15 degrees angle with 0-degree telescope in the middle. Suturing and knot tying practice is done using a 20 cm long 3-O Polyglycolic acid suture with HR26 needle in a 2 cm long incision over a 4 cm x 7 cm penrose drain. The angle between each instrument (telescope, needle holder, and grasper) and horizontal line (simulating horizontal patient lie) is less than 55 degrees (Figure 3). Practice is done at angles of 45 degrees, 25 degrees and 15 degrees respectively between instruments.

Figure 1: Angle Trainer made from cardboard box and covered with art paper Length = 16 inches, Width = 12 inches, Height = 8 inches

Figure 2: Opening (7 inches X 10 inches) on top of Angle Trainer for placing sutures as well as visual practice of suturing & knot-tying.

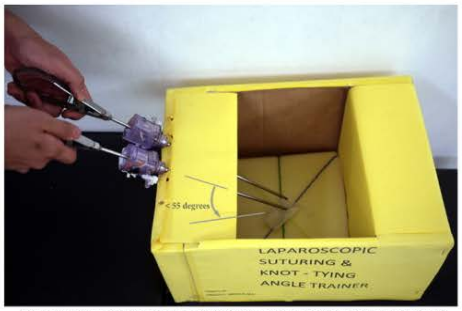

Figure 3: The angle between each straight instrument (telescope, needle holder, and grasper) and the horizontal line is less than 55 degrees.

Results: Practice on this Home-made Angle Trainer is done in two sets. In the first set, sutured penrose drain is placed in oblique 135 degrees position relative to telescope axis simulating laparoscopic suturing in pyeloplasty, partial nephrectomy, or ureteral surgery (Figure 3). In the second set, sutured penrose drain is placed in perpendicular 90 degrees position relative to telescope axis simulating laparoscopic suturing in prostatectomy, cystorrhapy or pelvic surgery (Figure 4). At 45 degrees angle between needle holder and grasper, practice is performed by making the 1st suture with 3 knots followed by 2nd to 5th sutures. Similar practice is then done at 25 degrees angle and 15 degrees angle respectively between instruments.

Conclusion: Presented is a Home-made Angle Trainer for practice in laparoscopic suturing and knot-tying at different angles of 45 degrees, 25 degrees and 15 degrees before performing L.E.S.S. surgeries.

Figure 4: At 15-degrees angle between instruments, perpendicular suturing an incision over Penrose drain placed at 90-degrees sutured-object position along "green string."

ABSTRACT 4

A SINGLE CENTRE PROSPECTIVE 5 YEAR CLINICAL EXPERIENCE WITH ROBOTIC-ASSISTED TRANSPERINEAL PROSTATE BIOPSY IN PATIENTS WITH PREVIOUS NEGATIVE BIOPSIES

Law ZW[1], Ho H[2], Teo J[2], Huang HH[2], Yuen JSP[2], Cheng CWS[2]
[1] *Yong Loo Lin School of Medicine, National University of Singapore*
[2] *Department of Urology, Singapore General Hospital*

Introduction: iSR'obot™ Mona Lisa (BiobotSurgicals pte ltd, Singapore) is a robotic system that performs ultrasound-guided transperineal prostate biopsy (rTPB) in Singapore General Hospital. A 3D model of the prostate is reconstructed based on the US images. After the urologist approves the biopsy plan, the robot assists biopsy to the planned location. We evaluated modifications made to this system and correlated clinical outcomes and detection rates with each modification.

Methods: This institution review board-approved prospective clinical trial included 278 men with previous negative biopsies and rising PSA levels. Between Sept 2006 and Jun 2012, 4 modifications were made (Table 1) and 284 biopsy sessions were performed. Mechanical accuracy is calculated by the distance (mm) between the tip of biopsy needle on real-time US and planned biopsy location. Biopsy time was defined from time of insertion to removal of the TRUS probe. We evaluated the following in 4 different versions of iSR'obot™ Mona Lisa: patient demographics and clinical outcomes. Post-rTPB complications were evaluated.

Table 1: Summary of modification made to iSR'obot™ Mona Lisa

	Technical Modification	**Clinical Impact**
Mechanical Accuracy	Automated pivot changing procedure to reduce error caused by manual positioning pivot point. Improved calibration tool and process.	Improves the actual versus planned biopsy accuracy.
Ultrasound Image Quality	Specially designed ultrasound probe coupler was used to enhance its contact with the prostate.	Improves the ability to delineate the prostate in a shorter duration.
Prostate Modeling	Semi-auto 3D prostate modeling.	Shorten the biopsy planning duration.
Robot Maneuverability	Reduction of robot dimension by more than half (17x22x35cm to 12x15x30cm).	More accurate alignment of robotic arm to the prostate gland.

Results: Overall, 68 patients (24.5%) were diagnosed with CaP, 27 (39.7%) had CaP with GS≥7. Mechanical accuracy improved from 2.5mm to 1.5mm. Median biopsy time shortened from 35(±14) min to 19(±5) min. 2 patients had fever requiring admission for intravenous antibiotics. 41 patients (14.7%) had ARU post-rTPB, 85.4% (35) of these patients had prostate volume ≥30cm^3 (Table2).

Table 2: Patient demographics and clinical outcome

	Version 1	**Version 2**	**Version 3**	**Version 4**
Modification Interval	Sep 2006 – Jan 2007	Apr 2007 – Apr 2009	May 2009 – Feb 2011	Mar 2011 – Jun 2012
Biopsy Sessions	24	101	108	51
Median No. of Cores	21 (±4)	26 (±7)	28 (±11)	30 (±8)
CaP Detected	4 (16.7%)	25 (24.8%)	22 (20.4%)	17 (33.3%)
CaP with GS≥7	1 (25%)	10 (40%)	8 (36.4%)	8 (35.3%)
+ve Cores With ≥50% Involvement	3	6	8	6

Conclusion: With 5 years of system improvement and clinical experience, we have overcome its learning curve. We achieved reduced biopsy time, increasing detection rates and diagnosis of clinically significant CaP maintaining low risk of serious complications. The iSR'obot™ Mona Lisa is a safe and useful for patients requiring rebiopsies.

ABSTRACT 5

COMPREHENSIVE ANATOMIC DESCRIPTIOIN OF RENAL INNERVATION USING 3D COMPUTER-ASSISTED MODELING

Andrew Emon Heidari B.S[1,2], Ryan Leary B.A[3],
Achim Lusch M.D[4], Jaime Landman M.D[4]
[1] *University of California Irvine Biomedical Engineering,* [2] *Beckman Laser Institute*
[3] *University of California Irvine School of Medicine*
[4] *University of California Irvine Department of Urology*

Introduction: Recent technological advances have allowed for treatment of hypertension using intravascular ablation of the autonomic nervous system (ANS) as it enters the kidney hilum. To refine this novel technique, an understanding of the spatial distribution of the ANS is essential. To date, a comprehensive description of renal innervation from the great vessels to the renal parenchyma has not been performed. We combined histopathology with 3D computer assisted imaging to create a three-dimensional comprehensive model of renal innervation.

Material: A series of histological cross sections of the kidney hilum were obtained from a human cadaveric kidney specimen. Each section was taken at 3mm intervals in the sagittal plane. Images of each histological section were taken at magnifications that ranged from 0.3X to 20X optical zoom such that fine detailed structures could be resolved. Images were then imported into ImageScope (Aperio; Vista, CA) software, whereupon the cross section of each artery, vein and nerve was traced and annotated. The annotated images were then imported in sequence as 2-D planes into SolidWorks (Waltham, MA, USA). Anatomical structures were identified in each slice and traced utilizing spline traces to closely map the lumen and contour of each structure. Arteries are labeled in red, veins are labeled blue, the collecting system (calyces and renal pelvis) is labeled yellow, and nerves are labeled as light blue.

Results: Tracings of adjacent histologic slides were then converted into 3-D structures by lofting volumes. In this way we were able to create a 3-D structure from a series of 2-D cross sections.

Figure: 3-D volumetric rendering of the kidney hilum created in SolidWorks. Arteries are shown in blue, veins shown in red, and nerves are shown in light blue. The model was then used to precisely characterize the path of all nerves as well as distances from other anatomic structures.

Conclusion: A 3-D rendering of the kidney hilum was created using sequential histological slices. This model allows for visualization and understanding of the spatial distribution of the renal autonomic nervous system anatomy. Comprehensive understanding of the renal ANS will have significant short and long-term clinical ramifications.

ABSTRACT 6

EVALUATION OF DIFFERENT REGION OF INTEREST (ROI) STRATEGIES FOR CHARACTERIZATION OF UPPER URINARY TRACT STONES DETECTED ON COMPUTERIZED TOMOGRAPHY

Vikram M. Narayan[1], Shahab Bozorgmehri[1], Joseph Ellen[1], Muna Canales[1], Benjamin Canales[1], and Vincent G. Bird[1]

[1]*Department of Urology, University of Florida College of Medicine, Gainesville, FL*

Introduction: Composition of a given calculus is of particular importance in the selection of optimal treatment for urinary tract stone disease. The use of computed tomography (CT) has become a common and routine imaging modality in the diagnosis of urinary lithiasis. Moreover, CT images are now routinely retrievable within individual workstations allowing for basic image manipulations by the clinician. Among such manipulations include the ability to measure the CT attenuation value in Hounsfield units (HU) over a region of interest (ROI) on the image. Studies have shown correlation between HU values and stone composition, which is useful in surgical decision-making. However, stone HU measurements are currently not standardized, and may lead to variable reporting of results. We investigated a number of ROI stone assessment strategies in order to characterize variability and direct a more standardized assessment.

Methods: From our institutional database we identified patients undergoing stone surgery with extraction of stone for analysis, and who underwent CT imaging. We assessed demographics, stone size, and stone chemical analysis. HU measurements were performed at transverse and coronal cuts that included stone, with four ROI techniques (identified by letter); (A) largest ROI possible fitting into stone, (B) two equal sized circular ROIs on stone, (C) 3-5 smaller ROIs randomly placed on stone, and (D) largest ROI fitting into stone at all stone inclusive cuts. Measurements were done in abdominal and bone windows. Data was collated and recorded. Stones that were ≥80% composition were identified for separate analysis. Means and standard deviations for the HU attenuation values were calculated and compared across different techniques, windows, and planes using ANOVA.

Results: 122 patients were included. Median age was 54 years. Mean stone size was 12.5 mm, standard deviation (SD) 7.6. Stones for subtype analysis included calcium oxalate monohydrate (31), calcium oxalate dihydrate (4), calcium phosphate-brushite/OH (4), and uric acid (12). Mean HU in abdominal window identified by ROI technique were (A) 443.53 (SD 254.10), (B) 568.65 (SD 366.98), (C) 560.00 (SD 318.19), and (D) 332.42 (SD 207.29). HU means were significantly different when comparing across ROI techniques (controlling for window and plane, $p<0.0001$), abdominal vs. bone windows (controlling for plane and ROI technique, $p<0.001$), and transverse vs. coronal planes (controlling for window and ROI technique, $p<0.001$). This was true when considering all stones together as well as within pure stone subtypes, except the underpowered calcium phosphate-brushite/OH subtype.

Conclusions: HU attenuation values measured on CT images to assess stone density vary significantly depending on the window, plane, and ROI technique in which the measurements are made. Current literature that describes correlation between HU values and stone composition likely do not take into account a clinician's individual differences in making ROI measurements. Additionally, the measurements made are performed on CT images that have been reconstructed using post-capture image processing software unique to different scanners, which likely represent approximations or averages of the original images. We recommend a standardized nomenclature be adopted to report stone HU density, as well further investigation into using raw unprocessed CT image data to perform HU measurements.

ABSTRACT 7

EVALUATION OF DURABILITY AND COST EFFECTIVENESS OF THREE SURGICAL SIMULATORS: MIMIC DV-TRAINER™, ROSS ROBOTIC SURGICAL SIMULATOR™, AND THE SIMULAB EDGE SYSTEM™

Michael del Junco, Ramtin Khanipour, Zhamshid Okhunov, Renai Yoon, Reza Alipanah, Elspeth M. McDougall, Jaime Landman

Department of Urology, University of California, Irvine

Introduction: There is an increasing demand for high-fidelity surgical simulation. We evaluated the cost of ownership (maintenance and overhead) of three high-fidelity surgical simulators: the Mimic dV-Trainer™, RoSS Robotic Surgical Simulator™, and the Simulab EDGE System™.

Methods: An equipment maintenance log was developed and prospectively used for each simulator. The number of breakdown incidents and annual service contract costs were documented for each surgical trainer as well as the total repair time and personnel time required to resolve each incident. Calculations were completed to determine the average number of incidents, overhead hours and cost, total maintenance cost, and total downtime on a per-month basis for each simulator. The period of observation began upon the date of first incident reported for each device. Data collection time was 8, 12 and 5 months each for the Mimic dV-Trainer™, RoSS Robotic Surgical Simulator™, and the Simulab EDGE System™ respectively.

Results: The average number of breakdown incidents per month were 1.09 for the Mimic dV-Trainer™, 0.68 for the RoSS Surgical Simulator™, and 1.53 for the Simulab EDGE System™. The mean time to repair each incident were recorded as follows: 4.13 days for the Mimic dV-Trainer™, 13.25 days for the RoSS Robotic Surgical Simulator™, and 2.43 days for the Simulab EDGE System™. The estimated mean monthly overhead costs were $136, $263, and $174 for the Mimic dV-Trainer™, RoSS Surgical Simulator™, and the Simulab EDGE System™, respectively. Significant limitations of this study include varying period of observation for the devices as well as varying frequency of simulator operation which was not documented. Moreover, none of the simulators were observed immediately after their purchase. Thus, each simulator may have variable ‘ware and tare’ due to this factor. Data is reported on a per-month basis. Estimated total operation cost per month were $953, $1,096, and $688 for the Mimic dV-Trainer™, RoSS Surgical Simulator™, and the Simulab EDGE System™, respectively.

Conclusion: While the Simulab EDGE System™ held the highest average incident breakdown per month, it was the most cost effective surgical simulator observed and also held the shortest mean time to repair each incident.

ABSTRACT 8

INDENTER STUDY: HIGHER ELASTICITY OF PROSTATE IS ASSOCIATED WITH LOWER TRACT SYMPTOMS

Jang Hwan Kim[1], Kwang Hyun Kim[2], Sey Kiat Lim[1], Bummo Ahn[3], Jung Kim[4], Koon Ho Rha[1]
[1] *Department of Urology, Urological Science Institute, Yonsei University College of Medicine*
[2] *Department of Urology, Ewha Womans University Mokdong Hospital, Seoul, Korea*
[3] *Korea Institute of Industrial Technology*
[4] *Department of Mechanical Engineering, School of Mechanical, Aerospace and Systems Engineering, Korea Advanced Institute of Science and Technology, Seoul, Korea*

Introduction: Numerous studies have shown that fibrotic changes in tissue architecture associated with aging and inflammation contribute to pathology and dysfunction in many organ systems. Recent study demonstrated that fibrotic changes of periurethral prostatic tissues were associated with increased mechanical stiffness and lower urinary tract symptoms (LUTS). We previously measured tissue elasticity of prostate tissue and developed a tissue elasticity map for localization of prostate cancer. In this study, we investigated the association of the elasticity of prostate with LUTS.

Methods: From August 2009 to December 2009, 48 consecutive patients without neoadjuvant therapy or previous prostate surgery, and underwent robot assisted radical prostatectomy by a single surgeon were included in this study. A novel palpation system was used to measure tissue elasticity on prostate specimens. The elasticity of the prostate was defined as the mean elastic modulus (kPA) of 21 sites from the posterior surface of prostate. All patients completed IPSS questionnaire prior to surgery. LUTS were defined as total IPSS score 8 or greater. Significant voiding symptoms were identified by a score of 5 or greater based on response to Q 1,3,5,6 and storage symptoms were identified by a score 4 or greater on response to Q 2,4,7.

Results: The median age of all patients was 66 years. Five patients (10.4%) had extracapsular extension and the median tumor volume was 0.75mL. The median elastic modulus of the prostate was 20.8kPa (IQR 15.6-22.9) and patients with elastic modulus greater than 20kPa were older (65.8 vs. 61.5, p=0.060) and had higher prostate volumes (47.4 vs. 41.6, p=0.205) than their counterparts. The incidences of LUTS (84.6% vs. 59.1%, p=0.047) and voiding symptoms (84.6% vs. 54.5%, p=0.022) were significantly higher in patients with elastic modulus greater than 20kPa. On multivariate logistic regression, higher elastic modulus (as continuous variable) was independently associated with voiding symptoms (OR 1.18, p=0.038) after controlling for age and prostate volume. Elastic modulus was not independently associated with LUTS and storage symptoms.

Conclusion: The elasticity of the prostate was independently associated with voiding symptoms. Our finding suggests that the elasticity of the prostate could be a potential risk factor for the development of LUTS.

Reference: Ahn B, Lorenzo EI, Rha KH *et al*. Robotic palpation-based mechanical property mapping for diagnosis of prostate cancer. *J Endourol* 2011; 25: 851-7

ABSTRACT 9 **BEST PAPER AWARD**

A NOVEL COMPACT SINGLE INCISION SURGICAL ROBOT WITH CONICAL REMOTE CENTER-OF-MOTION MECHANISM AND ROD ELBOW JOINT

Hyung-joo Kim , Hyun-do Choi, Jun-Won Jang, and Jong-hwa Won
Samsung Advanced Institute of Technology

Introduction: Single incision laparoscopic surgery (SILS) has recently been developed. In spite of the potential advantages of SILS techniques, there are limitations such as crowded space, weak tool strength, and mirror image manipulation. Surgical robot could resolve these problems; however, the current robot systems also have limitations such as decreased degree of freedom (DoF) and working space, weak joint force, and arm clashing. To overcome these technical obstacles, we developed the first prototype of a novel compact single incision surgical robot system providing high dexterity (9 DoF), strong tool strength (joint force), workspace, and intuitive control.

Methods: Conical Shape RCM Mechanism Design for Compact surgical robot. The RCM mechanism is mandatory for patient's safety. Parallelogram type RCM is the most widely used. The da Vinci system is a successful example of a parallelogram RCM. However, its huge size is the shortcoming of the currently used parallelogram, potentially inducing arm clashing and encroachment on the workspace of surgical assistants. This conical RCM is compact and avoids arm clashing by separating the motion area. The mechanism consists of a base frame, an inner cone, an inner rotator, and a linear instrument guide (Figure 1). This novel and simple kinematic structure can satisfy our design goals (compactness, workspace, no clashing, dexterity) with 9 DoF(4 DoF arm +5 DoF instrument).

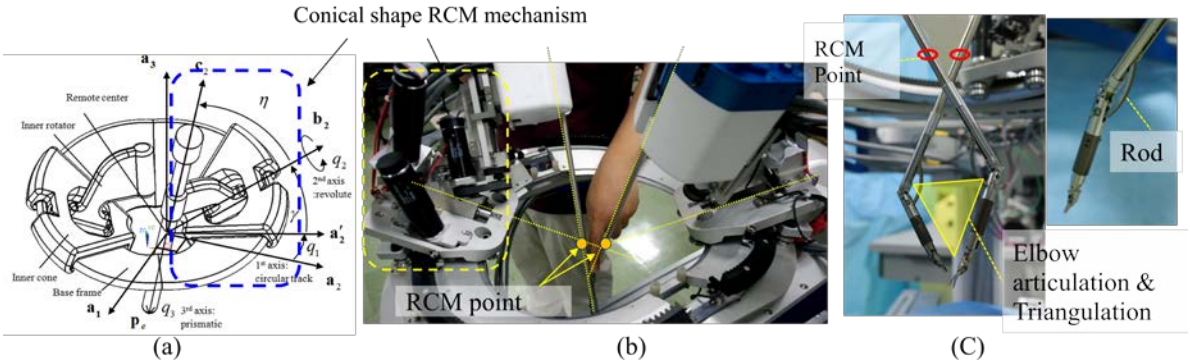

Figure: (a) Conceptual design and parameter definition of the conical shape RCM mechanism, (b) 1st prototype of cone actuator 4DoF, (c) surgical instruments 5DoF.

Rod Driven surgical Instruments. The articulated joints are required for triangulation and dexterity. However, joint is the main reason for weak strength of instrument. Therefore, instead of the currently used wire driven joint, we adopted rod link to elbow of 5 DoF instrument (Figure 1C). For joint force test, maximum 3kg was applied to the end of instrument and smooth motion was observed without a sudden divergence and unstable vibration.

Results: To evaluate the performance of the system, FLS test were performed by non-expert (by HD Choi) [peg transfer: 4m4s at 7th trial / suturing & knot tying: 2m57s at 8th trial] and an *in vivo* animal trial was performed to verify the design output of conical mechanism and rod instrument. In this 1st prototype trial, Endoscope was handled by assistant. He (HS Kwak) could handle the endoscope successfully without interference of arms or arm clashing.

Figure 2. *In vivo* animal test for design out verification (Nephrectomy Rt, porcine model, 35kg).

Conclusions: We could verify the design output of the conical RCM with rod link instrument. However, this first prototype did not include endoscope manipulating arms. The next steps will be making a second prototype that will include two instrument arms and an endoscope manipulating arm, and performing an *in vivo* study to evaluate the preclinical feasibility of the next generation prototype.

ABSTRACT 10

COLLECTION SYSTEM PERCUTANEOUS ACCESS USING 3D REAL-TIME TRACKING SENSORS: FIRST PIG MODEL *IN VIVO* EXPERIENCE

Estevao Lima [1,2], Pedro Rodrigues[1,3], Carlos Oliveira[1,2], Antonio Cicione[1,4], Emanuel Silva[1,2], Paulo Mota[1,2], Jorge Correia-Pinto[1,5], João Vilaça[1,3]

[1] *ICVS/3B's - PT Government Associate Laboratory, School of Health Sciences, University of Minho-Braga/Guimarães, Portugal,* [2] *Department of Urology, Hospital of Braga, Braga, Portugal,* [3] *Algoritmi Center, School of Engineering, University of Minho, Guimarães, Portugal,* [4] *Urology Unit, Magna Graecia University of Catanzaro, Catanzaro, Italy,* [5] *Department of Pediatric Surgery, Hospital of Braga, Braga, Portugal*

Introduction and objectives: Precise needle puncture of the renal collecting system is a challenging and essential step for successful percutaneous nephrolithotomy (PCNL). This work aims to evaluate the efficiency of a new real-time electromagnetic tracking (EMT) system for *in vivo* kidney puncture.

Materials and Methods: Six anesthetized female pigs underwent ureterorenoscopies in order to place a catheter with an EMT sensor into the desired puncture site and to ascertain the success of puncture. Subsequently, a tracked needle with a similar EMT sensor was navigated into the sensor inside the catheter. Four punctures were performed by two surgeons in each pig: one in the kidney and one in the middle ureter, on both right and left pig sides. The number of attempts and time needed to evaluate the virtual trajectory and to perform the percutaneous puncture were outcomes measurements.

Results: Overall 24 punctures were easily performed without any complications. Surgeons required more time to evaluate the trajectory during ureteral puncture than kidney (median 15 versus 13 seconds, range 14 to 18 and 11 to 16 seconds, respectively; p= 0.1). The median renal and ureteral puncture times were 19 and 51 seconds, respectively (range 14 to 45 and 45 to 67; p=0.003). Two attempts were needed to achieve a successful ureteral puncture. The presented technique demands presence of renal stone for testing.

Conclusions: The proposed EMT solution for renal collecting system puncture proved to be highly accurate, simple, and quicker. This method might represent a paradigm shift in percutaneous kidney access techniques.

ABSTRACT 11

BIOMECHANICAL PROPERTIES OF THE URETER: PRELIMINARY RESULTS

Yaniv Shilo[1], Joseph E. Pichamuthu[2, 3], Timothy D. Averch[1], Stephen V. Jackman[1], David A. Vorp[2, 3]

[1] *Department of Urology, University of Pittsburgh Medical Center, Pittsburgh, USA*
[2] *McGowan Institute for Regenerative Medicine, Pittsburgh, USA*
[3] *Department of Bioengineering, University of Pittsburgh, Pittsburgh, USA*

Introduction: Ureteral injuries such as perforation and avulsion are directly related to mechanical damage of the ureter. Understanding the biomechanical properties of this tissue may assist in engineering efficient devices for urological applications, a better comprehension of pathological events in the ureter and prevention of iatrogenic injuries. While few studies looking on the mechanical properties of the animal ureter were reported, specific data on the tensile strength and elastic properties of the human ureter is unavailable. The purpose of this work was to study the biomechanical properties of the human ureter.

Methods: After obtaining IRB approval, we harvested 6 human proximal ureters (4 male and 2 female) from patients who had nephrectomy for either renal cell carcinoma or nonfunctioning kidney from August, 2012 to February, 2013. The ureters were immediately placed in saline at 4°C and tested within 48 hrs. The ureter was then cut into multiple circumferentially- and longitudinally-oriented tissue specimens for tensile testing. Initial dimensions of each tissue specimen were measured and then mounted and stretched to failure after ten cycles of preconditioning in a uniaxial tensile testing machine. The corresponding force and displacement was recorded and stress-strain curve was plotted. Finally, stress at failure was noted as the tensile strength of the sample. Circumferential tensile strength was also compared in the proximal and distal regions of the specimens.

Results: The age of the patients studied was 66.5±10.8 (mean±SEM) years and BMI was 24.5±1.8. The tensile strength of the ureter in circumferential and longitudinal orientations were found to be 538±50 MPa and 1059±197 MPa, respectively ($p<0.03$). The circumferential strength in the proximal portion of the ureter was 501±41 MPa in comparison to 575±94 MPa in the distal portion ($p=0.15$).

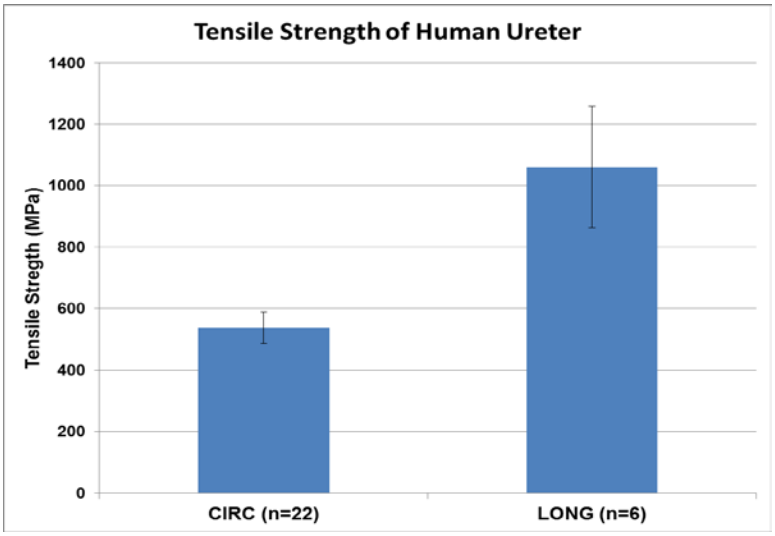

Conclusions: The circumferential tensile strength of the ureter was found to be significantly lower than the longitudinal. Additionally, the circumferential tensile strength of proximal segments of the ureter is lower than its distal segments, likely indicating the proximal portion of ureter is more prone to be damaged than the distal portion.

ABSTRACT 12 **TOP 10 ABSTRACT**

PRE-CLINICAL EVALUATION OF A MRI-SAFE ROBOT FOR ENDORECTAL PROSTATE BIOPSY

Govindarajan Srimathveeravalli[1], Chunwoo Kim[2], Doru Petrisor[2], Jonathan Coleman[1], Hedvig Hricak[1], Stephen B Solomon[1], Dan Stoianovici[2]

[1] *Dept. of Radiology, Memorial Sloan-Kettering Cancer Center, New York, NY*

[2] *Urology Robotics Lab, Johns Hopkins University, Baltimore, MD*

Introduction: The purpose of this study was to assess the feasibility and safety of using an MRI-Safe robot for image-guided transrectal needle placement and biopsy of the prostate using a canine model. The accuracy and precision of robot-assisted targeting was also determined. Finally, the possible interference of the robot with the quality of the MR spectroscopy imaging (MRSI) was also determined.

Methods: Healthy adult male beagles (n=6) were used in an Institutional Animal Care and Use Committee approved study. MR spectroscopy images acquired before and after placing the robot were compared to examine any possible changes in the spectroscopic signature due to the presence of the robot. Then, under robot assistance, 4 to 6 needle placements were performed in each dog and images were acquired to measure targeting accuracy. In four animal experiments, seven core biopsies were obtained and the cores were analyzed for their quality and potential diagnostic value.

Results: A total of 30 locations, equally distributed on both sides of the urethra in the central and peripheral aspects of the prostate, were targeted under robot assistance. The mean targeting error was measured to be 2.58mm (SD 1.31mm). It was possible to place the needle in a single attempt in 3 minutes or less. Qualitative analysis of MRSI acquired before and after placing the robot did not indicate identifiable differences in the relative amplitude or location of the citrate and creatine peaks. Histopathology analysis of retrieved biopsy core indicated presence of prostatic tissues, sufficient for making a potential diagnosis. All dogs recovered and have been adopted.

Conclusion: Results of the study indicate that it is safe and feasible to use MR image guidance and robotic assistance to help the placement needles in the prostate. The use of the robot does not interfere with the spectroscopic signature of the healthy prostate and could be used for performing pathology – imaging correlation.

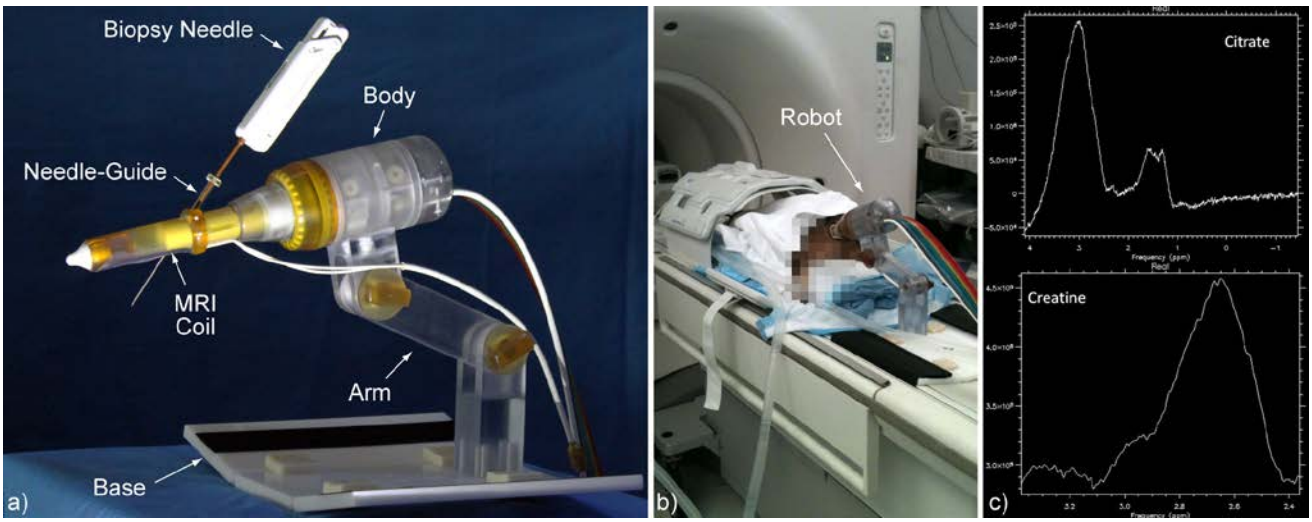

Figure: a) MRI-Safe Robot, b) Animal experiment, and c) MRSI graphs with built-in robot coil

Acknowledgement: Project supported by Award Number W81XWH0810221 from the Prostate Cancer Research Program of the Department of Defense. The content is solely the responsibility of the authors and does not necessarily represent the official views of the PCRP or the DOD.

ABSTRACT 13

MICRO-CRYOABLATION OF ILIOINGUINAL AND GENITOFEMORAL NERVE FIBERS FOR PATIENTS WITH PERSISTENT OR RECURRENT CHRONIC GROIN OR SCROTAL CONTENT PAIN

Ahmet Gudeloglu[1], Jamin Brahmbhatt[1], Yaron Har-Shai[2], Sijo Parekattil[1].
[1]*Winter Haven Hospital & University of Florida*
[2]*Carmel and Lin Medical Centers, Haifa, Israel*

Introduction: Chronic groin and scrotal content pain (CGSCP) is a debilitating condition. Previous studies have shown that 15% of patients are refractory to current treatment options (such as denervation of the spermatic cord). Cryoablation has been shown to be effective in ablating peripheral nerves in chronic pain syndromes. This study assesses the use of a novel micro needle cryoablation technique for the ablation of ilioinguinal and/or genitofemoral nerves in patients with chronic CGSCP.

Methods: Prospective database review: November 2012 to February 2013. 19 micro-cryoablation procedures (3 bilateral cases) in 16 CGSCP patients (4 female patients with chronic groin pain included). Under real time power Doppler ultrasound visualization, a micro-cryo needle (CryoShape Inc., New York, NY) was carefully placed via a 3-4 mm subinguinal incision to target branches of the ilioinguinal and genitofemoral nerves. Testicular arteries and veins were identified with the Doppler and micro-cryoablation was performed medial and lateral to the spermatic cord at the level of the external inguinal ring. A 1 cm diameter ice ball (Figure 1) was created with care taken to preserve the spermatic cord and vessels. Pain was assessed preoperatively and post-operatively using an externally validated pain impact questionnaire (PIQ-6, QualityMetric Inc, Lincoln, RI). Analysis was performed utilizing Mann-Whitney U test.

Results: There was a significant decrease in the mean PIQ-6 score from 72 (pre-op) to 42 at the 3 month post-op point ($p<0.0001$). At 3 months post-op, 74% (14) of the patients had a significant decrease in their pain: 63% (12) had complete elimination of pain and 11% (2) had a greater than 50% reduction in their pain score. The micro-cryoablation technique failed to provide pain relief in 5 patients. Complications were limited to 2 wound infections (treated with antibiotics).

Conclusion: This study, despite its small sample size, seems to indicate a possible benefit to using micro-cryoablation to ligate the ilioinguinal and/or genitofemoral nerve fibers in patients who have persistent or recurrent CGSCP. Further evaluation and longer follow-up are needed.

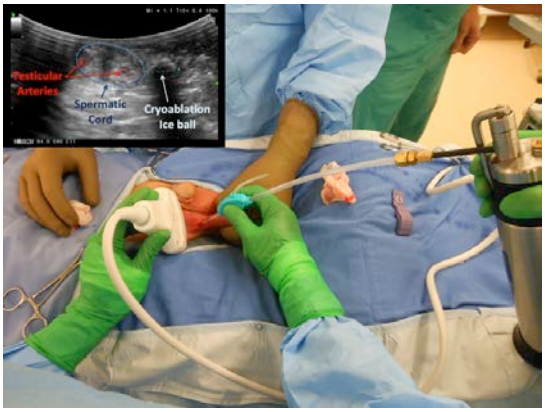

Figure 1: Direct visualization of ice ball formation during micro-cryoablation of peri-spermatic cord ilioinguinal and/or genitofemoral nerve branches

ABSTRACT 14

A NEW, TOTALLY POSTERIOR APPROACH TO ROBOT-ASSISTED LAPAROSCOPIC PROSTATECTOMY IMPROVES EARLY CONTINENCE RATES

Jang Hwan Kim, Sey Kiat Lim, Woong Kyu Han, Sung Joon Hong, Young Deuk Choi, Koon Ho Rha

Department of Urology, Urological Science Institute,
Yonsei University College of Medicine

Introduction: Preservation of the anterior suspensory apparatus (ASA) has been proposed to aid early recovery of continence after radical prostatectomy. ASA spans the ventral prostate and anterior bladder in continuity and will be disrupted if the bladder is dropped during prostatectomy. To our knowledge, current techniques universally involved the disruption of ASA at some point during robot-assisted laparoscopic prostatectomy (RALP). We developed a novel technique which does not require the bladder to be dropped during prostatectomy so as to maximize anatomic normalcy and improve continence outcome. We aimed to evaluate the safety, feasibility and outcomes of this totally posterior approach—RALP (TPA-RALP) with standard or extended lymph node dissection (PLND).

Methods: This was a prospective study involving 31 consecutive patients who underwent TPA-RALP from November 2012 to January 2013 by a single surgeon in a tertiary institution. Low to high-risk tumors were included in this study. Patients with metastatic diseases or suspected lymph node involvement (LNI) at diagnosis or on neo-adjuvant hormonal therapy were excluded. Tumors with extra-capsular extension (ECE) or seminal vesicle involvement (SVI) on pre-operative staging were not contraindicated

Results: The mean age, BMI, and PSA of the cohort were 65.7years, 23.3kg/m^2 and 14.1ng/ml, respectively. 16 (51.6%), 8 (25.8%) and 7 (22.6%) patients had biopsy Gleason scores of 6, 7, and ≥8 , respectively, and 9, 16, and 6 patients were of clinical T-stage 1, 2, and 3, respectively. The mean operative time, estimated blood loss, and length of hospitalization were 123 mins, 294 ml, and 4.5 days, respectively. 8 (25.8%), 18 (58.1%), and 5 (16.3%) patients underwent no PLND, standard-PLND, and extended-PLND, respectively. 29.1% of patients had pT3 tumors and 19.4% had high-grade tumors. Positive margin and complication rates were 16.1% and 9.7%. 26 (83.9%) patients had absolute continence (no leak) and 4 (12.9%) reported only drops of urine leak requiring only safety liners at 4 weeks post-surgery. The continence rate (0-pad used) of the cohort at 1 month was 96.8%.

Conclusion: Early results suggested that TPA-RALP, although technically more demanding was feasible and safe, and also led to excellent recovery of early continence.

ABSTRACT 15

PROSPECTIVE, RANDOMIZED COMPARISON BETWEEN MICROPERC AND RETROGRADE INTRA-RENAL SURGERY OF RENAL CALCULI LESS THAN 1.5 CM

Shashikant Mishra, Raguram Ganesamoni, Ravindra Sabnis, Mahesh R Desai

Muljibhai Patel Urological Hospital, Nadiad, Gujarat, India, 387001

Objective: To compare microperc and retrograde intra-renal surgery for the management of renal calculi less than 1.5 cm in size. The primary outcome studied was stone clearance rate. Secondary outcomes were operative parameters, complications and postoperative recovery.

Methods: Seventy patients presenting with renal calculi less than 1.5 cm in size were equally randomized to microperc and RIRS groups between February 2011 and August 2012 in this randomized controlled trial. Randomization was based on centralized computer generated numbers. Patients and authors assessing the outcomes were not blinded to the procedure. Microperc was done with 4.85-Fr (16 G) needle using 272 µm laser fiber. RIRS was done with Storz Flex-X2 uretero-renoscope. Parameters studied were stone clearance rates, operating time, need for double J stenting, intra-operative and postoperative complications with respect to Clavien-Dindo classification system, surgeon discomfort score, postoperative pain score, analgesic requirement and hospital stay. Stone clearance was assessed using ultrasonography and x-ray KUB at three months.

Results: There were 35 patients in each group. All the patients were included in the final analysis. Stone clearance rate in microperc and RIRS groups were comparable (97.1% vs. 94.1 %, $p = 1.0$). The mean operating time was comparable between the groups (51.6 ± 18.5 vs. 47.1 v 17.5, $p = 0.295$). Double J stenting was required in lower proportion of patients in microperc (20 vs. 62.8%, $p < 0.001$). Intraoperative complications were minor pelvic perforation in one patient in microperc group and transient hematuria in two patients of microperc group. One patient in each group required conversion to miniperc. One patient in microperc group needed RIRS for small residual calculi in first postoperative day. Hemoglobin drop was higher in microperc group (0.96 vs. 0.56 g/dl, $p < 0.001$). Incidence of postoperative fever (Clavien I) was similar in both the groups (8.6% vs. 11.4%, $p = 1.0$). None of the patients in the study required blood transfusion. Postoperative pain score at 24 hours (1.9 ± 1.2 vs. 1.6 ± 0.8, $p = 0.045$) was slightly higher in microperc group. Analgesic requirement was higher in microperc group (90 ± 72 vs. 40 ± 41 mg tramadol, $p < 0.001$). Hospital stay (57 ± 22 vs. 48 ± 18 hours, $p = 0.08$) was comparable in both the groups.

Conclusion: Microperc is a safe and effective alternative to RIRS for the management of small renal calculi. Microperc has similar stone clearance and complication rates when compared to RIRS. Microperc is associated with higher hemoglobin loss, increased pain and higher analgesic requirement while RIRS is associated with higher requirement for double-J stenting.

ABSTRACT 16

NOVEL LAPAROSCOPIC DEFOGGING AND CLEANING DEVICE FOR ROBOT-ASSISTED LAPAROSCOPIC PROSTATECTOMY (RALP)

Carson Wong, MD[1,2,3], Xiao Gu, MD, PhD[4], Motoo Araki, MD, PhD[5] and Sara M. Heider, BSc[1]

[1]SouthWest Urology, LLC, Middleburg Heights, OH, USA;
[2]Ahuja Medical Center, University Hospitals, Cleveland, OH, USA;
[3]Parma Community General Hospital, Parma, OH, USA;
[4]First Clinical Medical College at Yangzhou University, Yangzhou, China;
[5]Okayama University Graduate School of Medicine, Okayama, Japan

Introduction: We evaluate the Advanced Laparoscopic Care Kit (New Wave Surgical, Coral Springs, FL) as a novel set of accessories that defogs and cleans the laparoscope during RALP.

Methods: Laparoscope warming and cleaning equipment was replaced in our operating suite with the Advanced Laparoscopic Care Kit ("Care Kit") for 60 consecutive patients who underwent transperitoneal RALP. Observations and the features of the Care Kit are reviewed.

Results: The Care Kit includes a defogging device that heats an internal reservoir of surfactant based alcohol-free anti-fog solution to 120 F. The device remains heated for 5 hours. The heated surfactant acts as a soap that can quickly remove dried debris from the lens. Because the device is self-contained and hand held, it can be brought to the laparoscope with minimal displacement of the laparoscope from the trocar. The Care Kit also includes microfiber cleaning pads and a trocar cleaning sponge for removing debris trapped inside the trocar cannula. Subjectively, the Care Kit was simple to use by the bedside assistant and effective at maintaining optimal laparoscope visualization. Transfer of the laparoscope to the back table for warming intraoperatively was not required in all 60 cases. The Care Kit protects the laparoscope while it is initially lying flat on the back table from the dangers of scratching and falling associated with using traditional laparoscope warmers.

Conclusion: The Care Kit was effective in preventing fogging of the laparoscope during RALP and has the potential to minimize delays that can result from laparoscope defogging and cleaning.

ABSTRACT 17 **TOP 10 ABSTRACT**

IRREVERSIBLE ELECTROPORATION: OUTCOMES IN A MINIMALLY INVASIVE APPROACH TO RENAL TUMORS

Jonathan Melquist[1], Brian Caldwell[1], Joseph Caputo[1], Annie Darves-Bornoz[1], Jason Kim[1], Rahuldev Bhalla[2]

[1] *Stony Brook University Medical Center, Stony Brook, NY*

[2] *Urology Group of New Jersey, Millburn, NJ*

Introduction: Needle ablation of solid tumors is a valuable option in the treatment of urologic malignancies. The two most common modalities are radiofrequency ablation and cryosurgery, which rely on thermal destruction of treated tissue. A new treatment modality is Irreversible Electroporation (IRE), which induces cell death by non-thermal means, and has been successful in treating hepatic lesions. We report our pilot experience with the use of IRE on renal lesions.

Methods: Five patients received IRE ablation by either laparoscopic-assisted (4/5) or open (1/5) approaches after informed consent was obtained. Pre-ablation biopsies of all lesions were performed. Three to 7 bipolar NanoKnife® IRE Electroporate (AngioDynamics,Latham, NY) probes were positioned utilizing a computer-generated needle insertion field derived from pre-operative imaging. Probe spacing was no greater than 1.8 cm apart. IRE pulses were synchronized to the refractory period of the cardiac rhythm, and ablation occurred in 100 microsecond pulses from 1700-3000 volts for a total treatment course of 15 minutes. Patients were followed at regular intervals with contrast CT imaging.

Results: Average age of our patient was 68 years. The average size of the lesion 2.15±0.73 cm, and all were polar in nature. Three out of 5 were >50% exophytic while 2 of 5 were purely endophytic. Fox Chase Nephrometry scores were 5A, 5P, 6P, 6P, and 5P (www.nephrometry.com). Average operating time was 3.29 ± 0.66 hours. On surveillance imaging, 4 of 5 patients showed resolution of their renal lesions and stable scarring while one of 5 patients showed recurrence. Biopsy at that time confirmed diagnosed of persistent renal cell carcinoma and a laparoscopic partial nephrectomy was performed.

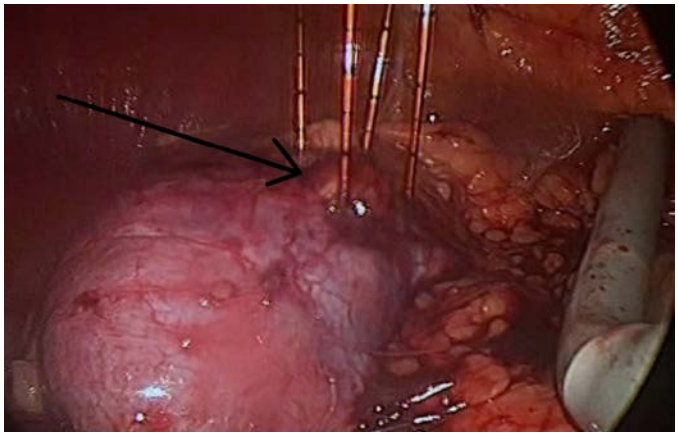

Figure: Laparoscopically-placed needles surrounding partially exophytic renal lesion.

Conclusion: IRE is a novel approach for ablating patients with renal lesions. A theoretical advantage to this treatment as compared to other minimally-invasive approaches is its non-thermal nature, which should permit ablation of problematic lesions near the renal hilum. Our pilot series shows promise. An expanded case series and long-term follow-up of patients may show IRE to be a valuable tool in the Urologist's armamentarium.

ABSTRACT 18

LONG-TERM OUTCOMES OF THE RESONANCE METALLIC URETERAL STENT FOR MALIGNANT AND CHRONIC BENIGN URETERAL OBSTRUCTION

Crystal Castaneda, Yungkhan Tan, Natasha Leigh, Edan Shapiro, Bailey Zampella, Mantu Gupta
Columbia University College of Physicians and Surgeons, Department of Urology
New York, New York, United States

Introduction: The least invasive method to manage ureteric compression from pelvic malignancies and chronic benign ureteral strictures is with an indwelling ureteral stent. The drawbacks of traditional polymeric stents can include failure to relieve hydronephrosis, particularly with very tight or long strictures, and the frequent need for stent changes. We described our initial experience with metallic Resonance ureteral stents (RS) in a previous multi-center study, however there is a paucity of literature on the long-term effectiveness of these stents in managing obstructed systems.

Methods: Candidates for metallic RS at our institution included patients with ureteral obstruction due to pelvic malignancy or chronic benign pathology, who had failed single or parallel stent placement, or at patient-request. After RS placement, patients were followed with serum creatinine measurements and renal ultrasonography immediately after initial placement and every 6 months thereafter. Success was defined as stable renal function and absent or improved hydronephrosis. Stents were changed at yearly intervals or earlier for symptoms or changes in renal function. Stent failure was defined as discontinuation of RS for another modality of management due to discomfort, hematuria, rising serum creatinine, or development of hydronephrosis

Results: Review of Columbia's Endourology database from 1999- 2012 yielded 73 Resonance stents placed in 28 renal units in 21 patients. Resonance stent placement was uneventful in 20 patients. RS was indicated in 22 (78.6%) renal units due to malignant obstruction. The median follow-up was 17 months (range: 0-64, 12 renal units for less than 12 months, 6 for 12-24 months and 10 for more than 24 months, of which 7 were managed with RS for more than 56 months). Eleven renal units (39%) were identified to have failed RS. Median time to RS management failure was 12 months. Median duration to each stent change was 9 months. Stent symptoms were seen in 17 patients (80%). This included dysuria (6 patients, 28.6%), frequency (4 pts., 19.0%), urgency (2 pts., 9.5%), and recurrent UTI (9 pts., 43%). Nine patients (43%) required early stent change (less than one year) due to stent symptoms.

Conclusion: The use of a metallic ureteral stent to relieve obstruction caused by pelvic malignancy or chronic benign stricture helps patients avoid the morbidity of nephrostomy tubes or more invasive surgical intervention with less frequent stent changes associated with polymeric stents and with possibly better relief of obstruction in these challenging patients.

ABSTRACT 19

CRITICAL EVALUATION OF MRI-TARGETED TRUS-GUIDED TRANSPERINEAL FUSION BIOPSY FOR DETECTION OF PROSTATE CANCER

Timur H. Kuru[1,2], Matthias C. Roethke[2], Jonas Seidenader[1], Tobias Simpfendörfer[1], Silvan Boxler[1], Khalid Alammar[1], Philip Rieker[1], Valentin I. Popeneciu[1], Sascha Pahernik[1], Heinz-Peter Schlemmer[2], Markus Hohenfellner[1], Boris A. Hadaschik[1]

[1] *Department of Urology, University Hospital Heidelberg, Heidelberg, Germany*

[2] *Department of Radiology, German Cancer Research Center (DKFZ), Heidelberg, Germany*

Introduction: Precise staging of prostate cancer (PC) is essential for individualized treatment decisions. MRI/TRUS fusion has shown encouraging results for detecting clinically significant prostate cancer. Here we critically evaluate MRI-targeted TRUS-guided transperineal fusion biopsy in clinical routine.

Methods: 347 consecutive patients with suspicion of PC were prospectively included. The median age of patients was 65 years (range 42-84). Mean PSA level was 9.85ng/ml (0.5-104). 49% of men had previous TRUS-guided biopsies, 51% underwent primary biopsy. All patients received MRI-targeted TRUS-guided plus systematic stereotactic prostate biopsies. Imaging data and biopsy results were analyzed and a self-designed questionnaire was sent to all men regarding further clinical history and adverse effects of the biopsy.

Results: 191 of 347 (55%) biopsy samples showed PC. 75% of biopsy proven PC was clinically relevant (NCCN criteria). On multiparametric (mp)-MRI, 104 men were reported as highly suspicious for PC and, in these, the tumor detection rate was 82.6% (86/104). Overall, targeted cores detected significantly more cancer than systematic biopsies (30% vs. 8.2%). In patients without cancer-suspicious MRI-lesions, 11.7% (11/94) were diagnosed with intermediate risk disease. Regarding adverse effects, 50.6% of patients (152/300) reported mild hematuria, 26% temporary erectile dysfunction and 2.6% needed short-term catheterization after biopsy. In three patients (1%) non-septic febrile urinary tract infection occurred.

Conclusion: MRI-targeted TRUS-guided transperineal fusion biopsy provides high detection rates of clinically significant tumors. mp-MRI still has some limitations, and therefore systematic biopsies should currently not be omitted. The morbidity of the transperineal saturation approach is reasonable and mainly self-limiting.

ABSTRACT 20

IN VITRO COMPARISON OF A STANDARD AND NOVEL ECHOGENIC NEEDLE FOR ULTRASOUND-GUIDED PERCUTANEOUS RENAL BIOPSY

Ashleigh Menhadji[1], Vien Nguyen[1], Ringo Chu[1], Jane Cho[1], Kathryn Osann[1], Philip Bucur[1], Puja Patel[1], Achim Lusch[1], Elspeth McDougall[2], Jaime Landman[1]

[1] *Department of Urology, University of California, Irvine*
[2] *University of British Columbia, Vancouver*

Introduction: Urologists are becoming increasingly aware of the importance of pre-treatment percutaneous renal biopsy of small renal cortical neoplasms. A barrier to the routine performance of ultrasound-guided percutaneous renal biopsy has been the technical challenges associated with the procedure. We evaluated a new modified needle which incorporates an echogenic needle tip, designed to improve the needle tip's visibility under ultrasound. We evaluated and compared the ultrasonic imaging quality of the echogenic needle (EN) and a standard needle (SN).

Methods: Forty-eight participants of varying levels of ultrasound experience were recruited to perform ultrasound-guided needle targeting using phantom models consisting of 2 cm water balloons ("cysts") embedded in an opaque gel mold. Each participant was blinded to the type of needle being deployed and was asked to identify and aspirate the balloon using both needles under ultrasound guidance. Both needles were tested at three ultrasound-aiming angles, (0, 15, and 30 degrees). The quality of needle visibility under ultrasound imaging was assessed via a questionnaire, including needle preference and a visibility score (Likert scale 1-10) at each aiming angle. Participants were stratified by level of ultrasound experience.

Results: For each angle tested, the EN received higher visibility ratings. Mean visibility scores for the EN versus the SN were 6.44 vs. 5.52 at 0 degrees ($p=0.001$), 7.77 vs. 6.96 at 15 degrees ($p=0.0004$) and 8.33 vs. 7.54 at 30 degrees ($p=0.0003$). Participants reported significantly greater comfort using the EN needle compared to the SN ($p= 0.001$). These results held true regardless of the sequence of needle tested first. Also there was a significant difference in visibility scores by angle, $p=0.0001$, with larger angles ($30>15>0$) having larger scores. This difference between angles varied by user experience, with the biggest differences seen in those with the least experience, $p =0.03$.

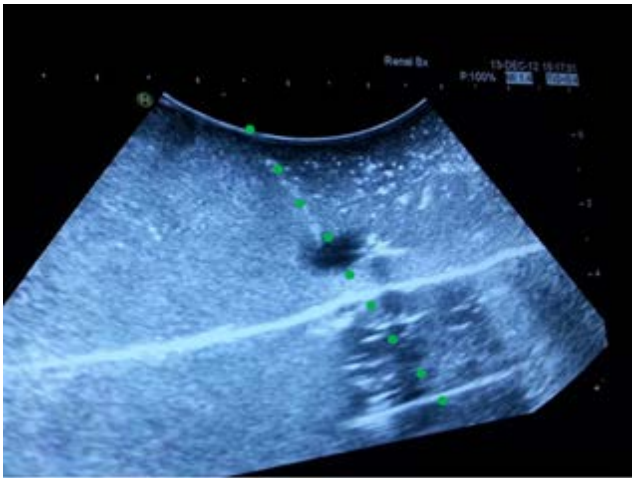

Figure: Echotip needle puncturing cyst at 30 degree angle

Conclusion: Use of the EN improved needle visibility and user comfort regardless of user level of experience, which may lead to its increased adoption during ultrasound-guided renal biopsy procedures.

ABSTRACT 21 **TOP 10 ABSTRACT**

BEVELED NEEDLE TRAJECTORY CORRECTION

Changhan Jun, Chunwoo Kim, Doyoung Chang, Ryan Decker, Doru Petrisor, Dan Stoianovici
Urology Robotics Laboratory, Johns Hopkins University, Baltimore, MD

Introduction: Needle insertion is a commonly performed component of minimally invasive procedures and clinical interventions and is extensively used for diagnostic and therapeutic purposes. Before insertion, the needle is typically aligned on target, with the common assumption that it will remain straight during insertion. However, this is seldom true, particularly with thinner needles. Resulting targeting errors may have a critical clinical impact. Needle bending depends on several factors that include the passage of heterogeneous tissues, physiological motion, physician skills, and also on the intrinsic physical properties of the needle, among which needle point geometry plays a critical factor. Two common types are the diamond (symmetric) and beveled (asymmetric) points, the latter actually inducing deflections by its inclined, rudder-like surface. Still, most needles are beveled, especially core biopsy needles. Several needle steering and deflection control methods have been proposed ([1]IJMRCAS, 2011; 7(2):138), including rotation, oscillation, and speed control. For beveled needles the beveled surface itself has been used for steering, by coupled needle rotation-insertion. We present a new method of steering beveled needles or holding them on a straight path.

Methods: Our AcuBot-RND needle driver robot was used in the experiments [1]. A mockup was built within a translucent box with a grid marked on a lateral surface, filled with 300 Bloom gelatin powder (FX Warehouse Inc., Florida) in solution with sorbitol, glycerin, and water. An 18gx20cm beveled point needle (MN 1820 Magnum core tissue biopsy needle, C.R. Bard, Covington, GA) was held by the robot.

First, needle insertion was done through the fixed needle-guide, to measure the natural lateral deflection of the needle. Then, the robot was used to tilt the needle-guide to prevent the deviation of the needle point from a straight path.

Results: Insertion through the fixed needle-guide appears to follow a circular trajectory curved towards the side of the bevel point. The trajectory lies in the plane defined by the bevel surface normal and needle axis. For 80mm insertion depth, the lateral deflection was 7mm. Tilting the exposed part of the needle *in the same plane and side* may be used to counteract the deflection, as shown in the movie. Controlled deflections were <1mm.

Conclusion: Beveled needles may be held on a straight path by counter-bending the needle in the opposite direction of the bevel. Modeling and/or feedback means currently under development are required for clinical implementation.

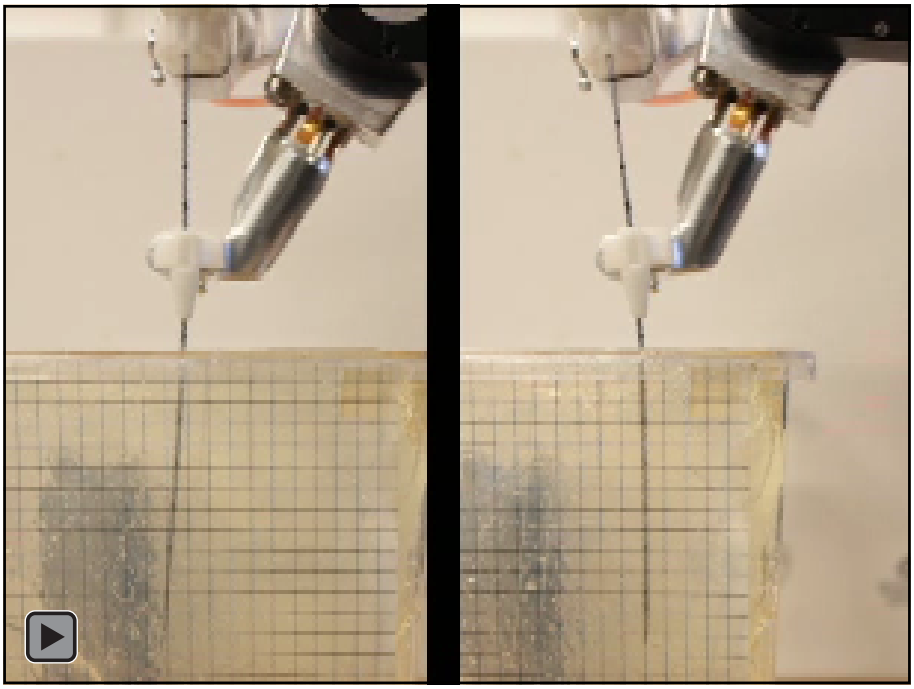

Figure: Uncontrolled curved (left) and controlled straight (right) needle paths. Please play the **MOVIE**.

ABSTRACT 22

WIRELESS TISSUE PALPATION TO LOCALIZE RENAL MASSES: PRELIMINARY ASSESSMENT ON LAPAROSCOPIC TRAINER MODEL

Aaron Benson[1], Marco Beccani[2], Christian Di Natali[2], Ryan Pickens[1], Pietro Valdastri[2], S. Duke Herrell[1]
[1] *Vanderbilt University, Department of Urologic Surgery*
[2] *Vanderbilt University, Department of Mechanical Engineering*

Introduction: Renal ultrasonography (US) is the only active intraoperative image guidance modality available for localization and subsurface imaging in minimally-invasive partial nephrectomy (MIPN). Ultrasonography is limited by lack of multiple dimensions, loss of real-time images after the probe is removed, need for laparoscopic port space and cabling to external monitors for use, and lack of organ surface mapping. Considering these disadvantages, we have developed a small, wireless laparoscopic tissue density probe to measure differences in sub-surface tissue density (similar to digital palpation) and which may provide a 3-dimensional map to localize underlying tissue density differences.

Methods: The proposed approach takes advantage of an external magnetic field source and an intraoperative wireless palpation device (WPD). The WPD can be introduced into the peritoneal cavity through a standard trocar and used to palpate the target with a laparoscopic grasper. Indentation pressure is obtained by a tactile sensor embedded in the tip of the WPD. WPD relative position with respect to the source of the magnetic field is obtained in real-time by on-board magnetic field sensors. Tissue indentation depth is obtained, integrating the WPD position as indentation pressure is detected. These data are used to derive the elastic module of the tissue being palpated and to create a bi-dimensional tissue stiffness map. Inside the WPD, a wireless microcontroller transmits the measurements acquired by the magnetic field sensors and the tactile element. The WPD is a cylindrical capsule with a diameter of 12.7 mm (compatible with access through a standard trocar for 12 mm instruments) and a length of 27.5 mm. The WPD was assessed against a traditional indenter to measure the elastic modulus of a PVC sample (Liquid Plastic, M-F Manuf.) with a thickness of 35 mm and a nominal elastic modulus of 64.49 kPa. The WPD was used to palpate the sample in a laparoscopic trainer model, using a standard 5-mm grasper. The same sample was then removed from the laparoscopic trainer model, and indented with a standard material characterization system.

Results: Elastic moduli obtained by interpolating the stress-strain data with least square fitting for the traditional indenter and for the WPD were respectively E_{TRAD}= 63.862 kPa (R^2 = 0.993) and E_{WPD} = 64.794 (R^2 = 0.995), the average relative error was equal to 1.45%. Indentation depth reached 1.22 mm with an indentation force equal to 1.2 N, which shows how WPD is able to detect stiffness of a soft material. The next step will be to use the WPD to map a soft tissue surface where masses are embedded, in order to assess the possibility of correctly defining buried tumor margins.

Conclusion: Current intraoperative US imaging for localization of urologic masses, such as in MIPN, is limited by 2-dimensional imaging, lack of real-time images to direct excision, and requires laparoscopic port space for use. The WPD operates completely intracorporeally, eliminating the need for laparoscopic port space. The WPD measured sub-surface tissue densities and associated mapping based on those densities could potentially assist in mapping excision of endophytic masses. In combination with general localization using ultrasonography, tissue density mapping could further improve the accuracy of renal mass excision, especially the primarily endophytic masses. From a practical standpoint, technology that could have been useful in minimally invasive surgery but was limited by size and wired connections has been re-invented in a small, wireless form suited for laparoscopic use.

ABSTRACT 23

ENDOSCOPIC FORCEPS FOR URETEROSCOPY: A COMPARATIVE *IN VITRO* ANALYSIS

Giovanni S. Marchini, Carl Sarkissian, Shubha De, Manoj Monga
Glickman Urological and Kidney Institute, Cleveland Clinic Foundation, Cleveland, OH

Introduction: The objective of this study was to compare different grasper devices in terms of opening dynamics, grasping effectiveness, safety, and influence on flexible ureteroscope deflection.

Methods: The Captura (2.8F, Cook Medical), Platinum (3.0F, Bard Urological), TriClaw (2.4F, UroGyn), Graspit (2.6F, Boston Scientific), and Boston Scientific Tricep (2.4F, 3.0F; 3.0F non-retracting) graspers opening dynamics were evaluated using high-resolution images; grip strength by measuring maximum tensional force applied while grasping stone models attached to an in-line load cell (Fig. 1A,B); safety profile by the maximum force required to perforate aluminum foil; impact on deflection by measurement of maximum deflection and bending radius after insertion of the grasper through a flexible ureteroscope. Grip strength and perforation forces were compared with Tukey's test assuming unequal variance.

Results: The TriClaw and Graspit had greater grip strengths than all other devices (Fig. 1C). Captura (1.92 N) and Tricep 2.4F (1.72 N) required the greatest forces to perforate aluminum foil. The Triceps and Captura required the least distance to attain a grasping width of 5 mm. Ureteroscope deflection was least impacted by the Tricep 2.4F (213º; 1.35 cm radius), Graspit (207º; 1.35 cm radius) and TriClaw (206º; 1.3 cm radius) (Fig. 2).

Conclusions: There are significant differences in opening dynamics, grip strength, perforation forces, and ureteroscope deflection among ureteroscopic graspers that may predict clinical performance capabilities.

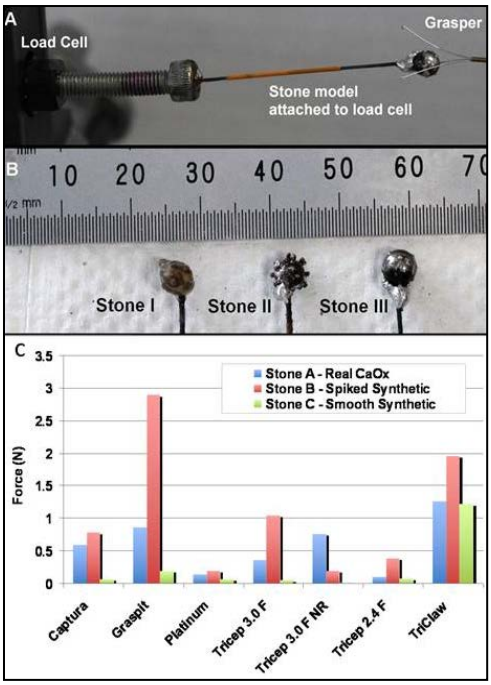

Figure 1A – Grip strength set up. (B): Three stone types designed to replicate common shapes. (C) Average maximum grip strength measurements for each grasper per stone.

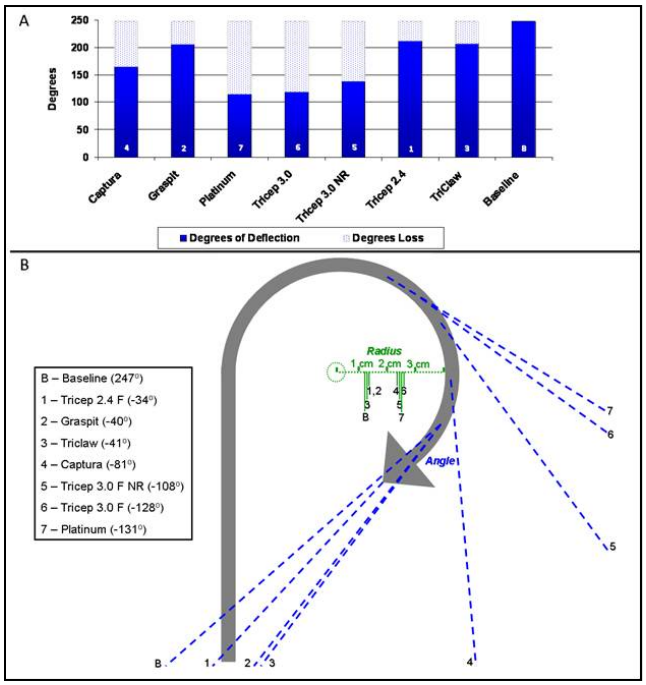

Figure 2: Total impact on the angle of ureteroscope deflection (A and B), and radii (B) varied among grasper devices.

ABSTRACT 24

INITIAL INVESTIGATION OF A 2450 MHZ MICROWAVE SYSTEM FOR ABLATION OF RENAL TISSUES

Karli Pease[1,2], Arturo Castro[1,2], Raymond J. Leveillee[1,2], Nelson Salas[1,2]

[1] *Joint Bioengineering and Endourology Developmental Surgical Laboratory, Division of Endourology, Laparoscopy, and Minimally-Invasive Surgery, Department of Urology, University of Miami Miller School of Medicine, Miami, FL, USA*

[2] *Department of Biomedical Engineering, University of Miami, Coral Gables, FL, USA*

Introduction: Microwave (MW) ablation can potentially produce faster heating over larger volumes of tissue with less susceptibility to heat sink compared to radiofrequency ablation. Two frequencies currently available for microwave ablation are 915 and 2450 MHz. A microwave ablation system which runs at 2450MHz for 2-8 minutes with a maximum power of 180 Watts is currently available. The objective of this experiment was to determine the effect of output powers on the resulting lesion size in an in-vivo porcine model when using the MicroSulis Acculis 2450 MHz MW system.

Methods: Up to two ablations per kidney were performed on 4 Yorkshire pigs (45-49kg) using the Acculis MTA System (Denmead, Hampshire UK) with a single cooled 1.8mm microwave needle. The needle was inserted 3.5 cm into the kidney at either the upper or lower pole parallel to Brodel's line. Five ablations per output power (60W, 120W, and 180W) were performed for 2 minutes followed by a 10 minute cool-down period. Animals were euthanized following the procedure and kidneys harvested for gross analysis of ablation sites. Axial diameter, minimum and maximum radii, and minimum and maximum transverse diameters of each lesion were measured and analyzed.

Results: Coagulation zones were largely spherical with a slight elongation in the direction of the needle shaft, although several lesions for 120W and 180W trials spanned the entire thickness of the kidney (anterior to posterior surface)(Figure 1). Axial diameters and minimum and maximum transverse diameters increased with increasing power output, ranging from 29.74±1.08 mm (60W) to 37.02±6.46mm (180W), 14.50±4.32 mm(60W) to 20.62±1.05 mm(180W), and 25.86±3.18 mm(60W) to 33.20±4.15mm (180W), respectively . Minimum and maximum radii did not show the same increasing trend from 120W and 180W. There were no statistically significant differences in the dimensions of the coagulation zones except between the axial diameter and transverse diameters when comparing 60 and 180 Watts.

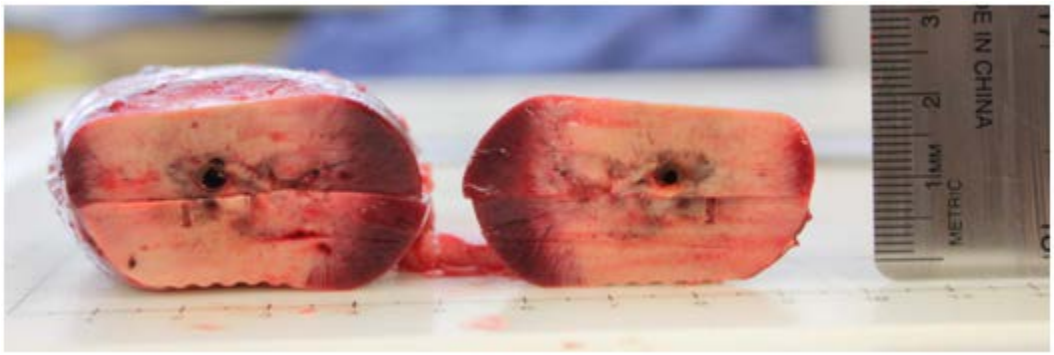

Figure: Transverse view of the kidney that was ablated with 180 Watts for 2 minutes.

Conclusion: MW at 2450 MHz is a minimally-invasive ablation modality that can achieve rapid increases in temperature to induce lesions of various sizes in renal tissue. Caution must be taken in selecting the proper output power, treatment time, and placement of the needle. Further studies to determine the relationship between the treatment parameters and ablation volume in the kidney are warranted.

ABSTRACT 25

ANTHROPOMETRIC RENAL ANATOMIC ALTERATIONS BETWEEN SUPINE AND PRONE POSITIONS IN PERCUTANEOUS RENAL ABLATION FOR RENAL CORTICAL NEOPLASMS

A. Lusch[1], L Findeiss[2], S Fujimoto[2], Z Okhunov[1], E. McDougall[1], J. Landman[1]
[1]*University of California, Irvine, Department of Urology, Orange, California, USA*
[2]*University of California, Irvine, Department of Radiology, Orange, California, USA*

Introduction: During percutaneous renal ablative cryoablation procedures performed in the prone position for renal cortical neoplasms [RCN] we noted significant anthropometric alterations for lung, colon and kidney positions compared to the preoperative supine CT scan. As such, we evaluated anatomic alterations between supine and prone CT scans.

Material and Methods: A total of 19 patients with RCNs underwent abdominal CT scanning in supine and prone positions. Data was collected on axial CT images with adjustment to the tilt. Data points included anterior/posterior, medial/lateral, cranial/caudal movement of the kidney and kidney rotation relative to distinctive anatomic positions (posterior vertebral body, perpendicular bisector of vertebral body). Further measurements included the amount of kidney covered by liver, spleen and lung, skin to tumor distance, amount of perirenal fat, distance of colon to kidney in the hilar position and anterior/posterior location of the colon compared to the kidney. Statistical analysis included a paired Wilcoxon Rank test with values < 0.05 seen as significant.

Results: Both kidneys are more anteriorly located in prone compared to the supine position: 4.72 cm vs. 4.29 cm [left] and 4.41 cm vs. 4.06 cm [right] (p=0.02 and p=0.03, respectively). On prone CT images the kidneys are also more cranially located: 80.4 mm vs. 60.8 mm [left] and 87.2 mm vs. 57.4 mm [right], (p=0.002 and p<0.001, respectively). The prone position is associated with a significantly shorter skin to tumor distance: 6.47 cm vs. 7.84 cm [right](p<0.0001) and 6.04 cm vs. 6.81 cm [left] (p=0.005). Further, the position of the colon relative to the hilum is closer in prone axial images: 1.02 cm vs. 1.32 cm [left] and 0.81 cm vs. 1.45 cm [right], (p=0.04 and p=0.33, respectively). The colon is more posteriorly located in prone vs. supine position on both sides: 1.21 cm vs. 1.04 cm [left] and 0.80 cm vs. 0.70 cm [right], (p=0.005 and p=0.005, respectively). A significantly larger amount of the kidney is covered by the right lung in prone (27.3 mm vs. 6.05 mm, p=0.0001).

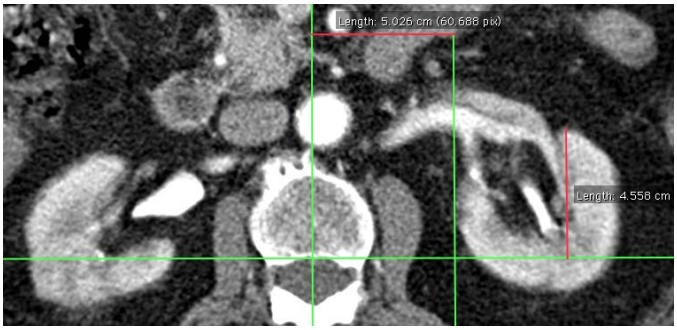

Figure: Measurement anterior/lateral and medial/lateral position of the kidney.

Conclusion: There are specific clinically relevant and reproducible anatomic differences between prone and supine positions. The kidneys are more anterior, more cranially located with an associated shorter skin to tumor distance in prone position. The colon is closer to the kidney, more posteriorly located on both sides and more kidney is covered by lung on the right side. The prone position may limit access, particularly for right upper pole tumors. Pre-procedure prone imaging may be helpful in selected cases.

ABSTRACT 26

TRANSPERINEAL OPTIMIZED PROSTATE (TOP) BIOPSY

Georgios Sakas[1, 2] Pawel Zogal[2]
[1] *GRIS, TU Darmstadt, Germany,* [2] *MedCom GmbH, Darmstadt, Germany*

Introduction: Today TRUS random biopsies are performed by a recommended 12-core scheme, which is difficult to validate, since the true location of each core within the prostate cannot be tracked adequately in TRUS [1]. With our transperineal BiopSee® 3D-ultrasound method [2] we can precisely place cores within each prostate zone [3]. With this work we propose a method automatically calculating an optimized core placement saturation scheme and calculating a "quality score" for each implant configuration.

Methods: We employ 3D-ultrasound and establish geometrical models for lesions, cores and prostate. We model lesions as a sphere of variable diameter d. For clinically relevant lesions of 0.5 cc this results to a diameter d=1cm. Cores are modeled as capsules (image left). For the prostate we either use true contours drawn on 3D U/S or follow the established ellipsoid model. We employ a hexagonal template grid enabling better prostate coverage. We calculate what the optimal number & placement of cores within the prostate can be by requiring optimal volume coverage by minimum cores number: According to our model, needles placed further than d apart can miss a lesion, whereas if needles are placed closer than d, volume parts equal to the volume of capsule overlap are oversampled (image left). Same is true for parts of the capsule out of the prostate border resulting to "partially wasted samples," as well as for needles placed too close to the prostate border (blue area of image right). By dividing the prostate volume by the volume of a core capsule and considering the above constrains (max. volume coverage, minimize under- & oversample, wasted capsules, number of cores), we can estimate the ideal number of needles for complete prostate volume coverage (image right). Accordingly, the percentage of covered volume is regarded as quality score, *i.e.* better implants topologies result to comparatively higher scores.

Results: First patients examined with TOP in Univ. Clinics of Heidelberg confirm the validity and ergonomy of our approach. Automatic scheme saves time and removes inter-operator variance. Core auras intuitively assist manual needle placement. Quality score helps to objectively estimate implant quality.

Conclusion: TOP has the capability to automate saturation protocols and remove operator dependency, as well as to assign individual "quality scores" to manual and/or automated core schemes.

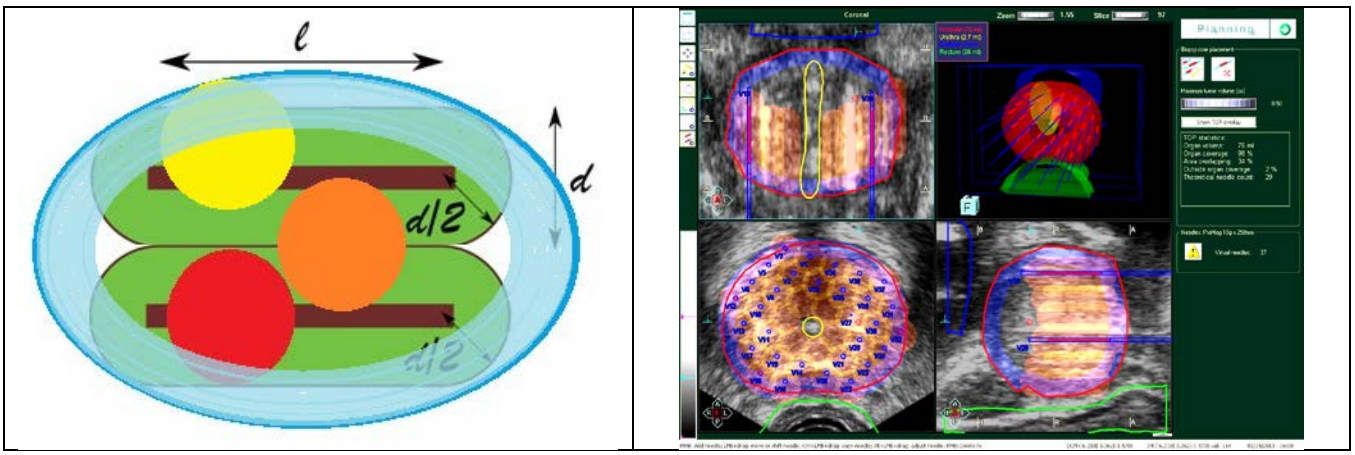

[1] Han *et.al*: Geom. Evaluation of Systematic Transrectal Ultrasound Guided Prostate Biopsy, *J. Urology*, Vol. 188, 2404-2409, 12/ 2012
[2] Hadaschik *et.al*: A Novel Stereotactic Prostate Biopsy System Integrating Pre-Interventional Magnetic Resonance Imaging and Live Ultrasound Fusion, *J. Urology*, Vol. 186, 2214-2220, 12/ 2011
[3] Kuru *et.al*.: Phantom Study of a Novel Stereotactic Prostate Biopsy System Integrating Preinterventional Magnetic Resonance Imaging and Live Ultrasonography Fusion, *JOURNAL OF ENDOUROLOGY,* Volume 26, Number 7, 807-813, 7/2012

ABSTRACT 27

NEW PROTOTYPE CHIP-ON-THE-TIP DIGITAL FLEXIBLE URETEROSCOPE: FIRST CLINCIAL FEASIBILITY STUDY

Mishra Shashikant[1], Sabnis Ravindra B, Desai Mahesh[1]
[1] *Muljibhai Patel Urological Hospital, Nadiad, Gujarat, India*

Introduction: A new prototype model for flexible ureteroscopy (Polydiagnost®) was developed. The mechanisms introduced were only one direction steering of the tip up to 270 degrees, bending fixation by lock at different angles on the handle, and 100% rotation transmission from the handle to the tip. The prototype has an 8 Fr sheath with a smooth, rounded tip having a chip on the tip digital camera, incorporated light fiber, and a 1.2 mm working channel. The proximal handle is made lightweight by the direct connection from the light fiber and digital camera to the processor via a connector.

Methods: The prototype model was used for a left mid calyceal 11 mm stone. VAS score of the surgeon was taken with respect to ease in overall handling, access, tip flexion, scope maneuverability in the calyces, visibility, digital output, and overall experience, using a scale of 1 to 10.

Results: The procedure could be completed successfully in 55 minutes. An access sheath (11/13, NAVIGATOR™) was placed before introducing the model. The stone was retrieved from the middle calyx with a 2.4 F, zero tip™ Nitinol basket and placed in the pelvis before fragmentation with a Holmium 200 micro LASER. The VAS score was 9 for overall handling, 5 for access, 4 for tip flexion, 4 for scope manipulation in the calyces, 5 for visibility, 6 for digital output, and 6 for overall experience with this prototype model.

Conclusion: This prototype model is an interesting development in the field of digital ureteroscopy, with promising clinical implications.

Figure: Prototype (Polydiagnost®) model for digital ureteroscopy

ABSTRACT 28

ROBOT-ASSITED LAPAROSCOPIC SACROCOLPOPEXY IN PATIENTS WITH PRIOR TRANSVAGINAL REPAIR OF PELVIC ORGAN PROLAPSE

Hajimirzaee F, Yates J, Fromer D, Lovallo G, Mora-Esteves C, Rusnack S, Ahmed M
Hackensack University Medical Center

Introduction: Robotic sacrocolpopexy (RALSC) has grown in popularity, with robotic assistance providing excellent visualization in the pelvis, and instrument mobility to facilitate the dissection and mesh manipulation. The role of RALSC in patients who have undergone prior transvaginal pelvic floor reconstruction (PFR) has not been well-defined.

Methods: All patients undergoing RALSC by Urologists at a single institution between 2008 and 2012 were included in the study. A retrospectively-maintained database was reviewed for relevant perioperative variables.

Results: A total of 67 patients underwent RALSC. Of these patients, 11 had undergone prior transvaginal PFR. The mean age of the patients was 58 years, mean parity was 2.8, and mean ASA was 2.1. Mean degree of apical prolapse was grade 3.5. Eighty-two percent were sexually active at the time of initial evaluation. Twenty-seven percent underwent concomitant transvaginal urethral sling procedure. There was one Clavien grade II complication, which was a pelvic abscess requiring long-term intravenous antibiotics. The mean total operative time was 149 minutes. Mesh erosion into the vagina did not occur in any of the cases. At a mean follow-up of 12.5 months (range 2-29), grade I apical prolapse was noted in two patients (18%), both of who were asymptomatic.

In comparison, the mean apical prolapse in patients without a history of PFR was grade 3.2. These patients experienced 3 Clavien grade II complications. Mesh erosion did not occur in any of these patients. Grade I to III apical prolapse recurred in 14 patients, at 17.9%, 5.4% & 1.8%, respectively. None of these patients were symptomatic.

Conclusions: RALSC can be safely performed in patients who have undergone prior transvaginal PFR. The complication rate is comparable to that of patients undergoing RALSC without prior PFR. Symptomatic apical prolapse occurred in one patient in the prior PFR group.

Table 1 Demographic and perioperative data

	Prior Transvaginal Repair (Mean)	No Prior Transvaginal Repair (Mean)
Mean Age	58.1	65.6
BMI	23.1	24.3
ASA	2.1	2.3
Mean Degree of Prolapse	3.4	3.2
% Sexually Active	82%	53.70%
Operative Time (min)	149.5	136.5
EBL (cc)	98.3	101.9
Follow Up (months)	12.5	15.8

Table 2 Post-Surgical Prolapse Recurrence

	Prior Transvaginal Repair	No Prior Transvaginal Repair
Grade 1 Prolapse (%)	18	17.9
Grade 2 Prolapse (%)	0	5.4
Grade 3 Prolapse (%)	0	1.8

ABSTRACT 29

EVALUATION OF A NOVEL DISPOSABLE DIGITAL CYSTOSCOPE

Joseph V. DiTrolio, M.D[1], Nina N. Harkhani[1], Michael D. LaSalle, MD[2]
[1] *UMDNJ/New Jersey Medical School, Newark, New Jersey USA*
[2] *St. Barnabas Medical Center, Livingston, New Jersey USA*

Introduction: Endoscopic urological procedures are the basis of modern urology. Technology has enhanced the image beyond the capability of the human eye. Those gains have come with increased cost, complexity, and fragility. Resistant bacterial strains present difficult treatment options and complex sterilization requirements. All these complexities beg for the development of an inexpensive, disposable, sophisticated urological endoscope.

Methods: We had the opportunity to evaluate and employ an FDA approved, 4.5mm diameter chip-on-the-tip disposable (CMOS) cystoscope with 21 Fr Operating Sheath from ProSurg®. Using a standard laptop (HP DV4), we were able to power the integrated LED light source and the chip-on-the-tip camera as well as store and transmit images to the laptop hard drive. At the time of cystoscopy, all that was required was the following:

1. Disposable cystoscope with Operating Sheath;
2. Bag of irrigation fluid with tubing;
3. Laptop/Tablet computer (Windows 7 or Windows 8); and
4. USB 2.0 Connecting Cable.

Results: Using the 21 Fr ProSurg NeoScope®, with Operating Sheath, we were able to insert into the male urethra, under direct vision, visualize the entire male urethra, sphincter, prostate, and enter the urinary bladder. The laptop was able to record an AVI video and take JPEG and BMP images. Complete endoscopic evaluation of the bladder, although not up to today's high-definition standard, was possible. The disposable Operating Sheath 21 Fr and the CMOS viewing endoscope 4.5mm allowed for good irrigation and instrumentation.

Conclusion: Cost to maintain and sterilize endoscopic equipment is approaching $60/case. Along with the amortization of initial equipment, one can make the case for a disposable cystoscope that costs under $100. Additionally, with the power light source, video monitor, and documentation device all being replaced by an everyday laptop/tablet computer only adds to the benefits. The needs of portability, disposability, and improving quality demand a functional, low-cost endoscopic system and warrants further evaluation.

ABSTRACT 30

EXTRACORPOREAL SHOCK WAVE LITHOTRIPSY (ESWL) COMPLICATIONS DEPENDING ON THE SHOCK WAVE RATE AND NUMBER

Maria C., Mitroi G., Nedelcuță C., Drăgoescu O., Turcitu N.
Urology Department; Craiova Emergency Hospital

Introduction: ESWL has revolutionized the treatment of upper urinary tract calculi and is considered the first-line therapy for more than 75% of the patients with urolithiasis, but it has been intuitively connected to various complications. These complications are mostly related to residual stone fragments, infections, and other effects on tissues, such as urinary, gastrointestinal, cardiovascular, genital, and reproductive systems. The destructive forces generated when cavitation bubbles collapse are ultimately responsible for stone fragmentation; however, they can also cause trauma to thin-walled vessels in the kidneys and adjacent tissues. Our study aims to analyze ESWL complications rates, considering the shock waves number and frequency.

Methods: The study was conducted over a 24 month period and included 344 patients with upper urinary tract calculi. All patients underwent ESWL, with 167 patients receiving with a shock wave frequency of 120 shock waves per minute, with an average number of shock waves of 3697 ± 378, and shock wave average intensity of 4.8 ± 0.9 kV (first group). For 177 patients, we used a lower shock wave frequency (60 per minute) and number (2819 ± 980), with an average intensity of 5.7 ± 0.6 kV (second group).

Results: There were no statistically significant differences between the two groups regarding age, sex, place of origin, clinical symptoms or presence of stone history, stone location or number. Complication rates were lower in the second group compared to the first group, as follows: macrohematuria 13 (7.3%) and 32 (19.2%) in the first group, superficial tissues damage 35 (19.8%) and 62 (37.1%), lumbar pain 21 (11.9%) and 38 (22.8%), and nausea 8 (4.5%) and 22 (13.2%). Other complications were similar, fever 3 (1.7%) and 2 (1.2%), larger residual fragments that lead to steinstrasse 16 (9.0%) and 19 (11.4%).

Conclusion: A decrease in shock wave number, rate and energy may improve ESWL safety, thus reducing the incidence of macrohematuria, superficial tissues damage, lumbar pain, and nausea. Preventive measures can be taken to minimize the frequency of these side effects. Modern lithotripters are optimized to be user friendly, and treatment is only moderately painful, but patient selection and optimized treatment protocols are necessary in order to maximize stone-free rates and to minimize side effects.

ABSTRACT 31

A NERVE COMPRESSION DEVICE AND ELECTROPHYSIOLOGICAL RECORDING OF NERVE RESPONSE TO PRESSURE COMPRESSIONS

Andrew Asmus[1], Joseph Sewell M.D.[2,3], Guangjian Wang Ph.D.[2], Gerald Timm Ph.D.[2,3]
Department of [1]Biomedical Engineering, [2]Urology, [3]Institute of Engineering in Medicine, University of Minnesota

Introduction: Repetitive compression of pelvic structures may cause neural injuries associated with urinary stress incontinence (USI). We developed a system to investigate electrophysiological response of isolated nerves to repetitive pressure compression. The goal is to validate the device in order to investigate the role of neural injury in USI and to develop strategies for mitigating such injuries.

Methods: Our system consists of a sealable electrophysiological chamber and a gas compression apparatus (Figure 1a). The compression is supplied by an air compressor and precisely controlled through a series of regulators connected to air-piloted directional control valves. A toggle valve allows input pressure to be controlled by the opening and closing of a valve that leads to a sealed nerve recording chamber. The sealable chamber consists of two air fittings that allow an entry point for the compressed air and a pressure transducer. The amount of pressure inside the chamber is adjusted by a precision regulator, which comes equipped with a locking nut to prevent inadvertent pressurization. Once the toggle valve is returned to the normally closed position the chamber returns to atmospheric pressure. Nerve compound action potential (CAP) is recorded in freshly isolated swine phrenic nerves. Standard electrophysiological methods were used for amplification and recording of the nerve signals.

Results: The pressure from the device was measured before (input pressure) and after (chamber pressure) it entered the nerve recording chamber. Both input and chamber pressures were linearly correlated with pressure increases on the settings of the regulator and they were well correlated ($R^2 = 1$, m=1) (Figure 1b). The chamber internal pressure can be precisely controlled from 47 mmHg to 450 mmHg. The pressure changes achieved by the opening and closing of the 3-way valve can be completed within 0.01 seconds enabling intermittent-compression on nerve preparations (Figure 1c). Pressure changes did not cause signal artifacts to nerve recordings. Baseline CAPs were recorded for their amplitude, conduction velocity, latency and duration. After baseline recordings the nerves were compressed at 100 mmHg for 10 minutes and allowed to recover for additional 10 minutes. Four nerve samples have been tested thus far. A total block of CAP by compression was seen in one sample. In other two samples compression reduced CAP conduction velocity by approximately 74% and increased CAP duration by approximately 110%. In the fourth sample compression did not cause significant changes. Changes in CAP returned to baseline levels after ten minutes recovery.

Conclusion: These preliminary results concur with CAP and nerve compression literature. It demonstrated our device's capability for investigating real-time effects of compression forces on neural physiology.

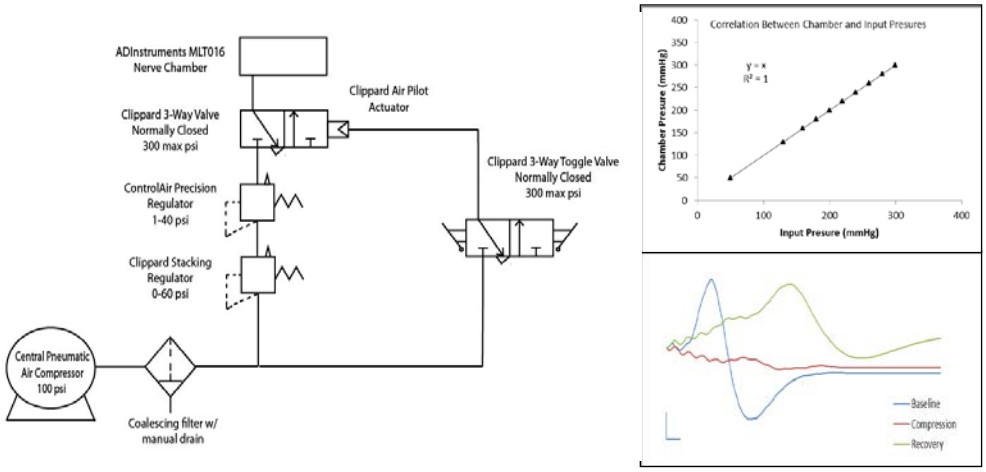

Figure: Test results and a diagram of the nerve compression system. a. Device diagram. b. correlation between input and chamber pressure. c. CAPs before, during and after the compression

ABSTRACT 32

GREENLIGHT HPS-120W VS GREENLIGHT XPS-180W LASER VAPORIZATION OF THE PROSTATE FOR BENIGN PROSTATIC HYPERPLASIA: A GLOBAL, MULTI-CENTER, AND PROSPECTIVE COMPARATIVE ANALYSIS

Pierre-Alain Hueber[1], Daniel Liberman[1], Tal Ben-Zvi[1], Henry Woo[2], Mahmood A. Hai[3], Alexis E. Te[4], Bilal Chughtai[4], Richard Lee[4], Matthew Rutman[5], Ricardo R. Gonzalez[6], Neil Barber[7], Naif Al-Hathal[1], Talal Al-Qaoud[8], Quoc-Dien Trinh[1], and Kevin C. Zorn[1]

[1] CHUM Section of Urology Department of Surgery, Centre Hospitalier de l'Université de Montréal, QC, Canada. [2] University of Sydney, Sydney, Australia. [3] Department of Urology, Oakwood Annapolis Hospital, Wayne, MI, USA. [4] Departments of Urology, Cornell Weill Medical College New York, NY, USA . [5] Department of Urology, Columbia University, New York, NY, USA. [6] Department of Urology, Baylor College of Medicine, Houston, TX, USA. [7] Department of Urology, Frimley Park Hospital, Frimley, Surrey, UK. [8] Department of Urology, McGill University, Montreal, QC, Canada

Introduction: The aim was to evaluate the surgical performance and impact of prostate volume (PV) of the new Greenlight XPS-180W laser system (AMS, Minnetonka, MI, USA) in comparison with the former generation HPS-120W system for the treatment of BPH by photo-selective vaporization of the prostate (PVP).

Methods: From July 2007 to March 2012, a total of 1809 patients underwent Greenlight laser PVP for the treatment of BPH performed at 7 international centers. 1187 cases were performed using the HPS-120W and 622 cases using the XPS-180W laser system. Preoperative data along with operative parameters were all collected prospectively.

Results: The XPS, compared to HPS, allowed significantly reduced laser and operative time, with a mean lasing time of 29.6 min vs. 65.8 min and total operative time of 53 min vs. 80 min, respectively ($p<0.01$ for both). The number of fibers used during the procedures was significantly reduced with the XPS system, 1.11 vs. 2.28 fibers ($p<0.01$) while total energy delivered was 250.2 vs. 267.7 kJ ($p=0.043$), respectively. Overall, using the XPS and HPS systems, the mean operative time (104.3 vs. 55.6 min), mean laser time (86.5 vs. 37.3 min), and mean energy usages (400 vs. 197 kJ) were all significantly increased according to PV >80 cc vs. <80cc. However, when stratified according to PV, XPS demonstrates significant advantages compared to HPS regardless of prostate size in all operative parameters ($p<0.01$).

Conclusion: The XPS-180W system exhibits reduced operative time and laser time with reduced total energy delivery, suggesting a significant increase in efficiency compared to the HPS-120W system. Overall, both with XPS-180W and HPS-120W mean operative time, laser time, and energy usage increased according to prostate size. This suggests that evaluation of PV should be a mandatory assessment as part of the pre-operative evaluation of Greenlight PVP because it has direct implications for the operating parameters, including operative time, and therefore can assist in more efficient scheduling of operating room time.

ABSTRACT 33

LASER ACTIVATED NANOSHELL ABLATION OF PROSTATE CANCER: A PILOT STUDY IN HUMANS

Joshua Stern MD[1], Elena Sazykina [2], Jon Schwartz[3]
[1] *Montefiore Medical Center, Albert Einstein College of Medicine*
[2] *Uro-Clinic 2000, S.A. de C.V., México City, México,* [3] *Nanospectra Biosciences, Inc., Houston, Texas*

Introduction: There are a number of temperature based technologies currently being evaluated for the treatment of localized prostate. These technologies are all challenged by the delicate balance between accurate targeting of a tumor bed and preservation of surrounding vital structures. Laser activated gold nanoshell (GNS) thermal ablation represents a new, minimally invasive emerging technology that offers precise, benign tissue sparing thermal ablation of prostate cancer. This technology has been evaluated previously in a subcutaneous tumor model. We here present our early experience in humans.

Methods: 150nm diameter GNSs with a dielectric silica core and a 15nm thick gold shell were provided by Nanospectra Biosciences, Inc. (Houston, TX.). Designed to optimize optical scattering and absorption properties, these particles can act as intense near infrared (NIR) absorbers that selectively accumulate within tumor neovasculature. A water-cooled optical fiber catheter terminated with a 1 cm-long isotropic diffuser was inserted trans-perineally once into each prostate hemisphere. The optical fiber was energized at 4.5 or 5.0 W from an 805 nm laser source for either 3 or 4 minutes. Patients underwent a radical prostatectomy 3 – 4 days after the laser procedure. The resected prostates were formalin-fixed, paraffin-embedded, sliced, and Hematoxylin and Eosin (H&E) stained for histopathological analysis. Sample from 2 pts were submitted for Nuclear Activation Analysis (NAA) in order to quantify localized GNS concentration.

Results: We are reporting on a safety and laser dosimetry study on 4 patients with localized prostate cancer. The aim was not to accurately ablate all known prostate cancer, as all of these patients subsequently underwent radical prostatectomy. Patients did not have US detected prostate lesions. Future study will follow a protocol of hemi-ablation and will focus on maximizing our laser targeting to a target lesion. All 4 patients had no changes in serum electrolytes measured at various points over the course of 6 months following GNS infusion. No patient reported any systemic or adverse reaction to nanoshell infusion. H&E consistently shows areas of ablation with sharp demarcation from areas of viable tissue. Figure 1 demonstrates areas of successful Pca tissue ablation (Gleason =6 (3+3)) with a very strict demarcation of our laser zone. Areas of un-ablated tissue represent zones where the laser did not pass. This study was not equipped to accurately target all areas of tumor and as such we are not surprised to see viable unablated tumor. In areas of laser ablation however, we do see very focal and precise tissue ablation (Figure 1). NAA data (Figure 2) shows nanoshell accumulation increased nearly 5-fold in cancerous tissue as compared to benign prostate (20.5µg/g and 4.5µg/g respectively).

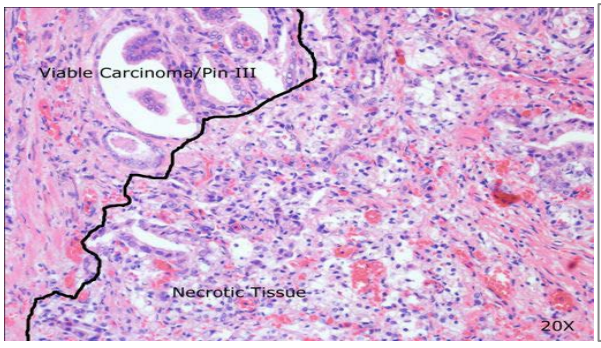

Figure 1. Sample H&E slide after laser ablation

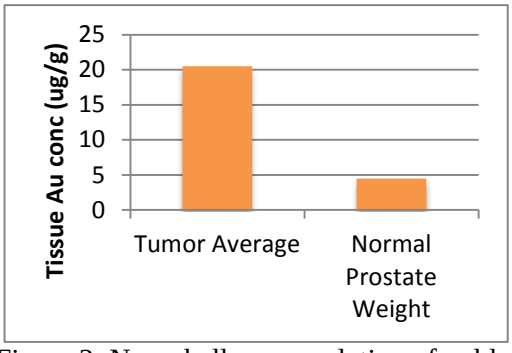

Figure 2: Nanoshells accumulation of gold.

Conclusion: Our data suggests that when targeted accurately, this new technology can focally ablate prostate cancer tissue. Future studies will focus on laser targeting. This pilot study provides evidence that systemically infused nanoshells preferentially accumulate in cancer tissue and that laser activation of these nanoshells can ablate Pca tissue successfully.

ABSTRACT 34

A NOVEL SYSTEM TO MEASURE FORCE ON PERINEAL ARTERIES DURING BICYCLING

Sujeeth Parthiban, Samuel J. Ohlander, James M. Hotaling, Amit Baftiri, Craig Niederberger
University of Illinois at Chicago, Chicago, IL.

Introduction: Several studies have raised concerns that bicycle riding may cause erectile dysfunction (ED). Although perineal artery compression has been suggested as a possible mechanism, the exact cause remains unknown. Previous studies relied on indirect methods and stationary bike models that do not accurately reflect real time or *in vivo* cycling conditions. The aim of this study is to measure the force exerted on the perineal arteries *in vivo.* We developed a portable perineal force-sensing device and used it to test different commercially available seat designs on a stationary bike and on the road to determine whether forces exerted on the perineal artery exceeds arterial occlusion forces.

Methods: A Rabbit core module 4000 based device was developed which can record and store force from 8 different sensors. 1 lb Flexiforce® (Tekscan Inc, Boston, MA, USA) sensors were selected to measure force because they are thin, flexible and virtually unnoticeable to the riders. The device was calibrated using an Instron 8500 high rate system to convert the recorded output from mV to force in Newtons (N). A GE Logic E-9 Doppler ultrasound (GE Healthcare, Milwaukee, WI, USA) probe was used to identify the left and right perineal arteries of 20 healthy men age 18-65, and a probe was used to apply increasing force on the perineum overlying the artery until cessation of flow was observed on ultrasound ($F_{occlusion}$). $F_{occlusion}$ was measured by 1 lb Flexiforce® sensors. Two 1 lb Flexiforce® sensors were fixed to the skin overlying each perineal artery. Subjects bicycled on a standard city road course for ½ mile using each of 6 seat designs. The protocol was repeated on a stationary trainer. Occlusion percentages (%t) were calculated as the percentage of a ride that perineal force ($F_{perineal}$) measured exceeded $F_{occlusion}$. A Paired t-test was used to determine statistical significance between the occlusion percentages in the stationary model versus that of the road model and between the occlusion percentages against a pre-determined threshold of 10% time occluded.

Results: Mean force required to occlude the perineal artery was 10.0 N, SD = 1.4 N. $F_{perineal}$ was greater than $F_{occlusion}$ in all subjects. Average %t was 28.1 % on the stationary ride vs. 44.1 % on the road ride. Mean difference in %t was 16.0% (p=0.01) greater in road vs. stationary In comparison to a pre-determined threshold of 10% occlusion, the average difference in %t was statistically greater than the threshold (p = 0.05) for each seat design on a road course. Our data demonstrates that no seat design prevents or significantly minimizes perineal artery occlusion.

Conclusion: We demonstrated that riders experience significantly greater occlusion on street rides than on stationary trainers. Future studies must rely on methods that measure perineal forces during road bicycling. Also our study demonstrates that no seat is ideal. We believe that no occlusion represents an ideal state, but using a pre-determined threshold of 10% time occluded, each of the six seats on a road course demonstrated a significantly greater time occluded over the threshold. Alternative solutions are necessary to prevent this common problem.

ABSTRACT 35 **TOP 10 ABSTRACT**

EVALUATION OF ACCEPTABILITY OF PHYSICAL SIMULATION MODEL FOR TRAINING OF LAPAROSCOPIC PYELOPLASTY

Lauren Poniatowski[1], Robert Sweet, MD[1], Troy Reihsen[1], Francois Sainfort, PhD[2], Sara L. Best, MD[3], Stephen V. Jackman, MD[4], Richard E. Link, MD, PhD[5], Wesley A. Mayer, MD[6], Stephen Y. Nakada, MD[3], J. Stuart Wolf, Jr., MD[7]

[1] *Department of Urology, University of Minnesota, Minneapolis, MN, USA*
[2] *School of Public Health, University of Minnesota, Minneapolis, MN, USA*
[3] *Department of Urology, University of Wisconsin, Madison, WI, USA*
[4] *Department of Urology, University of Pittsburgh Medical Center, Pittsburgh, PA, USA*
[5] *Department of Urology, Baylor College of Medicine, Houston, TX, USA*
[6] *Department of Urology, The Methodist Hospital, Houston, TX, USA*
[7] *Department of Urology, University of Michigan, Ann Arbor, MI, USA*

Introduction: The objective was to determine the acceptability and aspects of validity for a high-fidelity, low cost synthetic renal pelvis/ureter analogue model for use as a simulation model for training of laparoscopic pyeloplasty for practicing urologists.

Methods: A pyeloplasty simulator model was designed using organosilicate-based materials with incorporated assessment lines for use in post-task Black Light Assessment of Surgical Technique (BLAST)™. Post-task data collected included patency and twist angle at the anastomosis. Practicing urologists (N=12) participating in the 2012 AUA Mentored Renal Laparoscopy course performed a laparoscopic pyeloplasty procedure on the model and completed a post-task survey to evaluate acceptability, face, and content validity of the pyeloplasty model using a 5-point Likert scale. Combined performance data from the 2011 and 2012 AUA Mentored Renal Laparoscopy courses (N=35) was used to determine preliminary construct validity.

Results: Practicing urologists found the model acceptable by rating the model favorably in terms of the model improving their ability to safely perform a pyeloplasty procedure (mean = 4.33, SD = 0.651), and in improving preparedness to perform spatulation and anastomotic suturing (mean = 4.17, SD = 0.577). The model was given an average score of 3.92 (SD = 0.996) for ease of set up and use. Aspects of face validity including analogue tissue behavior (mean = 3.42, SD = 0.996), anatomical accuracy (mean = 4.17, SD = 0.389), and positioning and angle of the model (mean = 3.33, SD = 1.073) were rated favorably. For content validity, participants gave the model an average score of 4.33 (SD = 0.492) and 4.42 (SD = 0.515) for whether the model allowed the user to reproduce skills necessary for spatulation and anastomotic suturing, respectively. Practicing urologists who had performed a laparoscopic pyeloplasty procedure in the last 5 years outperformed those who had not in demonstrating patency (P <0.05) and minimal twisting (P <0.10) at the anastomosis, providing evidence of construct validity to the model.

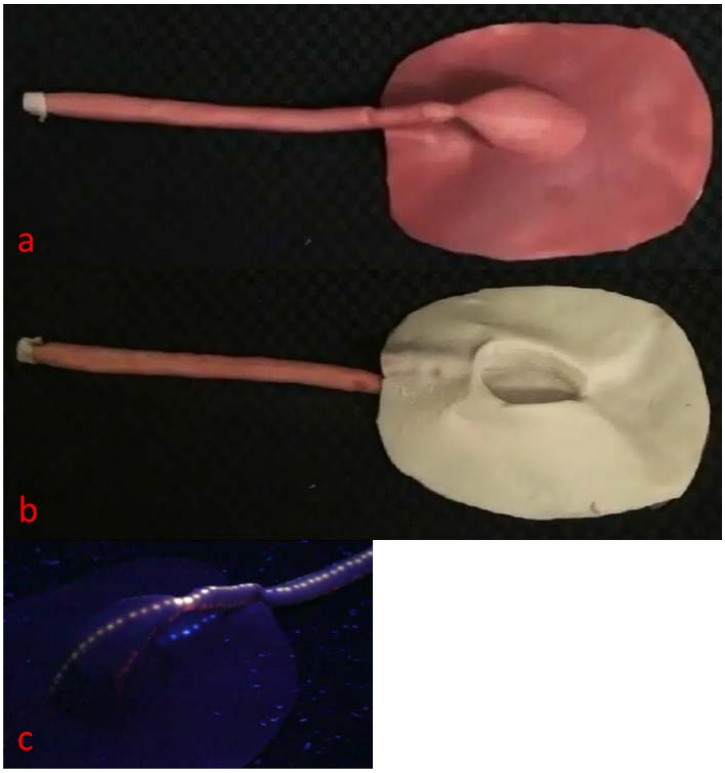

Figure: Pyeloplasty model under room lighting showing (a) exterior and (b) interior and (c) under UV lighting conditions showing BLASTTM assessment lines.

Conclusion: The BLAST™ pyeloplasty model demonstrated good acceptability and preliminary evidence of construct validity for training of laparoscopic pyeloplasty for practicing urologists.

ABSTRACT 36

ROBOTIC TRANSPERINEAL SATURATION BIOPSY APPROXIMATES THE "TRUTH" IN DEFINING LOW-RISK PROSTATE CANCER

Tay K.J.[1], Ho H.[1], Huang H.H.[1], Law Z.W.[2], Koh Z.J.[2], Yuen J.S.[1], Cheng C.W.[1]

1. *Department of Urology, Singapore General Hospital*
2. *Yong Loo Lin School of Medicine, National University of Singapore*

Introduction: Active surveillance and other less-invasive treatments are under-utilised in apparent low-risk prostate cancer, largely due to fears of under-sampling and under-grading with diagnosis by conventional trans-rectal ultrasound-guided (TRUS) prostate biopsy. Our objective was to assess the detection of higher-grade (Gleason>6) prostate cancer using robotic transperineal saturation biopsy (Figure 1) compared to the "truth" of radical prostatectomy in patients with TRUS biopsy detected low-risk prostate cancer.

Methods: This prospective cohort of patients had low-risk prostate cancer (Gleason score≤6, PSA≤10 and clinical ≤T2a) as diagnosed on TRUS biopsy between 2009 and 2012. The patients were grouped into: (A) those who underwent robotic transperineal saturation biopsy for further risk stratification, or (B) those who proceeded to radical prostatectomy immediately post-TRUS biopsy. Robotic biopsy for group A was performed using a novel device (BioXbot). Histological findings from the robotic biopsy and radical prostatectomy (whole-mount slides) were compared to original TRUS biopsy findings for upgrading of Gleason score.

Results: A total of 112 patients were included (group A 29 patients and group B 83 patients). Compared to original TRUS biopsy, upgrading of Gleason score from 6 to ≥7 in group A approximated upgrading in group B (20.7% vs. 34.9%, *p*=0.154). This approximation was even nearer to 63 men classified as very-low-risk (Epstein criteria) at original TRUS biopsy. Upgrading was seen in 22.7% of men in both group A and group B (*p*=1.000).

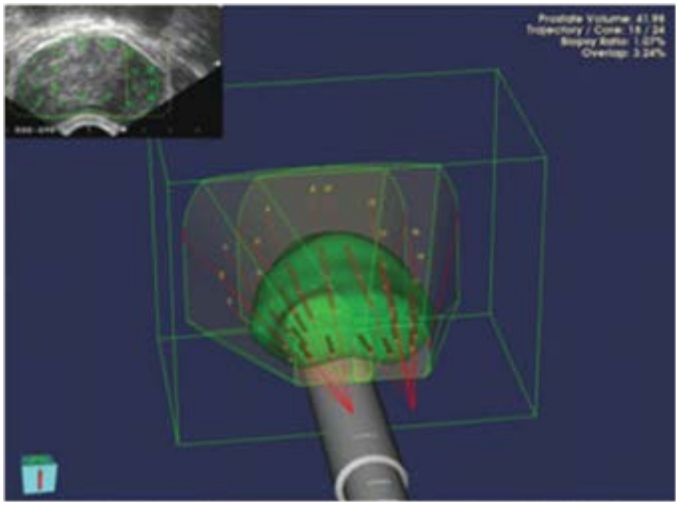

Figure: Grip strength set up. (B): Three stone types designed to replicate common shapes. (C) Average maximum grip strength measurements for each grasper per stone.

Conclusion: Compared to whole-mount histology as the final arbiter, robotic biopsy approximates the "truth" in defining low-risk prostate cancer. It may thus better select patients for less-invasive treatment.

ABSTRACT 37

CONTINUOUS VERSUS CONVENTIONAL BIPOLAR PLASMA VAPORIZATION OF THE PROSTATE AND STANDARD MONOPOLAR RESECTION—A RANDOMIZED COMPARISON OF A NEW TECHNOLOGICAL ADVANCEMENT

Bogdan Geavlete, Florin Stanescu, Cristian Moldoveanu, Marian Jecu, Leon Adou, Petrisor Geavlete
Department of Urology, Saint John Emergency Clinical Hospital, Bucharest, Romania

Introduction: This prospective, randomized study evaluated the efficiency and safety of a new energy source enabling a continuous bipolar plasma vaporization of the prostate (C-BPVP) to be achieved by comparison to the standard vaporization (S-BPVP) and to conventional TURP in medium size BPH cases.

Methods: A total of 180 BPH patients with prostate volume between 30 and 80 mL, maximum flow rate (Q_{max}) below 10 mL/s and International Prostate Symptom Score (IPSS) over 19 were equally randomized for C-BPVP, S-BPVP and classical TURP. All cases were evaluated preoperatively and at 1, 3 and 6 months after surgery by IPSS, Q_{max}, quality of life score (QoL) and post-voiding residual urinary volume (PVR).

Results: The mean operation time was significantly shorter in C-BPVP cases by comparison to conventional plasma-button vaporization and to monopolar resection (31.5 versus 40.6 and 49.8 minutes). Consequently, a substantial 22.4% and respectively 39.1% difference in surgical length was emphasized in favor of C-BPVP when compared to S-BPVP and TURP. Significantly lower capsular perforation (1.7% and 1.7% versus 8.3%), and intraoperative bleeding (1.7% and 3.3% versus 11.7%) rates as well as mean hemoglobin drops (0.4 and 0.6 versus 1.4 g/dL) were emphasized in the C-BPVP and S-BPVP series when compared to TURP. Also, significantly reduced mean catheterization periods (24.1 and 23.8 versus 73.6 hours) and hospital stays (2.1 and 2.2 versus 4.5 days) were described for the C-BPVP and S-BPVP groups. The rate of re-catheterization imposed by acute urinary retention (1.7% and 1.7% versus 6.7%) was significantly higher among the monopolar resection cases. At 1, 3 and 6 months, statistically superior IPSS and Q_{max} measurements were determined in the two bipolar vaporization study arms.

Conclusion: The new technical improvement of the BPVP procedure was able to reduce the surgical time by an average proportion of 20%. The plasma-button vaporization approach emphasized superior perioperative safety and improved follow-up voiding and symptom scores' parameters over conventional TURP.

ABSTRACT 38

THE CHARACTERISTICS OF MICROCIRCULATION IN RENAL CELL CARINOMA BY CONTRAST-ENHANCED ULTRASOUND (CEUS)

Motohiro Maeda, Tokunori Yamamoto, Momokaza Gotoh

Department of Urology, Nagoya University Graduate School of Medicine, 65 Tsuruma-cho, Showa-ku, Nagoya 466-8550, Japan

Introduction: To clarify the characteristics of microcirculation in renal cell carcinoma by contrast-enhanced ultrasound (CEUS).

Methods: From May 2008 to October 2009, CEUS was performed prior to surgery in 30 patients with renal masses. 10 of the 30 patients had cystic renal masses. The final diagnoses of all patients were pathologically confirmed. Contrast enhancement, as a function of time, was measured in two regions of interest (ROI)—tumor or solid component of cystic lesions and normal parenchyma—and TICs were obtained. The time to the contrast enhancement peak (TTP) intensity change from the baseline to peak (ΔI), and ΔI / TTP of the tumor and the normal parenchyma were measured from the TIC. In addition, we performed renal tumor biopsy under CEUS to confirm the characteristics of the TIC.

Results: Pathological diagnoses were renal cell carcinoma in all 30 patients. The TTP of the cancer was shorter than that of the normal parenchyma in all cases (6.0 ± 2.0 s vs. 10.4 ± 3.0 s; $p < 0.0001$). The ΔI did not differ between the cancer and normal parenchyma (21.3 ±5.9 db vs. 20.9 ± 7.0 db; $p = 0.68$); the ΔI / TTP of the cancer was significantly higher than that of the normal parenchyma (3.9 ± 1.4 db/s vs. 2.2 ± 0.94 db/s; $p < 0.0001$). TIC patterns of solid cancer and cystic cancer were very similar. TIC of the normal tissue and the cancer in pathology confirmed by renal biopsy for the tumor under CEUS also demonstrated similar to the characteristics of the TIC, respectively.

Conclusion: An objective and quantitative diagnosis of renal cell carcinoma by CEUS using a second-generation ultrasound contrast agent can be made by employing a TIC. The TIC patterns of solid and cystic cancers were very similar, despite their morphological and vascular differences. CEUS using a TIC is a promising tool in the diagnosis of cystic renal cancer.

ABSTRACT 39

A PROSPECTIVE COMPARISON BETWEEN NBI AND STANDARD WHITE LIGHT CYSTOSCOPY IN CASES OF NON-MUSCLE INVASIVE BLADDER CANCER

Bogdan Geavlete, Marian Jecu, Florin Stanescu, Cristian Moldoveanu, Leon Adou, Petrisor Geavlete
Department of Urology, Saint John Emergency Clinical Hospital, Bucharest, Romania

Introduction: The trial aimed to assess the impact of narrow band imaging (NBI) cystoscopy in cases of non-muscle invasive bladder cancer (NMIBC). A single centre, prospective comparison to the standard white light cystoscopy (WLC) was performed.

Methods: A total of 95 NMIBC suspected consecutive cases were enrolled. The inclusion criteria were hematuria, positive urinary cytology, and/or ultrasound suspicion of bladder tumors. All patients underwent WLC and NBI cystoscopy. Standard resection was performed for all lesions visible in WL and NBI-TURBT for only NBI observed tumors.

Results: The overall NMIBC and CIS patients' detection rates were significantly improved for NBI (96.2% versus 87.2% and 100% versus 66.7%). Also, on a lesions' related basis, NBI cystoscopy emphasized a significantly superior detection concerning the CIS, pTa and overall tumors (95.2% versus 61.9%, 93.9% versus 85.2% and 94.8% versus 83.9%, respectively). Additional tumors were diagnosed by NBI in a significant proportion of CIS, pTa, pT1 and NMIBC patients (55.5% versus 11.1%, 26.5% versus 10.2%, 30% versus 10% and 30.8% versus 10.3%) Moreover, pathologically confirmed positive tumoral margins secondary to white light TURBT were found at the NBI control in 10.3% of the cases. The postoperative treatment was significantly improved due to NBI results (16.7% versus 5.1%).

Conclusion: NBI cystoscopy represents a valuable diagnostic alternative in NMIBC patients, with significant improvement of tumor visual accuracy as well as detection. This approach provided a substantial amelioration to the bladder cancer therapeutic management.

ABSTRACT 40 **TOP 10 ABSTRACT**

IN VITRO COMPARISON OF A NOVEL FACILITATED ULTRASOUND TECHNOLOGY VERSUS STANDARD TECHNIQUE APPROACH FOR PERCUTANEOUS RENAL BIOPSY

Ashleigh Menhadji[1], Vien Nguyen[1], Jane Cho[1], Ringo Chu[1], Kathy Osann[1], Philip Bucur[1], Puja Patel[1], Achim Lusch[1], Elspeth McDougall[2], Jaime Landman[1]

[1] *Department of Urology, University of California, Irvine,* [2] *University of British Columbia, Vancouver*

Introduction: Advances in the understanding of the biology and epidemiology of renal cortical neoplasms (RCN) have made pre-treatment biopsy increasingly appealing. We evaluated a facilitated ultrasound technology (FUT) in which the needle can be passed through the transducer probe. The FUT allows the needle to follow a virtual "dotted line" on the monitor to the target. We compared the FUT to standard percutaneous biopsy technique.

Methods: Forty-eight participants, including 10 undergraduates, 11 medical students, 12 residents, 6 fellows and 9 attendings, were recruited. Participants performed ultrasound-guided biopsies on phantom ultrasound models using both the FUT and the standard (needle deployed percutaneously next to probe) biopsy technique in a randomized sequence. Phantom models consisted of pimento olives embedded in an opaque mold of Metamucil and Knox gelatin. Subjects were given up to ten attempts to achieve 3 complete specimens (core sample including green-red-green) from the olives. Subjects rated each biopsy technique.

Results: The mean time to obtain 3 complete biopsy specimens was significantly faster for FUT compared to the standard technique (140 seconds vs. 246 seconds, p = 0.0001). The mean number of attempts needed to obtain 3 specimens was significantly less with the FUT compared to the standard technique (4.3 vs. 5.6 attempts), (p=0.0007). Subjects also reported the FUT was significantly easier to use compared to the standard technique (p=0.0005). No significant order effect (standard versus FUT first) was observed. Level of experience did not affect any of the metrics tested with either technique.

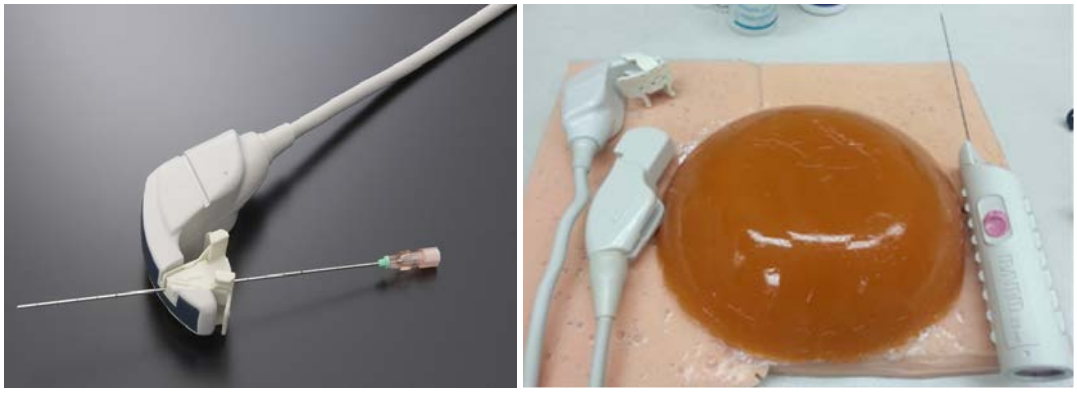

Figure: a) Close up of FUT probe with biopsy needle guide, courtesy of Hitachi Aloka©.
b) Total impact on the angle of ureteroscope deflection (A and B), and radii (B) varied among grasper devices.

Conclusion: The FUT increased the efficiency and efficacy of percutaneous biopsy for users of all experience levels. FUT may allow urologists with limited percutaneous renal biopsy experience to perform the procedure reliably and easily. Clinical evaluation of this technology is actively in progress.

ABSTRACT 41

COMPARISON OF RENAL PARENCHYMAL CLOSING PRESSURE DURING OPEN, LAPAROSCOPIC, AND ROBOTIC-ASSISTED RENAL RECONSTRUCTION

Ramtin Khanipour, Michael del Junco, Achim Lusch, Zhamshid Okhunov, Jaime Landman
Department of Urology, University of California, Irvine

Introduction: Contemporary options for extirpative renal surgery include open (OPEN), laparoscopic (LAP), and robotic-assisted (ROB) techniques. Renal reconstruction is a challenge, and patient outcomes are related to the quality of the parenchymal closure. In this *in vitro* study, we measured and compared renal parenchymal closing pressure with open, laparoscopic, and robotic-assisted technique.

Methods: Using an *ex vivo* porcine kidney model, we created a standardized 4cm simulated parenchymal partial nephrectomy defect in each kidney. Participants were stratified into three groups by level of training and expertise (medical students, residents and experts). Participants were instructed to close the defect by placing a surgical bolster and using a 2-0 vicryl suture with a Hem-o-lock® and Lapra-Ty® clips. Parenchymal closure was performed via open, laparoscopic and robotic-assisted techniques. During the reconstructive process a Force-transducer which converted mechanical force into an electrical signal was utilized to measure the amount of force applied with each technique. [Figure] Participants were asked to effectively close the renal defect over the bolster containing the force transducer. We recorded pulling force (PF) (force put on suture while closing the renal defect), closing force (CF) (force between edges of the renal defect after application of 2nd Hem-o-lock® and Lapra-Ty®) and on purpose performed tearing force (TF) (maximum pulling force applied on the needle end of the suture until the parenchymal tissue begins to tear) in Newtons. Each surgical technique was repeated in triplicate. Additionally we recorded the amount of time required to complete each task.

Results: A total of 23 participants were included in the study (8 medical students, 8 urology residents and 7 experts). There was no difference for PF between the various training levels or techniques (p=0.121, p=0.545 respectively). Regardless of training levels, CF and TF for ROB were significantly higher compared to LAP and open techniques (p=0.013, p=0.012 respectively). There was significant difference in time completing all tasks across all different techniques (p<0.001), OPEN vs. ROB vs. LAB (8.67 vs. 13.53 vs. 23.36 minutes respectively). Participants with greatest level of expertise demonstrated shorter times to complete shorter laparoscopic and robotic tasks.

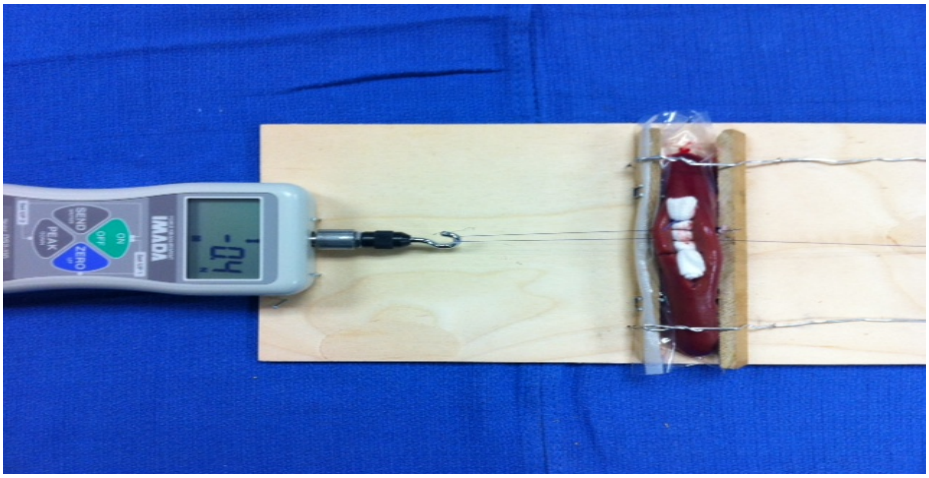

Conclusion: In this *in vitro* evaluation, all surgeons despite their level of expertise, place significantly higher closing force (CF) and tearing force (TF) during the robotic-assisted parenchymal reconstruction. The diminished haptic feedback and the higher tensile strength associated with robotic technology may lead to an increased parenchymal injury during renorrhaphy.

ABSTRACT 42

HISTOTRIPSY ACCURACY: CHARACTERIZATION WITH A NOVEL RED BLOOD CELL PHANTOM

Jon Cannata, PhD[1]. Jim Bertolina, PhD. [1], William W. Roberts, MD[2]
HistoSonics, Inc.[1] and University of Michigan Department of Urology[2]

Introduction: Histotripsy is a non-invasive, ablative, focused ultrasound technology that produces non-thermal tissue homogenization within a cigar-shaped acoustic focal volume. We sought to demonstrate the accuracy of histotripsy using a novel pelvic phantom with an insertable red blood cell prostate plug. The phantom is based on human CT data and contains a simulated bony pelvis in lithotomy position, a rectal channel for image probe insertion, and a prostate channel for prostate-plug insertion. The prostate plug consists of red blood cells suspended in an agarose hydrogel. Histotripsy ruptures red blood cells which in turn increases the optical transparency in the treated regions of the gel. Additionally, lesions in the phantom are visualized as hypoechoic regions on a B-Mode ultrasound image. Histotripsy was delivered from the VORTX R_X® prototype system which contains a 36-element piezoceramic composite array therapy transducer (700 kHz, 13-cm diameter circle shape, focal length 11cm, focal volume approximately 10 mm axial and 4 mm diameter) and a 7 MHz transrectal imaging probe. The imaging and therapy systems are mechanically linked such that the imaging plane tracks the treatment focus. A manual contouring tool is used to define the target volume prior to treatment and the target indicator (crosshair) is constrained by the target volume.

Methods: Histotripsy was performed on 6 phantom prostates. In the first four, the targeting cross-hairs (representing the center of the bubble cloud) were first positioned at the center point of the target volume and then driven repeatedly along a single line in the x and y axis through the center point producing a (+) pattern (16mm length, 16 mm width). In the remaining 2 phantom prostates, the cross-hairs were translated through a 16x16x11 mm volume. Following each treatment, an ultrasound volume was acquired and the extent of treatment within and beyond the target volume was recorded. The prostate plug was then removed and sectioned at 5 mm increments in the transverse plane (+ pattern) or longitudinal plane (box pattern) allowing visual assessment of treatment effect and measurement of the treated zone to validate the US measurements.

Results: In the four phantoms treated with the (+) pattern, the sum of treatment effect beyond both ends of the planned x-axis path of the cross-hairs was 2.5 mm and beyond the y-axis path was 1.75 mm. In the two phantoms where the entire box volume was treated, the sum of maximal extent of homogenization beyond the limit of the excursion of the cross-hairs was 1mm, 0 mm, and 9 mm along the x, y, and z-axes respectively.

Conclusions: The maximal "overshoot" of histotripsy treatment effect beyond the margin of the traced volume is consistent with the dimensions of the focal volume. When planning histotripsy treatment, homogenization can be expected to occur 5 mm beyond the center of the bubble cloud along the axial (z-axis) and 2 mm beyond the center of the bubble cloud along the x and y axes.

Funding: NIH R01DK087871. Disclosure: WWR has equity, royalty and consulting interests in HistoSonics, Inc.

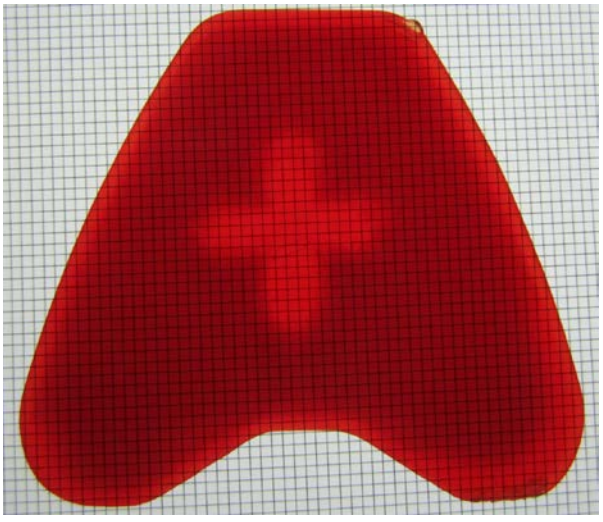

Figure: Transverse section of prostate plug from pelvic phantom after treatment with histotripsy. Grid line spacing is 1mm.

ABSTRACT 43

LASER POWER SETTINGS AND STONE CAPTURE IN A PERCUTANEOUS LITHOPAXY MODEL

Giovanni S. Marchini, Aayushi Rai, Shubha De, Carl Sarkissian, Manoj Monga
Glickman Urological and Kidney Institute, Cleveland Clinic Foundation, Cleveland, OH

Introduction: The purpose of our study was to test the efficiency of four different laser settings on stone fragmentation with and without stabilization of the stone with an entrapment device

Methods: Spherical stone phantoms were created using the BegoStone® plaster. Lithotripsy of one stone (1.0g) per test jar was performed with Ho:YAG laser (365µm fiber; 1 minute/trial). Four laser settings were tested: I - 0.8J, 8Hz; II - 0.2J, 50Hz; III - 0.5J, 50Hz; IV - 1.5J, 40Hz. Uro-Net (US Endoscopy, Mentor OH) deployment was used in 3 of 9 trials. Post-treatment, stone fragments were stained though a 1mm sieve; after a 7-day drying period fragments and unfragmented stone were weighed. Uro-Net nylon mesh and wire frame resistance were tested (laser fired for 30s). All nets used were evaluated for functionality and strength (compared to 10 new nets). Student's T Test/ANOVA were used to compare the studied parameters; significance was set at $p<0.05$.

Results: Laser settings I and II caused less damage to the net overall; the mesh and wire frame had worst injuries with setting IV; setting III had an intermediate outcome; 42% of nets were rendered unusable and excluded from strength analysis. There was no difference in mean strength between used functional nets and non-used devices (8.05 vs. 7.45lbs, respectively; $p=0.14$). Mean post-laser stone weight was significantly lower than baseline for all laser settings ($p<0.001$). Stone fragmentation with laser setting IV had the highest impact on stone weight loss (11.18%; $p<0.001$; Figure 1). Settings I and II had the smallest impact ($p<0.01$) and setting III performed better than the first two ($p<0.01$) but worse than the IV ($p<0.01$). Setting IV was the most efficient for lithotripsy (1.9 ± 0.6mg/s; $p<0.001$; Figure 2) with or without net stabilization; setting III was superior to I and II only if a net was not used.

Conclusion: Fragmentation efficiency increases with higher laser energy settings. Laser lithotripsy is not optimized by stone entrapment with a net retrieval device which may be damaged by high energy laser settings.

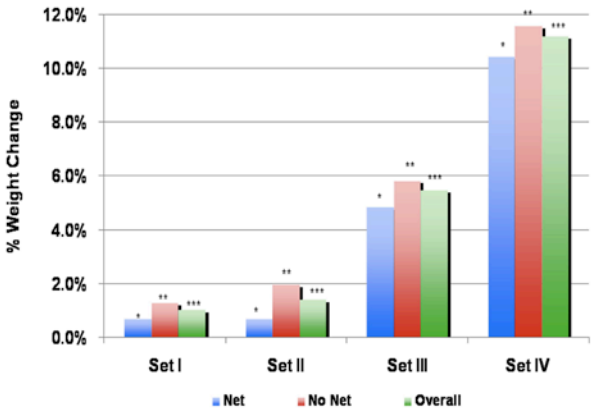

Figure 1 - Relative weight difference for each laser setting considering overall performance and separate trials with and without the stone entrapment device.

** **ANOVA**: p=0.001; **Tamhane's**: settings I and II < IV (p<0.01); setting III < IV (p<0.05)*
*** **ANOVA**: p<0.001; **Tamhane's**: settings I and I < III and IV (p<0.01); setting III < IV (p<0.01)*
**** **ANOVA**: p<0.001; **Tamhane's**: settings I and I < III and IV (p<0.01); setting III < IV (p<0.01)*

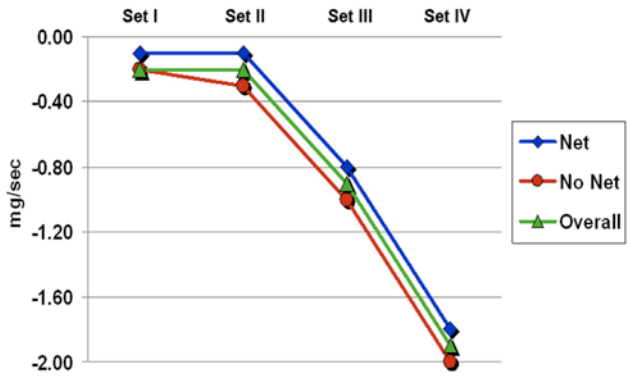

Figure 2 – Influence of laser settings and entrapment device on fragmentation efficiency characterized by absolute weight reduction per second of lithotripsy.

ABSTRACT 44

MAGNETIC RESONANCE IMAGING/ULTRASOUND (MR/US) FUSION-GUIDED PROSTATE BIOPSIES: AN INITIAL REPORT

Simpa S. Salami, Arvin K. George, Oksana Yaskiv, Baris Turkbey, Eran Ben-Levi, Robert Villani, Karin Beecher, Robert Moylan, Nancy M. Lee, Jason Naidich, Louis R. Kavoussi, David N Siegel, Ardeshir R. Rastinehad

Hofstra North Shore LIJ School of Medicine, New Hyde Park, NY, USA

Introduction: The Philips fusion biopsy system is currently being utilized at the National Institute of Health for targeted prostate biopsies (Pinto, J Urol. 2011). We report for the first time the cancer detection rates (CDR) for the MR/US fusion guided prostate biopsy platform (Philips) outside the NIH, a validation study.

Methods: Patients with previous diagnosis of prostate cancer (CaP) or found to have a suspicion of CaP on MRI were prospectively enrolled. The MRI included a T2, DWI, and DCE (3T with an endorectal coil) sequences and were reviewed by three radiologists (EB, RV, AR). All lesions identified were graded by number of sequences positive: low ($\leq$2), moderate/high suspicion (3). The MR/US fusion tracking system (Philips Healthcare, Canada®) was used to perform the fusion guided prostate biopsies. The 'protocol' biopsy included a standard 12-core biopsy and the MR/US fusion biopsy of the suspicious MR targeted lesions. Our institution's pathologist reviewed the biopsies.

Results: A total of 53 patients with mean age and PSA of 65.4 years and 7.1ng/mL respectively were enrolled. Overall CDR was 67.9 % (36/53). Nine (17%) patients were classified as low suspicion by MRI, of which 4 patients were found to have cancer and 2 of these patients had Gleason 6 CaP. Also, 44 (83 %) patients were classified as moderate/high suspicion by MRI, of which 32 (72.7 %) patients were found to have cancer (Table). Nine (9) cancers were missed by the MR/US fusion biopsy: 6 were Gleason 6 low volume ($\leq$ 40%) cancers; 1 was Gleason 7 low volume (5%) cancer; and the remaining 2 were missed targets due to user error.

Conclusion: The MR/US fusion biopsy platform can stratify patients in to risk groups. 72.7 % of patients with a moderate/high suspicion lesion(s) were found to have CaP on the 'protocol' biopsy. Though a small data set, the results supports the comparableness of MRI-directed biopsies to a traditional 12-core biopsy in detecting CaP. This may lead to image-guided approach to screening for prostate cancer in the future.

MRI Suspicion for Prostate Cancer	Gleason Grade	Protocol Biopsy CDR (%)	Fusion Biopsy CDR (%)	Standard 12-Core Biopsy CDR (%)
Low 9 Patients (17%)	**6**	2 (22.2)	0 (0)	2
	7	2 (22.2)	1 (11.1)	1 (11.1)
	8 – 10	1 (11.1)	1 (11.1)	1 (11.1)
Moderate/High 44 Patients (83%)	**6**	12 (27.3)	9 (20.5)	12 (27.3)
	7	15 (34.1)	12 (27.3)	13 (29.6)
	8 - 10	5 (11.4)	4 (9.1)	3 (6.8)
Total (53)		36 (67.9)	27 (50.9)	32 (61.2)

ABSTRACT 45

VALIDATION OF A SIMULATION TOOL TO SUPPORT ROBOTIC-ASSISTED SURGICAL TRAINING

Lee White[1], Jed White[1], Anna Skinner[2], Sabrina Whitehurst[3], Andrew Fielding[3], Ernest Lockrow[3], Thomas Lendvay[1], Jerome Buller[3]

[1] University of Washington, Seattle, WA, [2] Anthrotronix Inc., Silver Spring, MD

[3] Uniformed Services University of the Health Sciences, Washington D.C., DC

Introduction: We endeavor to compare training surgeons on the dV-Trainer with a standard da Vinci-based training using a curriculum of Fundamentals of Laparoscopic Surgery tasks. Performance on a cystotomy and sutured closure on a live pig was used to measure training effectiveness. Training surgeons to safely and effectively use the da Vinci surgical robot is time and resource-intensive. Training directly on a robot is the gold-standard but requires access to a robot. Offline training has to compete with the use of the robot in surgeries and training novice users during actual surgeries has ethical and patient-safety drawbacks. Training using a virtual reality simulator is one option. The dV-Trainer by Mimic Technologies, Seattle, WA, allows users to interact with a virtual surgical environment using controls that resemble the da Vinci master console.

Methods: 20 robotics-naïve subjects including residents, fellows and staff in surgical specialties were enrolled and put through a basic da Vinci on-line Intuitive Surgical didactic training module followed by a training on the use of the da Vinci standard surgical robot. Baseline Spatial Abilities Tests were performed. Subjects then trained on either the da Vinci or the dV-Trainer to proficiency. Finally, subjects performed the criterion task surgery. The da Vinci motion and video was recorded using SurgTrak™ and the subject's hand motions were tracked using Accelegloves by Anthrotronix. Performance was assessed using data from the various systems and using the validated Global Evaluative Assessment of Robotic Surgery (GEARS), structured assessment tool performed by an experienced surgeon. GEARS grading was executed by a group of experienced surgeons who performed a grading calibration session to establish agreement on the scoring criteria.

Results: Graders achieved excellent agreement demonstrated by Cronbach's Alpha = 0.910. No significant difference was found between groups for three acceleglove-based measures of hand motion analysis ($p>0.05$ for all comparisons). No significant performance difference was measured between the two training curricula as measured by task time [1467.2 sec. (da Vinci) vs. 1275.6 sec. (dV-Trainer), $p=0.420$] or mean GEARS score [14.15 (dV-Trainer) vs. 15.1 (da Vinci), $p = 0.559$]

Conclusion: Neither curriculum trained surgeons to perform surgery independently. We did not detect a difference between training curricula as measured by surgical performance, suggesting comparability. The ability of this study to detect such a difference was limited however by the wide variation in subject performance and the low number of subjects which was due to the difficulty and cost of using animal surgeries to measure surgical performance.

Source of Funding: This prospective randomized study was funded by the AMEDD Advanced Medical Technology Initiative (AAMTI) from the Department of Defense.

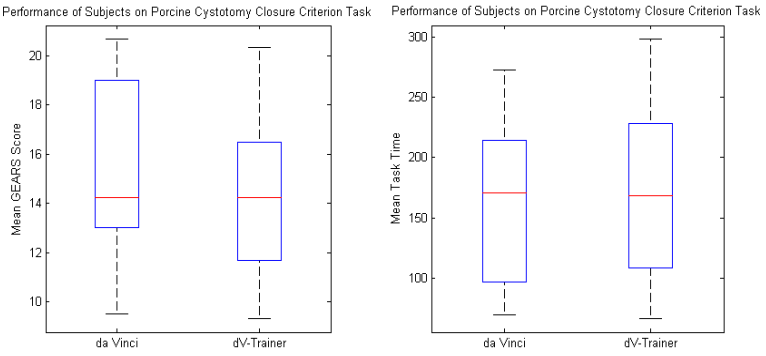

Figure: Performance of the two groups on a cystotomy closure task did not differ as measured by GEARS score nor task time.

ABSTRACT 46

COMPARISON OF OPTICS AND PERFORMANCE OF DISTAL SENSOR HIGH DEFINITION, DISTAL SENSOR STANDARD DEFINITION, AND FIBEROPTIC CYSTOSCOPIES

A. Lusch, P. Greene, C. Abdelshehid, A. Menhadji, P. Bucur, Z. Okhunov, J. Landman
University of California, Irvine, Department of Urology, Orange, California, USA

Introduction: We evaluated and compared characteristics of a new generation high definition distal sensor flexible cystoscope (HD-DS), a standard definition distal sensor cystoscope (SD-DS) and a standard fiber optic cystoscope (FO).

Methods: Three new cystoscopes (HD-DS, SD-DS and FO) were compared for active deflection, irrigation flow and optical characteristics. Each cystoscope was evaluated with an empty working channel and with various accessories. Optical characteristics (resolution, grayscale imaging, color representation, depth of field and image brightness) were measured using USAF/Edmund optics test targets and illumination meter. We digitally recorded a porcine cystoscopy in both clear and blood fields, with subsequent video analysis by 8 expert urologists via questionnaire.

Results: The HD-DS had a higher resolution than the SD-DS and the FO at both 20mm (6.35 vs. 4.00 vs. 2.24 lines/mm) and 10mm (14.3 vs. 7.13 vs. 4.00) evaluations, respectively ($p<0.00005$, $p<0.00005$). Color representation, depth of field ($p=0.00001$, $p<0.00005$) was better in the HD-DS. [Table 1] When compared to the FO, the HD-DS and SD-DS demonstrated superior deflection up and irrigant flow with and without accessory present in the working channel, whereas image brightness was superior in the FO ($p<0.00005$, $p=0.00003$, $p<0.00005$). Observers deemed the HD-DS cystoscope superior in visualization in clear and bloody fields, for illumination, resolution, as well as for the overall performance.

Conclusion: The new HD-DS provided significantly improved visualization in a clear and a bloody field, resolution, color representation and depth of field compared to SD-DS and FO. Clinical correlation of these findings is pending.

				Tukey-Multiple comparisons			
	FO	SD	HD	F-test	Pair-wise tests		
				p-value	FO vs SD	FO vs HD	SD vs HD
Resolution (lines/mm) at							
10 mm	2,24	4,00	6,35	<0.00005	0,00002	0,00002	0,00002
20 mm	4,00	7,13	14,30	<0.00005	0,00002	0,00002	0,00002
Depth of field							
5LP	9,00	14,67	14,67	<0.00005	0,00002	0,00002	0,00002
15LP	1,00	4,33	4,33	0,00001	0,00003	0,0001	0,01106
Illumination (LUX) at							
10mm	102367,00	54600,00	68633,33	<0.00005	0,00002	0,00002	0,00002
20mm	44666,67	23966,67	35366,67	<0.00005	0,00002	0,00002	0,00002
50mm	11393,33	6843,33	9496,67	<0.00005	0,00002	0,00002	0,00002
100mm	3750,00	2170,00	3046,67	<0.00005	0,00002	0,00002	0,00002

Table: Results optics

ABSTRACT 47

LAPAROSCOPIC VERSUS PERCUTANEOUS CRYOABLATION FOR THE SMALL RENAL MASS: LONG-TERM ONCOLOGIC AND FUNCTIONAL OUTCOMES

Dinesh Samarasekera, Ali Khalifeh, Riccardo Autorino, Jihad H. Kaouk
Glickman Urologic and Kidney Institute, Cleveland Clinic, Cleveland OH

Introduction: We previously described a comparative analysis of over 300 patients undergoing either laparoscopic (LRC) or percutaneous renal cryoablation (PRC) for an enhancing renal mass. Both LRC and PRC were found to have good short-term oncologic efficacy and preservation of renal function. However PRC was found to have a higher incomplete treatment rate (7.6% vs. 1.6%, p=0.0055) compared to LRC. We present our updated analysis with longer follow-up.

Methods: We retrospectively identified 419 patients in our thermal ablation database who underwent either LRC (n=267) or PRC (n= 152) for an enhancing renal mass between 1997 and 2012. Demographics, clinical characteristics, functional, and oncologic outcomes were analyzed. Renal functional outcomes were measured by absolute serum creatinine and estimated glomerular filtration rate (eGFR).

Results: There was no difference in patient demographics, clinical parameters, and tumor characteristics at baseline ($p > 0.05$). Mean tumor size was 2.5 ± 0.99 cm for the LRC group and 2.41 ± 0.92 cm for the PRC group ($p= 0.15$). Patients who underwent PRC were more likely to have a solitary kidney (48/152 vs. 49/267, $p = 0.002$). Mean follow-up was 51.1 ± 42.4 months for LRC versus 28.3 ± 20.0 months for PRC ($p < 0.001$). Mean eGFR at latest follow-up was 55.8 ± 28.5 versus 57.7 ± 24.7 mL/min/1.73 m^2 ($p=0.49$) for LRC and PRC respectively. The rate of incomplete treatment was 10.5% (28/267) for LRC and 15.8% (24/152) for PRC ($p=0.099$). Five-year Kaplan-Meier survival estimates were calculated and are included in Table 1.

Conclusions: LRC and PRC deliver equivalent oncologic and functional outcomes, but PRC had a higher rate of incomplete treatment (not statistically significant). However both methods are associated with acceptable efficacy and can be utilized as an alternative first-line treatment for select patients who are deemed unsuitable for surgery.

	LRC (%)	PRC (%)	Log rank
5-year Overall Survival	70.81	69.4	0.56
5-year Cancer Specific Survival	95.6	99.2	0.20
5-year Local Recurrence-free Survival	78.7	86.9	0.56
5-year Metastasis-free Survival	90.9	83.0	0.41

Table 1. Kaplan-Meier survival estimates.

ABSTRACT 48

MICROWAVE ABLATIONS AT 915 MHz IN *EX VIVO* AND *IN VIVO* PORCINE KIDNEYS

Karli Pease[1,2], Gideon Lorber[1], Raymond J. Leveillee[1,2], Nelson Salas[1,2]

[1] *Joint Bioengineering and Endourology Developmental Surgical Laboratory, Division of Endourology, Laparoscopy, and Minimally-Invasive Surgery, Department of Urology, University of Miami Miller School of Medicine, Miami, FL, USA*

[2] *Department of Biomedical Engineering, University of Miami, Coral Gables, FL, USA*

Introduction: Microwave (MW) ablation can produce faster heating over larger volumes of tissue with less susceptibility to heat sink compared to radiofrequency ablation. Permittivity, which is dependent on frequency, differs between the antenna and surrounding tissue, resulting in reflectivity loss. A 915 MHz microwave ablation system that offers frequency variability between 902-928 MHz to minimize reflectivity loss and enhance energy output without antenna tip cooling is currently available. The use of ex-vivo models is helpful in the preliminary assessment of the ablation geometry, but *in vivo* studies are needed to determine the effects of blood flow on the final ablation size and treatment time. The objective of this experiment was to determine the temperatures and resulting ablation sizes in ex-vivo and in-vivo porcine kidneys when using the MedWaves AveCure 915 MHz MW system.

Methods: Four ablations (two per kidney) were performed in either *ex vivo* or non-survival, *in vivo* porcine kidneys using the Medwaves AveCure 915 MHz System (San Diego, CA) in power mode at 24W with a single 16 gauge microwave needle. Each ablation was performed at a set temperature of either 96 or 106 ^{o}C and irradiation time of 3 or 5 minutes. The needle was inserted 4.0 cm into the kidney at either the upper or lower pole, parallel to the Brodel's line, and between the cortex surface and the collecting system boundary. Temperatures during and five minutes after treatment were measured with eight fiber optic thermal sensors placed 5 and 15 mm from the antenna axis. Gross lesion volumes, maximum temperatures, and total treatment times (irradiation time plus time between pulses) for each ablation were recorded and compared.

Results: Coagulation zones were ellipsoidal with the major axis in the direction of the needle shaft. Lesion volumes were generally smaller *in vivo* than *ex vivo* under similar parameters, with exception of those at 96^{o}C for 3 minutes, due to longer treatment time. Coagulation volumes increased with increasing time and temperature, except for those in-vivo at 96^{o} C between 3 and 5 minutes due to the number of power stoppages during the 5 minute treatment. A large cyst may have affected the lesion size and temperature during the *in vivo* trial at 106^{o} C and 3 minutes. Reverse powers over 12W and subsequent system disruptions were experienced as early as 2 minutes and 37 seconds (96^{o} C, 5 min, *in vivo*) into the irradiation cycle in all 5 minute trials and resulted in the inability to complete the irradiation, as noted by the maximum temperature variability (Table 1). *Ex vivo* cases required longer total treatment time than *in vivo*.

Table 1: In-vivo ablation data

Trial	Volume (cm^3)	Max Temp (^{o}C)	Time to complete ablation (min:s)
1	1.711	72.49	4:05
2	1.083	84.75	6:15
3	2.100	101.86	5:06
4	3.318	96.06	8:05

Table 2: Ex-vivo ablation data

Trial	Volume (cm^3)	Max Temp (^{o}C)	Time to complete ablation (min:s)
1	0.771	96.65	11:05
2	1.735	85.05	12:03
3	3.562	93.62	7:53
4	6.165	88.02	8:20

(Trial legend: 1: 96^{o}C, 3 min; 2: 96^{o}C, 5 min; 3: 106^{o}C, 3 min; 4: 106^{o}C, 3 min)

Conclusion: A 915 MHz MW system with temperature feedback near the probe tip and variable frequency and power output is capable of inducing lesions of various sizes in renal tissue without the need for cooling. Reverse power may still be an issue, though, which is dependent on the location of the probe in the kidney. Further studies must be performed to determine the effect of blood flow, as well as the effect of varying treatment parameters on ablation volumes in renal tissue when using the AveCure 915 MHz system.

ABSTRACT 49

ZERO ISCHEMIA ROBOTIC PARTIAL NEPHRECTOMY: SEQUENTIAL PRE-PLACED SUTURE RENORRHAPHY TECHNIQUE

Emad R. Rizkala, Ali Khalifeh, Riccardo Autorino, Dinesh Samarasekera, Humberto Laydner, Jihad K. Kaouk

Center for Laparoscopic and Robotic Surgery, Glickman Urological and Kidney Institute, Cleveland Clinic, Cleveland, Ohio

Introduction: To describe a robotic partial nephrectomy technique that eliminates renal global ischemia, while decreasing parenchymal bleeding.
Methods: Prior to tumor resection, a suture is placed through the parenchyma, adjacent to the tumor and deep to the planned edge of resection. The tumor resection is performed using robotic scissors and begun between the tumor edge and the pre-placed suture and continued along the excision margin until some bleeding is encountered. A second suture is placed into the already excised parenchyma. This is repeated until the mass is completely excised, while suturing the parenchyma simultaneously.
Results: Fourteen patients underwent this technique between April 2008 and January 2013 by a single surgeon. Median age was 66 years and 64.3% (N=9) were male. Median BMI was 27.5 Kg/m2. Median R.E.N.A.L nephrometry score was 6.5. Median tumor size excised off clamp was 2.2 cm. Three patients had multiple tumors. Median estimated blood loss (EBL) was 192.5 mL. Median operative time was 160 minutes. There were no Clavien grade 3 or 4 complications. One patient had a post-operative ileus and one patient had a blood transfusion and deep vein thrombosis. One patient had a positive tumor parenchymal margin, but negative excisional bed margin. Median hospital stay was three days and median follow-up of 8.4 months.

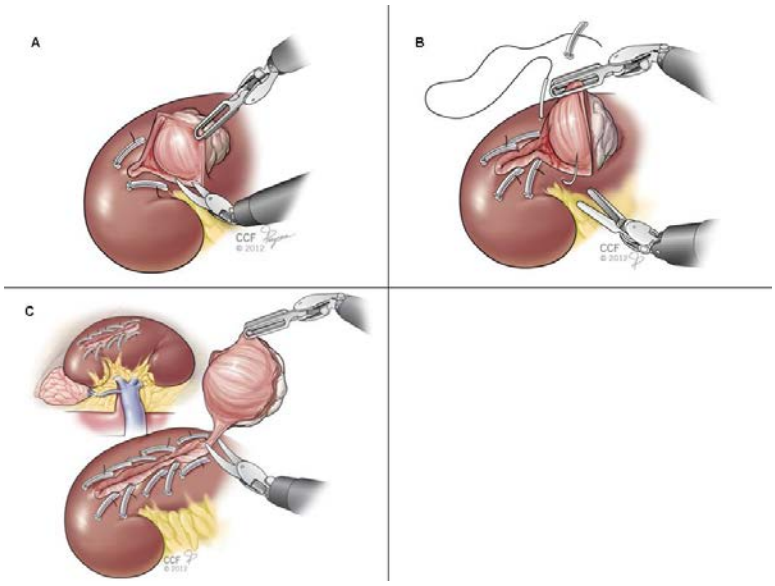

Figure: (A) 2-0 Vicryl suture with a knot and Hem-o-lok clip fixed to the free end is placed through the parenchyma, deep to the planned edge of resection and brought through the other side of the parenchyma, (B) Sequential 2-0 Vicryl stitches are placed adjacent to the tumor margin when parenchymal bleeding is encountered. This step is repeated as the tumor is gradually resected, (C) Completed excised tumor with tightened sequentially placed sutures fastened by Hem-o-lok clips to

Conclusions: Sequential pre-placed suture renorrhaphy technique is a safe and effective technique that is useful in renal function preservation by limiting or eliminating WIT, while aiding in maximizing nephron preservation, especially in those patients with solitary kidneys and multiple tumors.

ABSTRACT 50

DEVELOPMENT OF DEDICATED STONE DETECTION PROTOCOLS USING A RESEARCH-BASED ULTRASOUND IMAGER

Ryan S. Hsi[1], Bryan W. Cunitz[2], Barbrina Dunmire[2], Marla Paun[2], Jonathan D. Harper[1], Michael R. Bailey[2], Mathew D. Sorensen[1]

[1] *Department of Urology, University of Washington School of Medicine*

[2] *Center for Industrial and Medical Ultrasound, Applied Physics Laboratory, University of Washington*

Introduction: CT remains the gold standard for the detection of kidney stones but there are concerns regarding radiation risk. Ultrasound does not generate ionizing radiation, but is less sensitive and specific than CT. False positives may lead to unnecessary treatment. Existing ultrasound systems are optimized for characterizing soft tissue inhomogeneities and blood flow, but not hard structures such as stones. No dedicated stone detection algorithms are commercially available. Using a research ultrasound engine, unique signal processing algorithms can be implemented to generate alternative displays of the ultrasound image. The goal of this study was to evaluate the performance characteristics of a research-based ultrasound imager and to develop algorithms to improve kidney stone detection.

Methods: Patients referred for the evaluation of kidney stones with a recent CT (within 60 days) were recruited to undergo a renal ultrasound study with the Verasonics ultrasound imager. The Verasonics device has a research-based platform and allows the raw ultrasound signal to be captured, processed, and optimized. Blinded reviewers of the CT and ultrasound images separately recorded the location of each stone within the upper, middle, lower poles, and the renal pelvis/UPJ. Performance characteristics were calculated based on whether a stone or stones were seen (yes/no) in each of the four regions. The raw data from selected true positive and false positive stones were analyzed and processed using new algorithms. The first new algorithm rescaled B mode data and added green color to the image on bright echoes apparent on stones (Figure 1). The second algorithm used Doppler mode and processing similar to that which produces twinkling artifact (Figure 1).

Results: In 9 patients with 17 renal units, there were 27 stones with mean size 4.4 ±3.3 mm. Compared to CT, the research ultrasound imager had a sensitivity of 80%, specificity 90%, PPV 76%, and NPV 92% with B mode alone. With the first algorithm, false positive stones showed fewer color pixels than with true stones. With the second algorithm, little or no color appeared on the stone image on false positives, but was present on true stones. Thus, the second algorithm may help avoid identifying false positive stones.

Conclusion: The performance characteristics of the Verasonics research ultrasound imager compares favorably to commercially available ultrasound machines. The raw signal data captured by the ultrasound machine can be used to develop algorithms dedicated to stone detection. Efforts are underway to validate these protocols clinically to determine if they improve the accuracy of stone detection.

Funding: Work supported by NIH DK43881, DK092197 and NSBRI through NASA NCC 9-58.

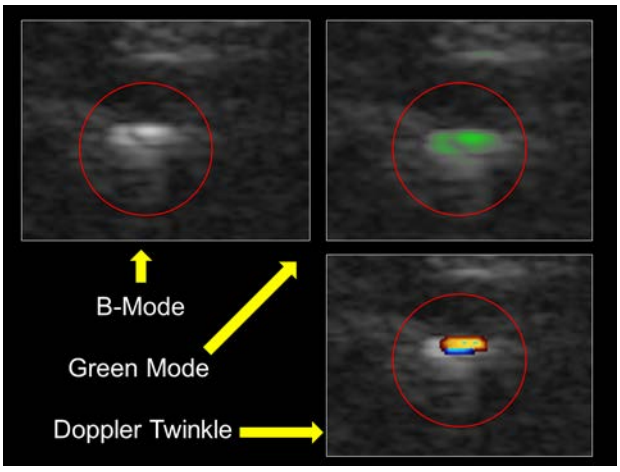

Figure: B-Mode and two experimental algorithms of the same stone

ABSTRACT 51

DYNAMIC CONTRAST-ENHANCED AND DIFFUSION-WEIGHTED MRI CORRELATE WITH HIGHER GRADE PROSTATE CANCER WITH EXTRACAPSULAR EXTENSION

Tay K.J. [1], Yuen J.S. [1], Thng C.H. [2], Jara-Lazaro A.R. [3], Ho H[1], Law Y.M. [4], Tan P.H. [3], Cheng C.W.[1]
[1]Department of Urology, Singapore General Hospital, [2] Department of Diagnostic Radiology, National Cancer Centre Singapore, [3] Department of Pathology, Singapore General Hospital, [4] Department of Diagnostic Radiology, Singapore General Hospital

Introduction: Early aggressive prostate cancers may be under-classified as low-risk at diagnosis due to under-sampling. A strategy to identify early aggressive cancers would better stratify patients to appropriate treatment. We aim to correlate dynamic contrast-enhanced (DCE) and diffusion-weighted (DWI) MRI findings with whole mounted radical prostatectomy specimens for prostate cancer detection.

Methods: All patients undergoing radical prostatectomy for prostate cancer were recruited. MRI scans using T2-weighted, DCE and DWI sequences specially angled in a plane perpendicular to the urethra were performed pre-operatively. Radical prostatectomy specimens were sliced whole mount at a plane perpendicular to the urethra with a thickness corresponding to the interval of the MRI slices. Areas suspicious of tumor on MRI were recorded by a radiologist blinded to histological diagnosis. Correlation was performed jointly by the radiologist, pathologist and urologist referring to the whole mount prostatectomy specimen.

Results: Seven patients undergoing radical prostatectomy were recruited. Median PSA was 7.2 (4.8–14) ng/dl. Prostatectomy Gleason score was 3+4 in 3 patients and 3+3 in the other 4. Two of the Gleason 3+4 nodules exhibited microscopic extracapsular extension and positive correlation was found between the whole mounted specimen and DCE and DWI MRI in these 2 nodules. The other 5 glands with organ-confined disease demonstrated no lesions on DWI and high flow areas on DCE corresponding only to stromal hyperplasia.

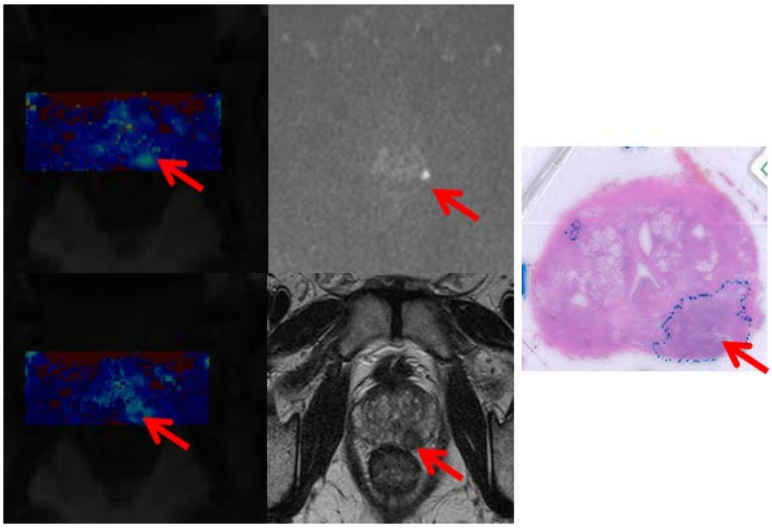

Figure: High flow areas and restricted diffusion at left PZ correlate with tumour area (Gleason 4+3 with microscopic extracapsular extension). MRI images (Clockwise from top left): DCE (F sequence) showing high flow (light blue) at left PZ, DWI sequence showing restricted diffusion at left PZ, DCE (V1 sequence) showing high flow (light blue) at left PZ), T2w sequence showing tumour nodule at left PZ. Prostatectomy whole mount slide: Areas of tumour at left PZ outlined in blue.

Conclusion: This pilot study suggests that combined positive findings of DCE/ DWI MRI may be correlated with biologically aggressive prostate cancers. DCE/DWI MRI may play a role in identifying lesions for targeted biopsy.

ABSTRACT 52

COMPARISON OF CURRENT URINARY DIAGNOSTIC TECHNIQUES FOR BIOPSY PROVEN TRANSITIONAL CELL EPITHELIAL CANCER AGAINST A MULTI-GENE URINARY DETECTION TEST

Joseph V. DiTrolio, M.D.[1], Maggie Cocca[1], Michael LaSalle, M.D.[2]
[1]*UMDNJ/New Jersey Medical School, Department of Urology, Newark, New Jersey USA*
[2]*St. Barnabas Medical Center, Department of Urology, Livingston, New Jersey USA*

Introduction: Modern Urology is dependent on non-invasive laboratory studies to assist in the diagnosing and monitoring of transitional cell epithelial cancers. A multitude of studies are currently available, most have a subjective component, none of which have become the gold standard. This study compares *Cxbladder*, a multi-gene urinary test to urinalysis, NMP22, cytology and standard DNA studies for accuracy in monitoring these patients, along with a comparison to tissue pathology from biopsy specimen.

Methods: A total of twenty-five patients were in this study, with pathology-proven transitional cell carcinoma, and were evaluated over an eighteen month period with multiple urinary screening tests. *Cxbladder* and the other noninvasive diagnostic tests were compared to tissue pathology. Specimens were collected prior to tissue biopsy when appropriate. *Cxbladder* uses MRNA to reconstruct cell DNA and evaluates for five (5) different gene expressions quantitatively which represent a pattern found in urological epithelial cancers.

Results: None of the urinary detection tests consistently predicted transitional cell epithelial cancer in the twenty-five cases with biopsy-proven cancer with 100% accuracy. Urine cytology with DNA and FISH when available, had the lowest accuracy <20%. Cxbladder, a multi-gene urinary test by Pacific Edge Diagnostics (New Zealand) had the highest accuracy in predicting cancer or recurrences >50%, followed by a standard urinalysis and NMP22. Aggressiveness of the epithelial tumor pathology only minimally affected the efficacy of the non-invasive urinary diagnostics.
Biopsy-proven epithelial cancer detection was only slightly better than 50%. Patients presenting with microscopic hematuria post-treatment for bladder tumor could not consistently separate tumor recurrence from the healing process, as accuracy was below acceptable levels.

Conclusion: Non-invasive urinary detection testing is an evolving and improving science; however, most have a subjective component and are only slightly better than a standard urinalysis. The Art of Medicine requires not only a collection of data in monitoring these patients, but the ability to integrate diagnostic, pathological, radiological and clinical findings to make an accurate

ABSTRACT 53

TRANSRECTAL HIGH INTENSIVE FOCUSED ULTRASOUND THERAPY BY ABLATHERM® IN LOCALIZED PROSTATE CANCER—EXPERICNES OF 15 YEARS

Thüroff, Stefan[1,2], Tilki, Derya[1,4], Chaussy, Christian [1,3]

[1] Harlachinger Krebshilfe e.V., Muenchen, Germany; [2] Dept. of Urology, Klinikum Muenchen-Harlaching

[3] Dept. of Urology, University of Regensburg ; [4] Dept. of Urology, Ludwig-Maximilians-University, Muenchen

Introduction: To present long-term cancer control and morbidity of high intensity focused ultrasound (HIFU) after neoadjuvant transurethral resection of the prostate (TURP). Evaluation of risk of metastatic induction by TURP and explanation of evolution of HIFU application and technology since 1996.*

Methods: Prospective Harlaching HIFU database—since 1996—was searched for patients with primary localized PCa (T1-2, N0, M0, PSAi <50 ng/ml) and follow-up > 15 months; Patients with previous long-term ADT, locally advanced PCa, or other PSA-influencing therapy were excluded. All patients were treated completely by Ablatherm® HIFU device. Evaluation was performed in aggregate and by stratification according to chronological cohorts and risk group (D'Amico criteria), PSA Nadir, and Gleason score. Phoenix definition was used for biochemical failure. Statistical analysis was performed using the Kaplan-Meier method, univariate and multivariate analysis employing a Cox model.

Results: Of 704 study patients, 78.5% had intermediate- or high-risk disease. Mean follow-up was 5.3 (1.3–14) years. Cancer-specific survival was 99%, metastasis-free survival 95%, and 10-year salvage treatment-free rates were 98% in low-risk, 72% in intermediate-risk, and 68% in high-risk patients. PSA Nadir and Gleason score predicted biochemical failure, side effects showed to be moderate. Included HIFU retreatment rate was 15% since 2005.

Conclusion: Long-term follow-up with HIFU therapy showed a high overall rate of cancer-specific survival and an exceptionally high rate of freedom from salvage therapy requirement in low-risk patients. The presented data of 10-year outcomes may warrant the possible closing of the investigational phase of HIFU.

* Thüroff, S., Chaussy, C., Evolution and outcomes of 3 MHz High intensity focused ultrasound therapy for localized prostate cancer over 15 years, The Journal of Urology (2013), doi: 10.1016/j.juro.2013.02.010.

ABSTRACT 54

PROSPECTIVE CONTROL TRIAL: FLEXIBLE FIBER-OPTIC CO2 LASER VS. MONOPOLAR CAUTERY FOR ROBOTIC MICROSURGICAL DENERVATION OF THE SPERMARIC CORD

Jamin Brahmbhatt, Ahmet Gudeloglu, Sijo Parekattil
Winter Haven Hospital & University of Florida

Introduction: Microsurgical targeted denervation of the spermatic cord is a treatment option for patients who have chronic testicular or groin pain. This procedure requires precise tissue dissection to ensure ablation of small diameter nerve fibers (thought to be causing pain) while preserving spermatic cord vessels and the vas deferens. CO_2 laser ablation offers a predictable and precise tissue interaction due to its high absorbance in water. Prior studies have shown a lower risk of peripheral tissue injury compared to monopolar or bipolar cautery. This study assesses the use of the flexible fiber-optic CO_2 laser in targeted robotic microsurgical denervation of the spermatic cord (RMDSC).

Methods: A cadaver model was utilized to develop a four-arm RMDSC technique using the da Vinci robotic platform (Intuitive Surgical, Sunnyvale, CA) and flexible fiber-optic CO_2 laser system (OmniGuide, Cambridge, MA). RMDSC with the CO_2 laser was performed on one spermatic cord side and standard monopolar electrocautery was used for the RMDSC on the contralateral side (control). 9 cross sections of the spermatic cord from each side were evaluated by a pathologist (blinded to the technique and procedure performed). The cord was assessed for any internal vascular or vassal injury and also assessed for peripheral thermal/cautery artifact. Student T test was conducted for analysis of the thermal injury.

Results: On microscopic pathology evaluation (basic H&E staining), the mean peripheral thermal damage in the spermatic cord was 0.17mm (0.15mm-0.25mm) on the side performed with CO2 laser ablation and was significantly less compared to the contralateral monopolar cautery side at 0.72mm (0.60mm-0.75mm) (p<0.001). There was no vascular or vassal trauma evident in either technique. The black diamond micro-forceps were able to handle the flexible fiber optic laser probe without any difficulty. The use of the CO2 laser appeared to provide easier tissue plane dissection compared to monopolar cautery.

Conclusion: The flexible fiber optic CO2 laser is a promising alternative to standard monopolar electrocautery for RMDSC. Advantages appear to be decreased peripheral tissue damage and dissection ease. Future studies are needed to assess its clinical potential in microsurgery.

Figure 1: Robotic handling of the flexible CO2 laser fiber and pathologic identification of decreased thermal injury compared to standard monopolar electrocautery.

ABSTRACT 55 **TOP 10 ABSTRACT**

FINE TILT TUNING OF A LAPAROSCOPIC CAMERA BY LOCAL MAGNETIC ACTUATION: TWO-PART LAPAROSCOPIC NEPHRECTOMY EXPERIENCE ON HUMAN CADAVERS

Ryan Pickens, M.D.[4,5] Massimiliano Simi [1,2,4], Arianna Menciassi, Ph.D.[1],
S. Duke Herrell, M.D [3,4,5], Pietro Valdastri, Ph.D.[2,4]

[1]The BioRobotics Institute of Scuola Superiore Sant'Anna;[2]STORM Lab, Department of Mechanical Engineering, Vanderbilt University [3]Department of Biomedical Engineering, Vanderbilt University [4]Vanderbilt initiative in Surgical Engineering (ViSE);[5]Vanderbilt University Medical Center, Department of Urologic Surgery

Introduction: Magnetic coupling is one of the few physical phenomena capable of transmitting forces across a physical barrier. This ability enables an entirely new paradigm for surgical instruments: they can be mobile and a separate incision is no longer needed for each surgical tool or camera. Magnetic Anchoring and Guidance Systems (MAGS), introduced in 2007 by UT Southwestern Medical Center, harness magnetic forces to steer and operate completely insertable intracorporeal tools via externally handheld magnets. An issue with this system is the fact constant external pressure to the abdominal wall has to be applied to achieve any upward/ downward tilt motioning. To overcome this problem, the concept of Local Magnetic Actuation (LMA) can be applied. LMA, achieved by a mix of anchoring and local actuation couples of permanent magnets linked across the abdominal wall, consists in changing the orientation and/or the position of one magnet of the actuation pair, causing magnetically coupled surgical camera to locally move on the inside. Building on the LMA concept, we developed a softly-tethered miniature magnetic camera that does not require manual motion of the external handle to achieve tilting of view in the vertical plane.

Materials and Methods: The LMA camera used in this study consists of two main parts, head (local actuation module) and tail (anchoring module) - linked by a flexible joint - resulting in a 95 mm long and 12.7 mm wide cylindrical device, with a weight of 20 g. The tail module embeds two magnets for anchoring, stabilization and manual rough positioning. The head module incorporates a couple of donut-shaped magnets (diametrical magnetization) that can be rotated by an internal miniature motor to achieve local actuation when coupled with an external static magnetic field. The operations were carried out in the Vanderbilt Cadaver Laboratory in accordance with all ethical considerations and regulations related to cadaveric experiments. Four different fresh tissue cadavers (3 males and 1 female) were used for this study.

Results: We first placed two laparoscopic ports in the abdomen and achieved a pneumoperitoneum. We then placed the LMA camera into the abdomen and measured its total range of motion that averaged 80 degrees. A trained laparoscopic surgeon then performed a standard laparoscopic nephrectomy using the LMA camera. All five cases were successful.

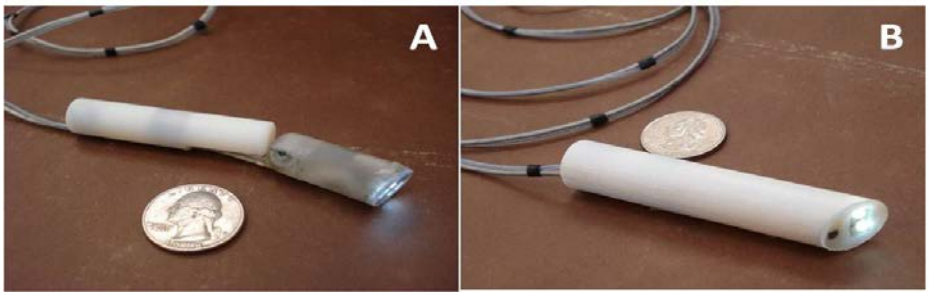

Fig.1 The two fabricated prototypes: the LMA camera (A) and the MAGS camera (B)

Conclusion: Cadaver trials described in this work let us conclude that LMA is an effective strategy to provide magnetic cameras with wide and high-resolution vertical motion.

ABSTRACT 56

SUCCESS OF PERCUTANEOUS ABLATION FOR RCC IS DEPENDENT UPON TUMOR SIZE: A MULTI-INSTITUTIONAL STUDY

Sara L. Best,[1] E. Jason Abel,[1] Ali Khalifeh,[2] Meghan Lubner,[1] Sutchin Patel,[1] Stephen Y. Nakada,[1] Jihad H Kaouk[2]

[1] *University of Wisconsin School of Medicine and Public Health, Madison, WI*

[2] *Glickman Urological and Kidney Institute, Cleveland Clinic, Cleveland, OH*

Introduction: Tumor diameter is a predictor of outcomes in renal cell carcinoma (RCC) after surgery but few studies have evaluated the impact of tumor size after percutaneous ablation. Success in prior ablation studies has been difficult to interpret since not all cases were biopsy-proven RCC. As such, the objective of this study was to evaluate the impact of tumor diameter on disease free survival in biopsy proven RCC patients treated with percutaneous ablation.

Methods: With IRB approval, institutional databases identified all patients with organ-confined, biopsy proven RCC treated with primary percutaneous ablation from 2 institutions and comprehensive clinical and pathologic data was reviewed for each patient. Ablation failures were categorized as incomplete ablation (persistent enhancement on the initial post-ablation imaging study), local recurrence (new enhancement on a follow up imaging study or biopsy-proven viable tumor), or metastatic..

Results: From 2003-11, 90 RCC patients were treated with percutaneous cryo-, radiofrequency, or microwave ablation and met inclusion criteria. Core biopsy revealed 66 clear cell, 18 papillary, 1 chromophobe and 5 unspecified renal carcinomas. 62 were low grade (Fuhrman 1 or 2 or "low") and 9 were high grade (Fuhrman 3 or 4 or "high"). The mean patient age was 64 years (range 41-87) and mean tumor size was 2.6cm (range 1.0-5.8cm). Following initial ablation, 81% of patients remained cancer-free with mean follow up of 31 mo ± 21.9. Disease free survival improved to 90% after repeat ablation was performed in 9 patients. Of the 17 failures, 5 were incomplete ablations, 9 were local recurrences and 3 patients developed metastatic disease. In 2 of 3 patients who developed metastases, there was a prior history of RCC that was not treated with ablation. Patients with tumors <3cm were more likely to remain disease-free after one or two ablation sessions (91 and 95% versus 64 and 82%, p=0.0003 and 0.036). Tumor diameter was ≥3cm in 12/17 (70.6%) patients who failed percutaneous ablation. Six of these patients underwent successful reablation and remain NED.

Conclusion: Percutaneous ablation provides excellent outcomes, particularly in patients with tumors < 3 cm (95% disease free). Patients with tumors ≥3cm should be counseled about the higher retreatment and failure rates.

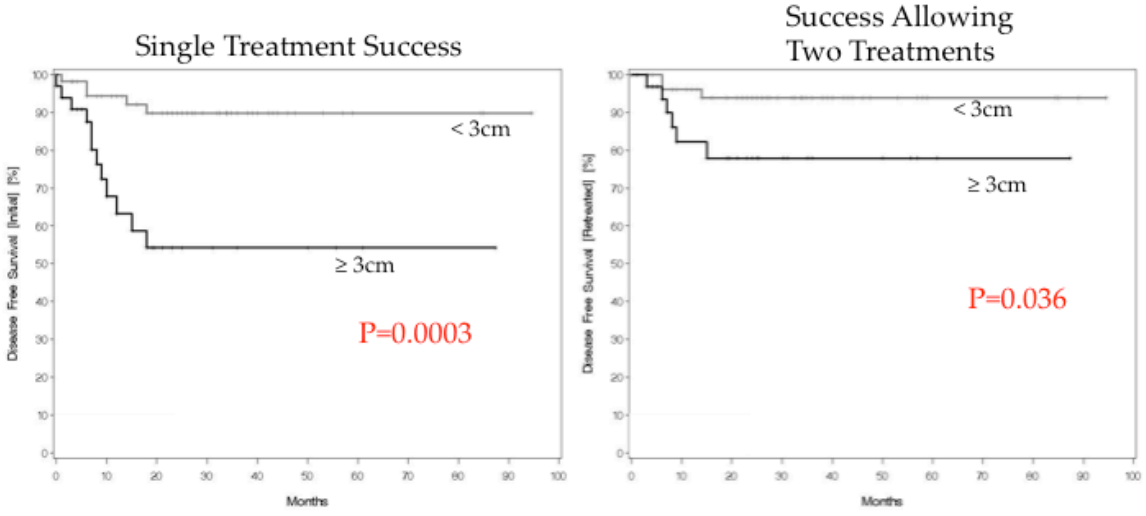

ABSTRACT 57

SILHOUETTE METALLIC COIL REINFORCED STENTS: PARMOUNT IN TREATMENT OF MALIGNANT URETERAL OBSTRUCTION

Andrew Leone [1],Sammy Elsamra[2], Michael Maddox[1] Shadi Al-Ekish[1] Dragan Golijanin[1]
Joseph Renzulli[1] Gyan Pareek [1]
[1] Brown University/RIH [2] LIJ Urology

Introduction: Malignant ureteral obstruction (MUO) is a challenging clinical entity associated with high failure rates with traditional ureteral stents. The Applied Silhouette metallic stent has demonstrated greater resistance to extrinsic compression in ex-vivo laboratory tests and is commonly used at our institution. We evaluated our experience with these stents, specifically assessing their efficacy and durability.

Methods: All patients with biopsy proven MUO confirmed with preoperative imaging (CT/ Ultrasound/MRI) who underwent placement of Silhouette ureteral stents at a single academic institution from January 2011 to September 2012 were identified. Pathology of MUO, pre and post-stent creatinine, time to subsequent stent exchange or stent removal, or death was recorded for each patient. Stent failures were defined as patients requiring unplanned stent exchange or percutaneous nephrostomy tube placement as a result of a rising creatinine or worsening hydronephrosis.

Results: A total of 49 stents were placed in 27 patients (35 renal units in 19 females & 8 males). Stent placement was successful in all cases. Etiologies of MUO are listed in Table 1. Fourteen (52%) of the patients had Silhouette stents placed as conversion from prior standard stent and 13 (48%) patients had primary Silhouette stent placement. Nine patients (33%) died with the stent in place without evidence of failure. The median time to follow up was 142 days. All 8 patients with creatinine greater than 1.5 pre-stent demonstrated improvement in creatinine. There were no failures noted with Silhouette stents requiring unplanned stent exchange or percutaneous nephrostomy tube drainage.

Conclusion: To our knowledge, this is the only study demonstrating the clinical utility of the Silhouette stent for those with MUO. Deployment of the Silhouette stent was technically feasible in 100% of our cohort. Further, no stent failures were identified after Silhouette stent placement. Silhouette stents should be considered as a first line option for decompression of MUO.

Table: Etiology of malignant ureteral obstruction

	Number Patients
All patients	27
Metastatic prostate cancer	5
Colorectal and anal cancer	5
Ovarian cancer	4
Uterine/cervical	5
Unknown primary	3
Other	5

ABSTRACT 58 **TOP 10 ABSTRACT**

A NOVEL PARABOLOID INTRACORPOREAL LITHOTRIPTOR: CAD ANALYSIS AND *IN VITRO* COMPARISON WITH HOLMIUM LASER

Rawandale-Patil AV, Patni L G, Mulay A, Patil PA.
Institute of Urology Dhule, Maharastra, India 424001

Introduction: The present project was an attempt to augment the pulverization properties of the pneumatic lithotripter. The paraboloid probe tip was designed and compared it with Holmium laser for stone pulverization.

Methods: The "Paraboloid lithotripter' was CAD designed, fabricated and patented. The probe tip was modified into a Paraboloid shape. CAD analysis and *in vitro* comparison (with laser) of the pulverization and propulsion dynamics was carried out in a standard underwater hands-free bench arrangement using phantom stones. Pulverization study end points were: Impacts at which (1) a dent was produced in the stone (at point contact); and (2) the stone bivalved or the probe bore through the stone (follow up impacts). *In vitro* propulsion was also studied. The data were analyzed using SPSS for different energy subgroups.

Results: The Spear head at 2, 3, and 4 bars was equally efficient to 6, 10, and 15 watts laser respectively. *In vitro* analysis: The Paraboloid at 2, 3, and 4 bars was equally efficient to 6, 10, and 15 watts laser respectively, in causing the first dent (see table). Effect of bivalving stone correlated with incremental energy levels. Low propulsion of the phantom stones was observed as a result of crumple zone effect at the point of contact.

	Energy source (N=20)								
	PL (2 bars)	Laser 6W	p value	PL (3 bars)	Laser 10W	p value	PL (4 bars)	Laser 15W	p value
Strokes to First dent	1.2 (1-2)	1.4 (1 – 2)	>0.05	1	1.2 (1 – 2)	>0.05	1	1	>0.05
First dent Success	20 (100%)	20 (100%)	>0.05	20 (100%)	20 (100%)	>0.05	20 (100%)	20 (100%)	>0.05
Strokes to Bivalve	4.85 (3-7)	NA	NA	3.8 (2–5)	NA	NA	3.2 (2–4)	NA	NA
Bivalve Success	20 (100%)	0	<0.05	20 (100%)	0	<0.05	20 (100%)	0	<0.05
Strokes to Bore through	NA	8.3 (7–10)	NA	NA	5.05 (4–6)	NA	NA	2.3 (2 –3)	NA
Bore through: Success	0	20 (100%)	<0.05	0	20 (100%)	<0.05	0	20 (100%)	<0.05
Propulsion (mm@45º)	4 (3-7)	3.4 (2-4)	>0.05	4.7 (4-8)	4.2 (3-5)	>0.05	6.1 (4-9)	5 (3-6)	>0.05

N= Number of Phantom stones. PL= Paraboloid lithotripter.
NA= Not applicable

Discussion: Lasers are expensive as compared to pneumatic lithotripters. They pulverize hard stones but prove time consuming in scenario of large stone bulk. Conventional flat tip lithotripter may poise difficulties in pulverizing hard stones. Paraboloid tip lithotripter incorporates the advantage of conventional pneumatic and laser and increases the efficiency of the conventional pneumatic lithotripter manifold as follows-CAD analysis: The Paraboloid tip generates impact pressure of 3570 bars at “point contact.” As fragmentation progresses (“follow-up impacts”) the tip pressure exponentially decreases while the lateral/centrifugal forces increase. This converts the probe tip into a lateral firing/impacting energy source resulting in mechanical separation/bivalving of stones.

Conclusions: The Paraboloid lithotripter generates highly focused impact force with low propulsion (comparable to laser), at point contact. As stone pulverization progresses; the tip forces exponentially decrease and the probe converts into a lateral firing energy source resulting in pulverization into larger fragments (suitable for PCNL). Thus, the paraboloid lithotripter has all the advantages of laser at point contact and the advantages of pneumatic lithotripter at follow-up hits, akin to being a bimodal energy source.

ABSTRACT 59

LASER LITHOTRIPSY RETROPULSION VARIES WITH STONE MASS

Michael Robinson, Joel Teichman
Department of Urologic Sciences, University of British Columbia, Vancouver, BC, Canada

Introduction: The Ho:YAG laser fragments stones by a photothermal mechanism. As fragment debris is ejected off the stone surface, it exerts a force in the opposite direction producing retropulsion. As pulse energy is increased, ablation crater volumes and retropulsion both increase. Previous research showed an overall benefit using low pulse energy at high pulse frequency. Retropulsion limited fragmentation efficiency as pulse energy increased. However, retropulsion has not been characterized for larger stones. We hypothesize that retropulsion would be minimal if treating a large renal or bladder calculus even at high pulse energy.

Methods: Stone phantoms were constructed to uniform cube sizes of 0.5 cm x 0.5cm x 0.5 cm (0.1 cm^3), 1.0 cm x 1.0 cm x 1.0 cm (1.0 cm^3), 1.5 cm x 1.5 cm x 1.5 cm (3.4 cm^3), 2.0 cm x 2.0 cm x 2.0 cm (8 cm^3), 2.5 cm x 2.5 cm x 2.5 cm (15.6 cm^3), and 3.0 cm x 3.0 cm x 3.0 cm (27 cm^3). Phantoms were positioned in a horizontal, cylindrical tube in a water bath and irradiated with a 365 um fiber using Ho:YAG pulse energies 0.5 to 3.5 J at 5 Hz. 10 pulses were applied. 10 trials were conducted per experimental condition. Displacement was measured. Analysis of variance was used for statistics.

Results: At any given pulse energy, retropulsion decreased as stone volume increased, $p<0.01$. At any given stone phantom volume ≤ 3.4 cm^3 (1.5 cm x 1.5 cm x 1.5 cm), retropulsion increased as pulse energy increased, $p<0.05$. However, for stones ≥ 15.6 cm^3 (2.5 cm x 2.5 cm x 2.5 cm), mean retropulsion was 0 mm, even at 3.5 J pulse energy.

Conclusion: For most ureteral stones, low pulse energy at high frequency delivers efficient fragmentation, low retropulsion, and small fragments. However, for larger bladder and renal stones, high pulse energy risks little retropulsion. The results support our hypothesis that large stones may be treated efficiently with increased pulse energy. More study is warranted to establish ideal parameters for Ho:YAG lithotripsy.

ABSTRACT 60

ADVERSE EVENTS RESULTING FROM LASERS USED IN UROLOGY

Abdulaziz M Althunayan, Mohamed A Elkoushy, Mostafa M Elhilali, Sero Andonian
Division of Urology, Department of Surgery, McGill University, Montreal, QC, Canada

Introduction: Endourologic procedures such as prostate tissue ablation and lithotripsy use different types of lasers with different wavelengths such as Neodymium-Doped Yttrium Aluminum Garnet (Nd:YAG), Holmium: YAG (Ho:YAG) and Potassium Titanyl Phosphate (KTP) lasers with the following wavelengths 1064 nm, 2100 nm, and 532 nm, respectively. Currently, there is no data regarding adverse events (AEs) to patients or operators resulting from the use of these lasers. Therefore, the aim of the present study was to collate world reports of such AEs.

Methods: The Manufacturer and User Facility Device Experience (MAUDE) database of the United States Food and Drug Administration (FDA) was searched using the term "Laser for gastro-urology use." In addition, the Rockwell Laser Industries (RLI) Laser Accident Database was searched for the following types of lasers: Nd:YAG, Ho:YAG, and KTP.

Results: Both databases were last accessed on October 1, 2012. Overall, there were 394 AEs (160 in FDA MAUDE database from 1992 to 2012 and 234 in RLI database from 1970 to 2005). Most of the AEs (192/394 or 49%) were related to generator failure or fiber tip breaking, especially with smaller laser fibers. While there were 20 AEs harming medical operators, 126 AEs resulted in harm for non-medical operators using Nd:YAG and KTP lasers. Interestingly, all 131 AEs resulting in eye injuries were associated with the use of Nd:YAG and KTP lasers as a result of improper eye protection; none were reported with Ho:YAG lasers. Most of the reported eye injuries resulted from non-medical laser uses. These eye injuries were serious ranging from mild corneal abrasions to total vision loss**.** Overall, there were 36 (9%) AEs resulting in patient harm including 7 (1.7%) mortalities; 3 deaths from ureteral perforation and retroperitoneal bleeding using the Ho:YAG laser (two in 2003 and one in 2005) and 4 deaths from air embolisms using the Nd:YAG laser (in 1987, 1988, 1989 and 1990). Two other patients with air embolisms from Nd:YAG laser survived. Other reported patient injuries included bladder or ureteral perforation resulting in urinary diversion in a patient, minor skin burns, internal burns, and bleeding.

Conclusion: Most of the AEs reported relate to equipment failure. There were no eye injuries reported with the use of Ho:YAG lasers. Caution must be exercised when using lasers in urology including wearing appropriate eye protection when using Nd:YAG and KTP lasers.

Laser type	**Ho: YAG**		**Nd: YAG**		**KTP**		**Overall**
Database	FDA	RLI	FDA	RLI	FDA	RLI	FDA and RLI
No. of AEs	87	53	48	161	25	20	394
Generator or Fiber Failure	72	48	26	30	16	0	192
Harm to operator (medical)	9	2	0	4	5	0	20
Harm to operator (non-medical)	0	0	0	109	0	17	126
Eye injury	0	0	0	113	1	17	131
Harm to patient	6	3	2	18	4	3	36
Death	3	0	0	4	0	0	7

Table 1: AEs reported in FDA MAUDE (1992-2012) and RLI (1970-2005) databases

ABSTRACT 61

THE SURGICAL SPECTACLE: A SURVEY OF UROLOGISTS VIEWING LIVE CASE DEMONSTRATIONS

Sammy Elsamra, Hector Motato, Justin Friedlander, Daniel Moreira, Brian Duty, Arthur Smith, Zeph Okeke
Smith Institute for Urology, Hofstra North Shore-LIJ Medical School

Introduction: Live case demonstrations (LCD) performed today are a far cry from the often gory spectacle they once were before the advent of anesthesia, aseptic technique, and modern interactive audiovisual teleconferencing. While many societies use LCDs at national and international meetings, it is unclear if there is any educational benefit over video demonstration or if viewers transfer what they observed into practice. Therefore we sought to evaluate perspectives of urologists on live and taped surgery.

Methods: An anonymous paper survey was distributed to all attendees of the live surgery session at the AUA 2012 national meeting (Atlanta) and the 3rd International Challenges in Endourology meeting (Paris). Descriptive statistics and Wilcoxon signed-rank tests were used.

Results: Atlanta: 181 forms were collected from 23 residents, 16 fellows, and 135 urologists in practice. A total of 36% (64 of 179) cited academic setting of practice, 71% stated they performed the surgery demonstrated in their practice and 83% stated they would incorporate what they viewed into their practice. About 40% stated they would not allow themselves to be a patient for a LCD and 19% did not choose yes to characterize LCD as ethical. Paris: 72 forms were collected from 10 residents, 13 fellows, and 47 urologists in practice. A total of 61% cited academic setting of practice. 96% stated they perform the surgery demonstrated in their practice and 94% stated they would incorporate what they viewed into their practice. About 43% stated they would not allow themselves to be a patient for a LCD and 28% did not choose yes to characterize LCD as ethical. Likert response for how beneficial LCD, unedited videos, and edited videos (for both meetings) are shown in graph 1. Viewers in Atlanta selected very helpful or helpful for both live surgery and unedited videos more than edited videos. In Paris, viewers selected very helpful or helpful for live surgery more than both edited and unedited videos (Wilcoxon Signed-Rank $p<0.001$).

Conclusion: Urologists feel LCDs are beneficial and applicable to their practice. LCDs are preferred over videos (only edited in Atlanta and both edited and unedited in Paris). The large majority considers LCD ethical and would volunteer themselves for LCD.

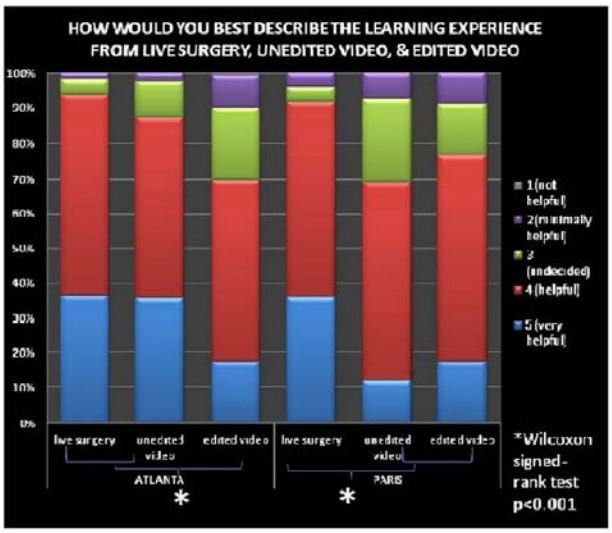

ABSTRACT 62 **TOP 10 ABSTRACT**

ACTIVE REMOVAL OF BUBBLE SHIELDING IN SWL: AN *IN VITRO* STUDY

Alexander P Duryea[1], William W Roberts[1,2], Charles A Cain[1], Hedieh A Tamaddoni[1], Timothy L Hall[1]
[1] *Department of Biomedical Engineering, University of Michigan, Ann Arbor, MI, USA*
[2] *Department of Urology, University of Michigan, Ann Arbor, MI, USA*

Introduction: Cavitation plays a complex role in SWL stone comminution. While bubble activity at the stone surface has been identified as a crucial component of the comminution process, bubbles that persist along the path of shock wave propagation can attenuate the energy that ultimately reaches the stone. This later phenomenon, often referred to as 'shielding,' limits the efficacy of SWL stone treatment. The effect is more pronounced at high shock rates, as bubbles induced by the tensile phase of the wave have less time to dissolve between successive shocks. In this regard, an increase in shock-shock efficiency has been reported using slower shock rates. In this study we attempt to achieve similar efficiency at high shock rate using additional acoustic pulses designed for the active removal of residual bubbles.

Methods: Cystine-mimicking model stones were held within a vinyl finger cot measuring 2 cm in diameter and 3 cm in height. SWL was delivered using an electrohydraulic research system designed to simulate the acoustic output of the Dornier HM3. All treatments were performed using a 20 kV charging voltage, which generates an acoustic shock wave having a P+/P- of 34/8 MPa. Bubble removal pulses were generated using a separate unfocused piezoelectric transducer driven at 370 kHz. A 100 ms burst at an amplitude of 500 kPa was used to sonicate remnant bubbles following each shock. Preliminary work indicates that this pulse scheme acts to remove remnant bubbles by stimulating their coalescence from a very large number into a small number of microscopic bubble nuclei. Model stones were treated with 2000 shocks using six different schemes: **(1)** SWL at 2 Hz; **(2)** SWL at 2 Hz with bubble removal pulses; **(3)** SWL at 1 Hz; **(4)** SWL at 1 Hz with bubble removal pulses; **(5)** SWL at 0.5 Hz; **(6)** SWL at 0.5 Hz with bubble removal pulses. Following treatment stone debris was collected and sieved to quantify efficacy. Five model stones were treated with each scheme.

Results: SWL delivered at 2 Hz produced minimal stone subdivision , with the majority of stone mass remaining >6 mm in size. The addition of bubble removal pulses at 2 Hz resulted in a drastic shift in fragment size, with the majority of stone mass reduced to <2 mm. SWL delivered at 1 Hz generated a broad distribution of fragment sizes, while 1 Hz with bubble removal pulses reduced the entire stone to <2 mm. SWL at 0.5 Hz reduced the entire stone to fragments <2 mm with or without the application of bubble removal pulses.

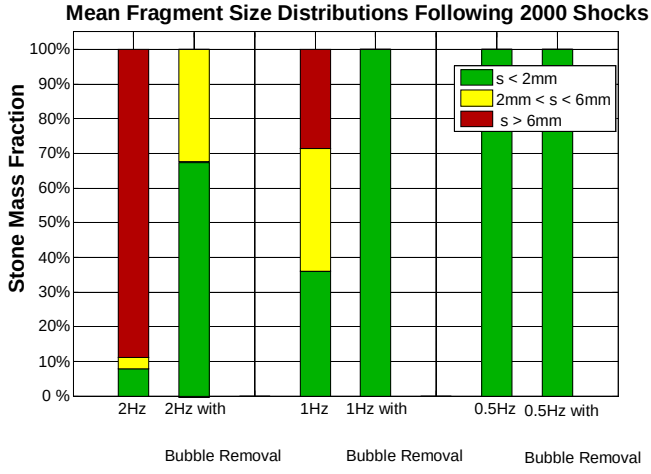

Conclusion: Bubble removal pulses dramatically improve SWL efficacy at higher rate (2 Hz), making the shock-shock efficiency more comparable to that achieved using slower shock rates (0.5 Hz). Maintaining this efficiency at high shock rate has the potential to drastically reduce treatment times in comparison to those typically achieved with conventional SWL.

Support and Disclosure: This work was funded by NIH R01DK091267. WW Roberts, CA Cain, and TL Hall have financial interests and/or other relationships with HistoSonics, Inc.

ABSTRACT 63 **TOP 10 ABSTRACT**

DESIGN OF STEERING MECHANISM AND SURFACE MOSAICS SOFTWARE FOR AUTOMATED BLADDER SURVEILLANCE

Xianming Ye, W. Jong Yoon
Department of Mechanical and Industrial Engineering, Qatar University, Doha, Qatar

Introduction: Automated cystoscopies can improve the accuracy and efficiency of postoperative surveillance of bladder cancer. A computerized pre-programmable steering mechanism has been proposed to steer an imaging probe to scan the entire bladder inner surface[1]. A further developed prototype with reduced size (Ø8×80 mm) consists of three segments connected in series (Figure 1).

Methods: Each segment of the mechanism is composed of two sub-segments that bend to the maximum of 90 degree in X- and Y- direction, respectively. The X/Y bending of each segment is controlled with thin wires (Ø0.25 mm) driven by DC-motors with precision position control. Translational motions and bending configurations of all segments are calculated by inverse kinematics to achieve desired positions and orientations of the camera. The central tunnel (Ø2 mm) of the steering mechanism allows the camera of an imaging probe to reach the distal end of the mechanism. The navigation of the steering mechanism is fully operational using a computer-based user interface within MATLAB environment enabling both manual and fully-automated scanning control.

With 3D path planning with optimized steering motion sequence, spiral scan trajectories are chosen to reduce the time for scan while maintaining the required percentage of overlap between neighboring image frames to help post-processing of the video. The total scanning process takes about three minutes to finish. In order to expediently review the bladder surface, a 3D stitching software which reconstructs the surface of the whole bladder from endoscopic video using structure from motion have been separately developed. The software was tested on endoscopic videos acquired from a phantom model and an excised pig bladder using a primitive robotic steering mechanism (Figure 2)[2][3].

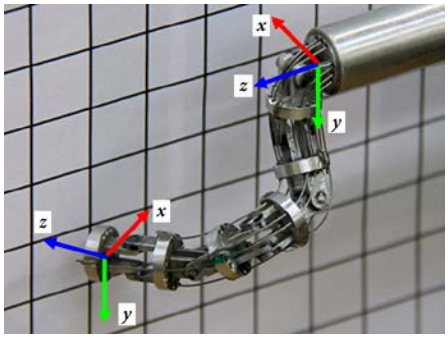

Figure 1: Steering mechanism with three segments connected in series

Results and Future work: The multiple degrees of freedom from this updated steering mechanism enable the imaging camera to retroflex, which makes it possible to obtain perpendicular views on the interested area of bladder surface. For example, this feature provides better visualization on the anterior region of the bladder. Pre-programmed steering motion control shortens the scan process and provides smooth motion of the camera. The 3D reconstruction software is under evaluation on videos acquired from this updated versatile steering mechanism using various sizes and shapes of *in vitro* and *ex vivo* models leaving lots of wealth of research to investigate whether/how these stitched maps impact a clinician's diagnosis.

Figure 2: Images captured from cystoscopic video within a bladder phantom, and the result of stitching and blending images together.

[1] Xianming Ye and W. Jong Yoon, Preliminary Design of a Bending Mechanism for Automated Cystoscope, The 8th IEEE International Conference on Automation Science and Engineering (CASE 2012), 257-262, August 20-24, 2012, Seoul, Korea.
[2] M. Burkhardt, T. Soper, W. Jong Yoon, and E. J. Seibel, Controlling the Trajectory of a Flexible Ultrathin Endoscope for Fully Automated Bladder Surveillance, IEEE/ASME Transactions on Mechatronics, 2013 (doi:10.1109/TMECH.2013.2237783).
[3] Timothy D. Soper; Michael P. Porter; Eric J. Seibel, Surface mosaics of the bladder reconstructed from endoscopic video for automated surveillance, IEEE Transactions on Biomedical Engineering. 2012; 59(6):1670-1680.

ABSTRACT 64

EVALUATION OF A NOVEL CORDLESS ENDOSCOPIC LIGHT SOURCE FOR OPTICAL QUALITY AND PERFORMANCE DURING FLEXIBLE CYSTOSCOPY

A. Lusch MD, P. Greene, C. Abdelshehid MD, Z. Okhunov, J. Landman MD
University of California, Irvine, Department of Urology, Orange, California, USA

Introduction: We compared a novel cordless LED light source (CLS, Cook Urological Inc., Spencer, Indiana) and standard Xenon light source (XLS) for optical quality and performance during cystoscopy.

Methods: We performed *in vitro* and *in vivo* comparison of the two light sources for contrast, optical resolution and color discrimination (using USAF test targets), image brightness at distances of 10mm/20mm/50mm/100mm, and battery durability. These metrics were also tested in a preliminary clinical evaluation in two office based cystoscopy procedures with both light sources.

Results: The flexible cystoscope showed identical resolution with both light sources (10mm/20mm distance = 3.56/2.0 line pairs/mm). Contrast evaluation as well as color representation was similar with both light sources. At a distance of 10 mm the CLS showed a maximum illumination 23% of the XLS maximum illumination. [Table] At distances greater than 10mm, the CLS showed superior illumination when compared with the XLS. CLS offers a 230 gram weight reduction due to the absence of the light cable. CLS lasted 47min on full power and 3.8hrs on 50% power. Observers deemed the cystoscope with CLS superior in handling, weight and similar in optical resolution and brightness during the cystoscopy. Heat generation at the tip of the LED light source was 55.7°C compared to >150°C at the tip of the light cable of the Xenon light source.

Conclusion: Compared to a SLS, the CLS is a cost effective and practical light source that offers acceptable illumination while offering superior endoscope performance during flexible cystoscopy. Lower temperatures may also make the CLS a safer alternative. Clinical correlation is pending.

Measurement	LED [100%] 10 mm	Xenon [100%] 10 mm	p-value
1	14300	98500	
2	14500	100000	
3	14400	100500	
4	14100	100200	
5	14300	99700	
6	14300	100100	
Mean	**14316,7**	**99833,3**	p<0.0001
STD	**132,9**	**703,3**	

LED light source attached to cystoscope

ABSTRACT 65

A BASIC NOVEL CONCEPT: PROSTATE-SPECIFIC COORDINATE SYSTEM

Doyoung Chang, Haixin Chen, Byongchang Jeong, Seungbae Lee, Chunwoo Kim, Changhan Jun, Doru Petrisor, Misop Han, Dan Stoianovici

Urology Robotics Laboratory, Johns Hopkins University, Baltimore, MD

Introduction: With current freehand transrectal ultrasound (TRUS) guided prostate biopsies the cores are often clustered, miss regions, and do not precisely follow the intended biopsy template (J Urol 2012; 188(6):2404). Biopsy targeting errors are on the order of 9 mm, too high to reliably target a clinically significant PCa tumor (0.5 cm^3, 5mm radius). Biopsy error factors include the imaging used, manual execution errors, the lack of quality control means, but also *a very basic factor* which is the lack of a general, commonly accepted system to define a prostate location precisely and accurately. Sextant biopsy schemata are commonly defined by regions (for example Left/Right x Medial/Lateral x Apex/Mid/Base). This definition is vague in a geometric sense and leaves room for subjective interpretation. Coordinates are typically used for the images, but these are not assigned relative to the prostate, are different from a session to another and across imaging modalities and procedures. Image-to-image registration (fusion) must be performed to use different sets of images and quality control is difficult. We propose a Prostate Coordinate System (PCS): *A reference frame that could be assigned to the prostate of the patient, with little variability among physicians, over time, and independent of the imaging used.* If successful, the PCS could be used in numerous aspects of PCa management and research: 1) to reference the locations of previous biopsies in active surveillance patients, 2) mark MRI abnormalities for TRUS-guided biopsy, 3) to use biopsy samples for longitudinal studies of biomarkers and chemopreventive agents, 4) to plan focal therapy in correlation with imaging and biopsies.

Methods: High-resolution 3D TRUS images of the prostate gland were acquired with the TRUS-Robot during the Tandem Robot-Assisted Laparoscopic radical Prostatectomy (T-RALP). Special software for PCS was developed with Visual C++ modules in the Amira Visualization platform (Visage Imaging Inc., San Diego, CA). Three urologists and 3 engineers were trained to manipulate the software. They were then asked to assign the PCS 5 times for 3 patients.

The assignment and location of the PCS are shown in Figure 1. This is based on selecting the center of the urethra at the base and apex points (B, A respectively in Figure 1a) on the central sagittal plane. The origin of the PCS is located in the middle of the AB segment and is aligned along the AB direction and the central sagittal plane. The directions of the PCS follow the LPS (Left-Posterior-Superior) standard anatomic system. The precision of defining the PCS was calculated as the radius of the minimal sphere enclosing the origins of the PCS.

Results: The average intra- and inter-operator PCS precision were 0.8 mm (SD 0.17) and 2.00 mm (SD 0.71), respectively. The average time of PCS assignment was 5.21 min (SD 2.17).

Conclusion: A PCS can be consistently assigned to the prostate of in 3D TRUS imaging. Further validation is necessary to confirm that the PCS can be consistently assigned over time and across other imaging modalities, such as MRI.

Acknowledgement: Supported by the Patrick C. Walsh Prostate Cancer Research Foundation.

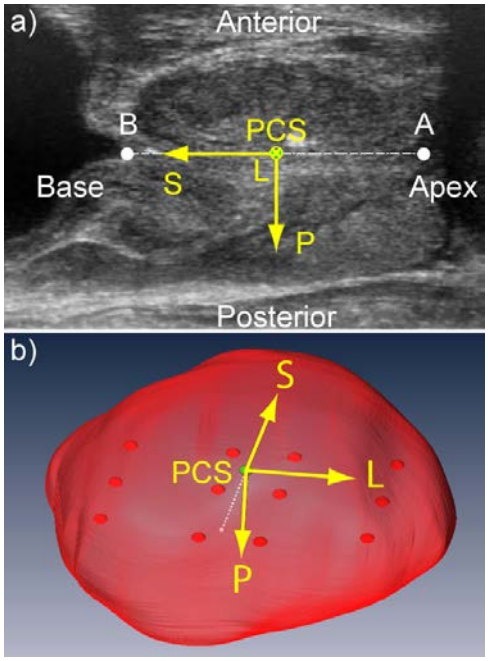

Figure 1: PCS Location: a) Central sagittal ultrasound through the prostate showing apex (A) and base (B) points, b) PCS with Left-Posterior-Superior coordinates.

ABSTRACT 66

EVALUATION OF THE IMPACT OF THREE-DIMENSIONAL VISION ON LAPAROSCOPIC PERFORMANCE

A. Lusch, P Bucur , A Menhadji, MA Liss, A Perez-Lanzac, Z Okhunov, E. McDougall, J. Landman
University of California, Irvine, Department of Urology, Orange, California, USA

Introduction: Recent technological advancements have led to the introduction of new 3-dimensional (3D) cameras in laparoscopic surgery. These novel optical systems may yield improved depth perception, spatial location, and precision when compared to conventional 2-dimensional (2D) laparoscopic equipment. We compared 3D vs. 2D performance using six standardized surgical tasks and stratified by level of laparoscopic experience.

Material and Methods: We performed a prospective, randomized educational study comparing a 0° 3D high definition camera with a conventional 0º 2D high definition camera using a high definition monitor (Karl Storz, Tuttlingen, Germany). [Figure below] All participants completed six standardized basic skills tasks utilizing laparoscopic tools. Quality testing scores were measured by dropped equipment, grasping attempts, and precision of needle entry and exiting. Additionally resolution, color distribution, depth of field and distortion were measured using optical test targets. After adjusting for level of training, 2D vs. 3D measurements were statistically analyzed using SPSS 10 (SPSS, IBM Corporation, Armonk, New York) and a p-value<0.05 was considered as statistically significant.

Results: 10 medical students, 7 residents and 7 expert surgeons were evaluated. There was a significant difference between levels of training and performance on all six-skill tasks and quality scores, except for cut the line quality score and peg transfer quality score. After adjusting for training level, there was a significant difference in performance between 2D vs. 3D environment in the number of rings left after completion of the ring transfer (p=0.041), number of rings threaded (p=0.0004), peg transfer completion time (p=0.047), and number of pegs left after completion of peg transfer (p=0.012). It also showed a significant difference for ring transfer quality score (p=0.046), thread the rings quality score (p=0.0002), knot tying quality score (p=0.004), and for peg transfer quality score (p=0.001). The three dimensional system also showed less distortion (p=0.0008), a higher depth of field (p=0.0004).

Figure: 3D optical system and set up

Conclusion: 3D laparoscopic equipment results in a significant improvement in depth perception, spatial location, and precision compared to the conventional 2D equipment. With this improved quality of vision even expert laparoscopic surgeons may benefit from 3D imaging. Clinical correlation is in progress.

ABSTRACT 67

CORRELATION BETWEEN THE PROSTATE SIZE AND LOCATION OF THE NEUROVASCULAR BUNDLES

Haixin Chen[1,2], Chunwoo Kim[1], Doru Petrisor[1], Misop Han[1], Dan Stoianovici[1]
[1]*Urology Robotics Laboratory, Johns Hopkins University, Baltimore, MD*
[2]*China-Japan Friendship Hospital, Urology Department, Beijing, China*

Introduction: The neurovascular bundle (NVB) sparing is associated with the sexual potency preservation following radical prostatectomy. A larger prostate size may pose more difficulties during surgery and result in delayed potency recovery (Urology 2008; 72(6):1263). A shorter NVB-to-prostate distance may pose challenges to nerve sparing. We studied the association between the NVB-to-prostate distance and prostate size.

Methods: Doppler ultrasound based navigation, such as the Tandem Robot Assisted Laparoscopic Prostatectomy (T-RALP, Urology 2011; 77(2):502), enables the intraoperative visualization of the NVB. Sets of 3D prostate images acquired during 31 T-RALP cases were analyzed.

Prostate size was calculated using the width, height, and length measured in the transverse and sagittal slices. The NVB-to-prostate distance was measured in the mid-gland transverse B-mode and Doppler slice. The shortest distance from the periphery of the Doppler signal to the contour of the prostate was measured (Figure 1). Distances on both sides of the prostate were measured.

Table: Prostate size and NVB-to-prostate distance

		Average	S.D.	Range
Prostate size [mL]		41.39	11.12	17.86-87.41
NVB-to-prostate distance [mm]	Left	2.72	1.21	0-7.03
	Right	2.96	1.49	0-7.71

Results: The average prostate size was 41 mL (range 18-87). The average NVB-to-prostate distance was 2.8 mm (range 0-7.7) (Table). Figure 2 shows the NVB-to-prostate distances vs. the prostate volume for 31 patients and both sides of the prostate. The NVB-to-prostate distance is inversely correlated to the prostate volume (p=0.0045).

Conclusion: In larger prostates, the NVBs are closer to the gland. Therefore, NVB sparing may be more challenging for larger prostates. These findings may explain why the early recovery of potency after RP is inversely related to the prostate size.

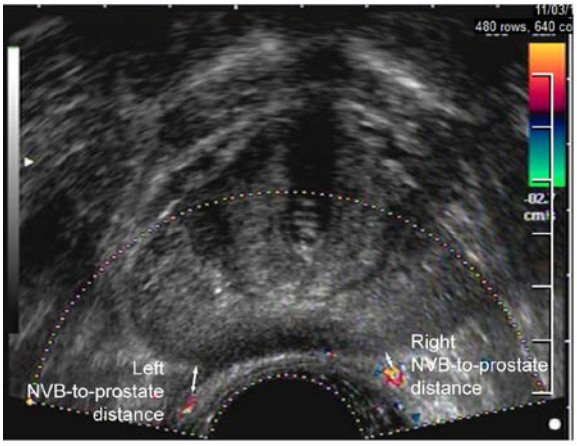

Figure 1: NVB-to-prostate distance

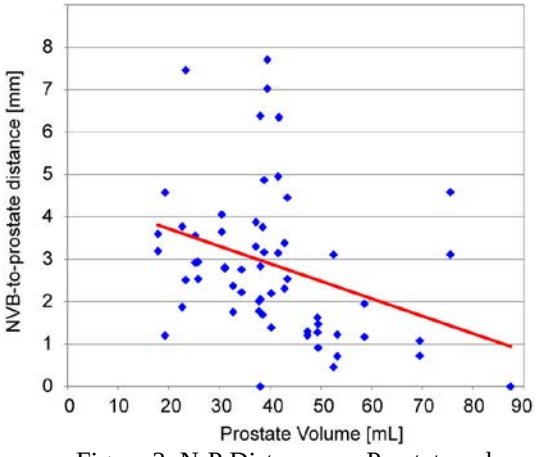

Figure 2: N-P Distance vs. Prostate volume

Acknowledgement: Study supported by award CA141835 from the National Cancer Institute, the Sidney Kimmel Comprehensive Cancer Center at Johns Hopkins, and Hitachi-Aloka Medical Systems.

ABSTRACT 68

COMPARISION OF THE iTRAINER AND STANDARD LAPAROSCOPIC TRAINER FOR BASIC LAPAROSCOPIC TASKS

Renai Yoon, Adam Kaplan, Philip Bucur, Martin Hofmann, Michael del Junco, Ramtin Khanipour, Naghmeh Ramezani, Reza Alipanah, Elspeth M. McDougall, Jaime Landman

Department of Urology, University of California, Irvine

Introduction: The use of laparoscopic trainers has well documented value in surgical education. Typically, laparoscopic trainers are expensive and are often located in an education center that may not be routinely accessible to trainees. As such, we developed the iTrainer (iT), which is an inexpensive, portable (small and lightweight) laparoscopic trainer that is based on the iPad imaging platform. The iT consists of a hardware component and software that is now in development. Here, we compare the iT and a standard pelvic trainer (SPT) in assessing surgical skills and for image quality, comfort, ease of use, and overall performance.

Methods: We engineered, designed and built the iT that engages an iPad 3 device as its optical system. Video and optics were provided by the iPad 3's 2048 x 1536 retina display and rear 1080p HD camera. A total of 34 subjects including undergraduate students (n=10), medical students (n=10), residents (n=4), fellows (n=6), and attending physicians (n=4) participated. Each participant was randomized to start on either the iT or the SPT and was assigned the thread-the-loops task. On each trainer, a 2-minute warm-up period was given to each subject followed immediately by a 2-minute testing period. Each subject's skill assessment score consisted of the product of their skill quality and the quantity of loops threaded. Quality was scored on a 0-4 scale, and quantity was scored on a 0-10 scale (max quality score = 4, max quantity score =10). Upon completion of the tasks, the subjects were given an evaluation sheet to provide feedback on image quality, comfort, ease of use, and overall performance of both training devices on a 1-5 scale.

Results: Statistical analysis showed no significant difference between mean +/- SD skill assessment for the task assigned on the iTrainer compared to the standard pelvic trainer ($p > 0.05$) for all groups tested with the exception of the medical student group ($p=0.03$). The group composed of attending physicians had the greatest mean skill assessment scores. Participants rated the mean overall performance and comfort similarly for both trainers, 3.382 and 3.735, iT and SPT, respectively. Higher mean feedback scores for image quality (4.294 vs. 3.235), resolution (4.147 vs. 3.147), and brightness (4.000 vs. 3.412) were given to the iTrainer.

Conclusion: We have demonstrated face, content, and construct validity for the iT. The iT is a portable laparoscopic training device. With regards to proficiency to perform the skills task, there is no statistical difference between the SPT and the iT among the groups tested with exception to the medical student group. Continued research and development for the iT is in progress.

ABSTRACT 69

TRANSVAGINAL HYBRID NOTES ROBOTIC DONOR NEPHRECTOMY

Ali Khalifeh, Riccardo Autorino, Humberto Laydner, Dinesh Samarasekera, Kamol Panumatrassamee, Shahab P Hillyer, Charles Modlin, Howard Goldman, Jihad Kaouk
Cleveland Clinic Foundation, Cleveland OH

Introduction: Based on our extensive experience with clinical and preclinical LESS, NOTES and robotic surgeries, we have conceptualized a novel approach for a transvaginal hybrid NOTES donor nephrectomy.

Methods: A 61year old lady volunteered to donate her kidney through this approach after thorough consent and IRB approval. The patient was placed in a right lateral decubitus position. Through a 4cm intra-umbilical incision, an 8mm trocar was tunneled through a fascial incision. To this port the left robotic arm would be docked. A SILS™ port was also placed through the same incision, accommodating a 12mm camera trocar and two 5mm assistant ports. A GelPoint™ port was placed transvaginally in the posterior fornix into which an 8 mm in a 12 mm bariatric trocar was placed. The right robotic arm was docked to that port. After dissection of the left kidney in preparation for extraction, the robot was undocked and the retrieval bag was inserted through the GelPoint™. The graft was bagged prior to vessel stapling and extracted without breaching of the bag. The kidney was delivered to a perfusion table, with a clean pair of gloves, without contamination with the bag exterior.

Results: Donor Nephrectomy was successfully completed without perioperative complications—WIT was 5.8 minutes, and EBL was 75cc. The patient was discharged after an uneventful 48 hour stay, with a stable GFR at 60mL/min/1.73m^2. The recipient was given pulse steroids for biopsy-proven acute rejection, and his GFR was 67mL/min/1.73m^2 on last follow-up.

Conclusion: Transvaginal hybrid NOTES robotic donor nephrectomy is feasible. Further advances in robotic technology are awaited for development of this approach and to foster its clinical application

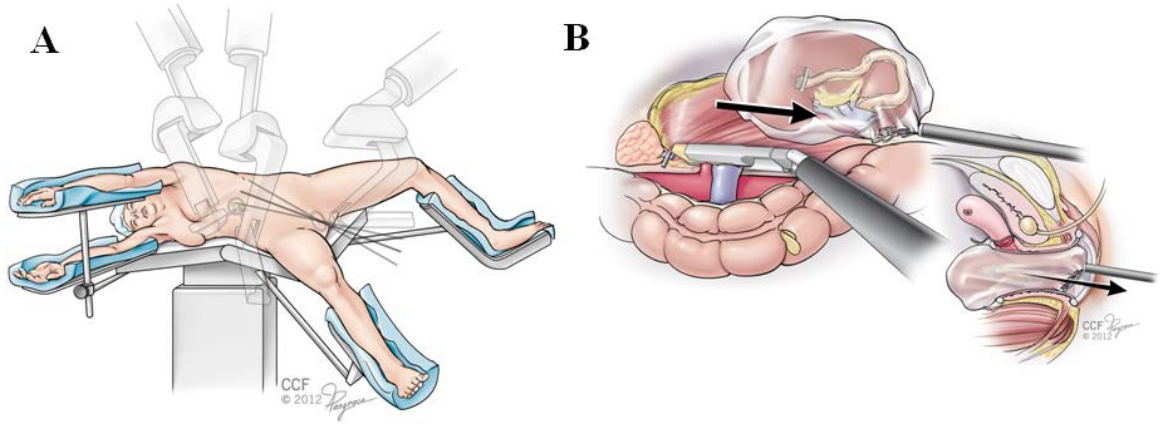

Figure. A. Patient positioning and Robotic arms configurations; larger range of motion of robotic arms made possible by the wide distribution of instruments. **B.** Graft is bagged into retrieval bag, followed by stapling of vessels and extraction through the vagina.

ABSTRACT 70

AUTOMATIC KIDNEY DETECTION AND SEGMENTATION FROM 3D ULTRASOUND IMAGE USING GRAPH SEARCHING AND LEVEL SET

Li Xin, Matthias Noll, Stefan Wesarg

Cognitive Computing & Medical Imaging, Fraunhofer IGD, Darmstadt, Germany

Introduction: Ultrasound is the preferred imaging modality for kidney disease diagnosis because it is real-time and low cost. Although ultrasonography is said to be the safest medical imaging technique, its speckle noise and poor signal-to-noise ratio poses a big challenge for designing automated detection and segmentation algorithms. The aim of this study is to design an automated method for detection and segmentation of the kidney in 3D ultrasound images, utilizing both image signal information and shape priors for graph searching and the Level Set algorithm.

Methods: We designed four major steps in order to localize and segment the kidney. In the first step the ultrasound is smoothed and downscaled using a multi-scale image pyramid. Additionally, we enhance the image contrast through histogram equalization. Secondly, Otsu's method is used to generate a threshold image that contains several kidney shape “candidates”. To find the kidney position among the potential kidney candidates, a graph based searching algorithm traverses the image with two step sizes equal to the two major kidney axes derived from a kidney shape model. For each graph node we then send 12 rays along the default image axes with a maximum travel distance matching the kidney shape size. We then detect the first zero-to-one crossing along each ray. The graph node with the highest count of zero-to-one crossings is selected as the kidney position. In the final step, seed points are placed with an offset d along the ray direction. Using all seed points the fast marching algorithm generates a coarse kidney shape from the preprocessed ultrasound image. The fast marching result, in turn is utilized to initialize the level set algorithm, which then produces the final and accurate kidney segmentation.

Results: Experiments were carried out for 62 three-dimensional ultrasound images of 8 healthy male and female volunteers. Figure 1(a) shows the contrast-enhanced ultrasound input. In Figure(b) the segmentation result of the proposed approach on the automatically detected kidney candidate is shown. The graph based searching procedure on the threshold image is illustrated in Figure 1(c). The proposed method was successfully applied in over 90% of the available test cases. In only 6 cases a kidney candidate could not be determined due to strong image artifacts such as acoustic rib shadows.

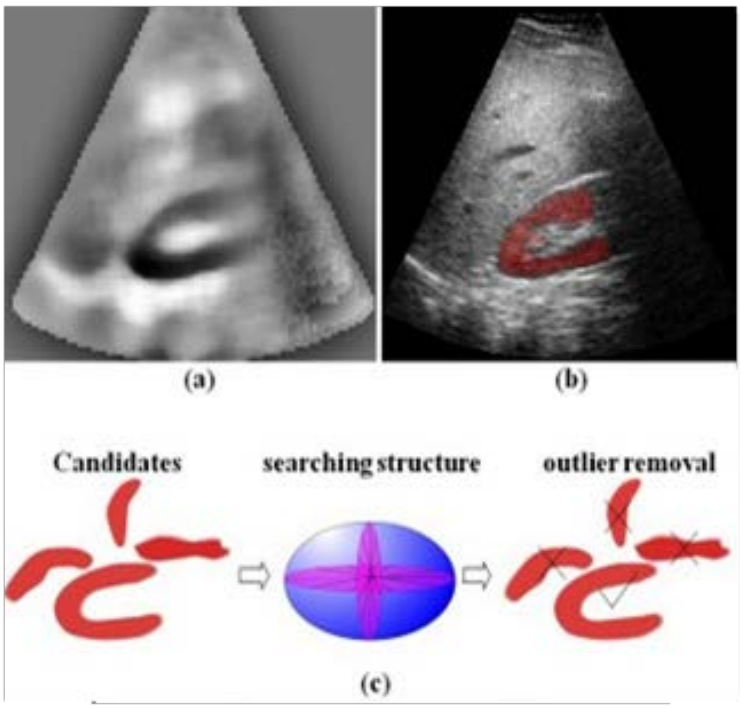

Figure: Steering mechanism with three segments connected in series

Conclusion: A method for automatic kidney segmentation in 3D ultrasound has been proposed. Both image signal information and object shape priors are used in the detection and segmentation process. Based on the segmentation result further diagnosis can be achieved.

ABSTRACT 71

PULSED FOCUSED ULTRASOUND AS A METHOD FOR NONINVASIVE TREATMENT OF URETEROCELES

Adam D. Maxwell[1,2], Ryan S. Hsi[1], Michael R. Bailey[2], Pasquale Casale[3], Thomas S. Lendvay[1,4]
[1] *Department of Urology, University of Washington School of Medicine*
[2] *Center for Industrial and Medical Ultrasound, Applied Physics Laboratory, University of Washington*
[3] *Department of Urology, Columbia University College of Physicians and Surgeons*
[4] *Division of Pediatric Urology, Seattle Children's Hospital*

Introduction: Ureteroceles are a thin, cyst-like out-pouching of the ureter opening to the bladder beyond the ureterovesical junction, and are associated with febrile urinary tract infections, urinary retention, and renal obstruction or injury. Current methods to treat ureteroceles include open surgical reconstruction, endoscopic puncture of the ureterocele wall, and observation. However, surgical procedures require general anesthesia and are invasive. We investigated the feasibility of performing ureterocele puncture noninvasively using focused ultrasound-generated cavitation to controllably erode a hole through the tissue.

Methods: Fresh bovine bladder was used to create two models for the ureterocele wall. The first was a bleb model created by injection of 1-2 mL dyed normal saline into the submucosal layer. The second was a denuded mucosal membrane separated from the muscular layer. The tissue was positioned in a degassed water bath and the target layer was aligned with the focus of a 1 MHz ultrasound transducer. Pulsed focused ultrasound was administered to create a visible hole in the wall. The pulse amplitudes employed were similar to those applied for extracorporeal shockwave lithotripsy, with peak positive pressure p_+ = 100-120 MPa and peak negative pressure of 17-20 MPa. Pulse duration and pulse rate were varied between different exposures. Time to puncture and puncture size was recorded. The use of ultrasound imaging as a method of targeting and treatment feedback was also explored.

Results: Focused ultrasound produced erosion of the wall and puncture (Figure 1) in times between 50-300 seconds, depending on ultrasonic parameters, focal alignment, and wall thickness. Dye was visible flowing from the punctures post-treatment, indicating the existence of a patent communication through the wall. The resulting hole diameters were between 0.5 to 3 mm and were highly consistent for a given acoustic exposure (n=4-6). No damage to the wall was apparent outside of the focal zone. Cavitation was visualized on B-mode ultrasound imaging within the focal zone as a hyperechoic region, providing precise targeting for the extent of erosion.

Conclusion: Focused ultrasound-induced cavitation can generate precise punctures in the inner bladder wall similar to those created endoscopically for treatment of ureteroceles. Results suggest B-Mode ultrasound imaging can be used for guidance the procedure. Future work will aim to minimize the treatment time and test the procedure in an *in vivo* porcine model.

Work supported by NIH 2T32DK00779-11A1, P01DK043881, and 2R01EB007643-05, and the National Space Biomedical Research Institute through NASA NCC 9-58.

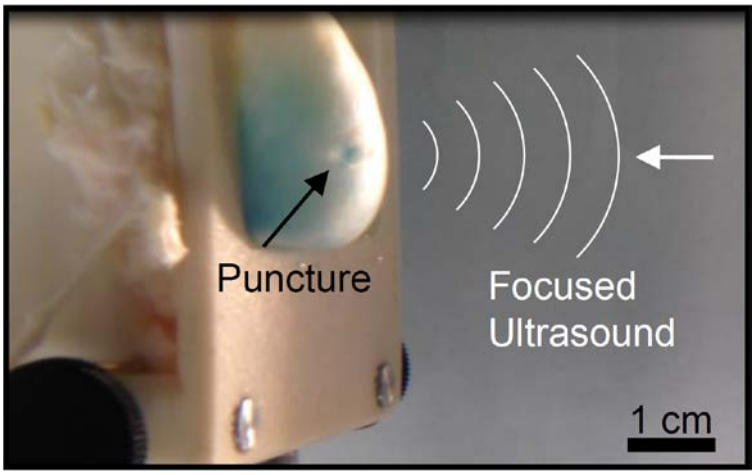

Figure: Puncture created in a bladder bleb after 180 seconds exposure of high-intensity ultrasound (indicated by white lines) focused onto the bleb wall.

ABSTRACT 72

FOCUSED ULTRASOUND REPOSITIONS *DE NOVO* CALCULI IN AN ESTABLISHED STONE-FORMING PORCINE MODEL

Ryan S. Hsi[1], Kristina L. Penniston[2], Thomas D. Crenshaw[3], Stephen Y. Nakada[2], Marla Paun[4], Barbrina Dunmire[4], Bryan W. Cunitz[4], Mathew D. Sorensen[1], Michael R. Bailey[4], Jonathan D. Harper[1]

[1] *Department of Urology, University of Washington School of Medicine*

[2] *Department of Urology, University of Wisconsin School of Medicine and Public Health*

[3] *Department of Animal Science, University of Wisconsin-Madison*

[4] *Center for Industrial and Medical Ultrasound, Applied Physics Laboratory, University of Washington*

Introduction: Our research group has introduced a non-invasive transcutaneous ultrasound device to potentially expel small stones or residual fragments after lithotripsy, or relocate an obstructing stone. Previous work has shown feasibility with endoscopically implanted stones, but it is unknown whether this technology could displace de novo stones potentially attached to the renal papilla. A porcine model with diet-induced hyperoxaluria has been demonstrated to develop calcium oxalate nephrolithiasis with stones growing attached to tissue. The purpose of this study was to demonstrate ultrasonic propulsion of de novo stones in a live, stone-forming porcine model.

Methods: Ultrasonic propulsion was performed using a Verasonics diagnostic ultrasound platform and a Philips/ATL HDI C5-2 commercial imaging transducer. In the surgery suite of our swine research center, sows fed the hyperoxaluria diet for 6 weeks were anaesthetized to effect with 4% isoflurane and then positioned in a lateral recumbency on a surgical table. Kidneys from three sows (190-210kg) underwent treatment using the device followed by euthanasia. Stone movement was visualized using real-time ultrasound. After treatment, stones were examined grossly and with micro-CT.

Results: Using B-mode ultrasound, all right-sided kidneys were adequately visualized while visualization of all left-sided kidneys was precluded by overlying bowel. No hydronephrosis was observed. Stones <3mm were identified in two of three kidneys on ultrasound at 10±1 cm depth, and stones were able to be moved within the collecting system. After euthanasia, stones were identified in all kidneys based on gross exam and on micro-CT. These stones appeared as calcium oxalate stone crystals on micro-CT.

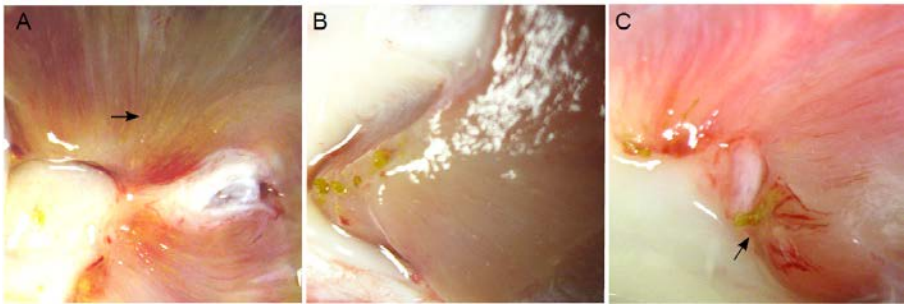

Figure: Evidence of crystal growth in porcine model of calcium oxalate lithiasis. (A) Transverse section of renal papilla showing crystals along the collecting ducts. (B) Stones at papillary tips. (C) Stones extruding from ducts of Bellini.

Conclusion: Ultrasonic propulsion of *de novo* calculi was demonstrated in the porcine stone model. In this model, <3mm stones grown attached to the papilla in a 200 kg subject were repositioned in the absence of hydronephrosis. This could expand the indications of this technology from residual fragments post-treatment to treatment of *de novo* stones.

Work supported by NIH DK43881, DK092197 and NSBRI through NASA NCC 9-58.

ABSTRACT 73

CONTRAST ULTRASOUND DISPERSION IMAGING IN PROSTATE CANCER DIAGNOSTICS

M. Mischi[1], M.P.J. Kuenen[1,2], M.P. Laguna Pes[2], J.J.M.C.H. de la Rosette[2], H. Wijkstra[1,2]
[1] *Eindhoven University of Technology, Electrical Engineering Department, the Netherlands*
[2] *Academic Medical Center, University of Amsterdam, Urology Department, the Netherlands*

Introduction: In the United States, prostate cancer (PCa) accounts for 28% and 10% of all cancer diagnoses and deaths in males, respectively. Although efficient focal therapies are available, their use is hampered by a lack of reliable imaging that enables accurate PCa localization. Contrast-ultrasound dispersion imaging (CUDI) has been proposed as a new alternative method for PCa localization based on dynamic contrast-enhanced ultrasound (DCE-US) data. Different from other DCE-US methods for cancer localization, invariably based on the assessment of blood perfusion, the intravascular dispersion of ultrasound contrast agents is directly influenced by the microvascular changes produced by those angiogenic processes supporting cancer growth. Characterization of the microvascular architecture opens therefore new possibilities for noninvasive assessment of PCa aggressiveness (cancer grading).

Methods: CUDI is performed after an intravenous injection of a 2.4-mL SonoVue® (Bracco, Milan) bolus. The bolus passage through the prostate is imaged by an iU22 ultrasound scanner (Philips Healthcare, Bothell) equipped with a transrectal probe (C8-4v or C10-3v). Contrast sensitivity is increased by employment of contrast-specific imaging. Time concentration curves (TCCs) are obtained at each video pixel after data linearization. Local dispersion is analyzed by assessment of the shape similarity between neighbor TCCs. As shown in Figure 1, a parametric dispersion map is generated that highlights angiogenic areas (in red color) and, therefore, aggressive cancer areas. A preliminary validation was performed at the Academic Medical Center University of Amsterdam by comparing the obtained dispersion images with the histology results after radical prostatectomy (Figure 1) in 12 datasets recorded from 8 patients.

Results: In all patients, the dispersion images showed a good agreement on a pixel level with the histology. The resulting average receiver operating characteristic (ROC) curve area was 0.89, with sensitivity and specificity equal to 77.3% and 86.0%, respectively. These results were superior to those obtained by all the tested perfusion parameters which were previously proposed in the literature.

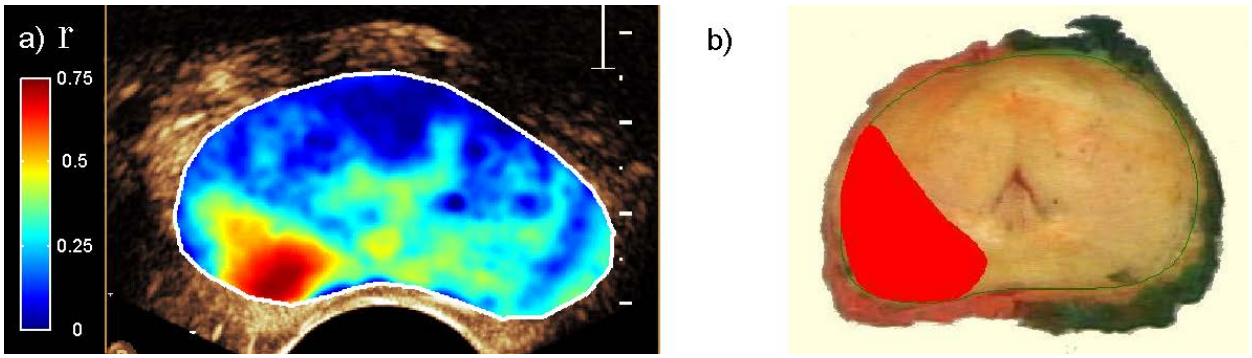

Figure: Dispersion map (a) with corresponding histology result (b).

Conclusion: Our preliminary results evidence a promising value of CUDI for PCa localization and motivate towards an extensive validation. Once validated, CUDI could support targeting of biopsy and focal-therapy, as well as therapeutic decision making based on noninvasive cancer grading.

ABSTRACT 74

TWO-CENTER EVALUATION STUDY USING THE XENX™ TO PREVENT STONE MIGRATION DURING LASER LITHOTRIPSY

Eugene Kramolowsky[1], Francesco Germinale[2] Idan Tamir[3], Ofer Zigman[3]
[1] *Virginia Urology, Richmond, VA*
[2] *Department of Urology, San Remo Hospital, Imperia, Italy*
[3] *Xenolith Medical, Herzlia, Israel*

Introduction: Stone retropulsion during ureteroscopic laser lithotripsy, leading to stone migration, is a well-known phenomenon accentuated by stone proximity to the kidney and can result in increased technical difficulty in stone removal and lengthier procedure times. Several commercially-available stone retention devices have various shortcomings, such as the need to introduce them in addition to a guide-wire and their limited capability to prevent stone migration. We report here the results of a two-center (and two-country) evaluation study of the XenX (Xenolith Medical), a novel stone retention device for proximal and distal stones, during holmium laser lithotripsy. The XenX incorporates a self-expanding retention element, which adapts to the ureter anatomy, and a guide wire – both integrated into one device. Moreover, due to its unique design, holmium laser lithotripsy may be conducted in close proximity to the XenX without compromising its capability to effectively prevent stone migration.

Methods: Between January 2012 and January 2013 seventeen (17) ureteroscopy procedures were performed using the XenX device in the USA, and in Italy, eight (8) procedures were performed between November 2012 and March 2013, for a total of twenty-five (25) ureteroscopy procedures performed using the XenX in two medical centers and in two different countries. Device evaluation included ease of deployment and positioning, stone migration prevention and urologist's perception of value. Mean patient age was 54 years (range 23-74). Twenty one (21) patients had a single stone and the remainder had two. Stones were located in the distal (46%), mid (11%), or proximal (43%) ureter. Mean stone size was 61.67 mm^2 (range 15-140). Secondary endpoints were reduction in laser and overall operation time, intraoperative complications, and stone migration prevention. Patients were followed for 30 days post-operatively.

Results: Generally, the XenX was advanced as a guide-wire past the stone and the braided mesh that comprises the stone retention element was deployed past the stone between the stone and the kidney. The XenX effectively blocked retrograde stone migration during holmium laser lithotripsy while allowing free fluid (urine and irrigation) flow in all patients. Stones fragmented to sub-mm size did not pass through the mesh and were removed by basketing or flushed into the bladder. Finally, in some cases the procedure ended with retracting the braided mesh into its sheath and the XenX was used as standard guidewire to position a catheter or an ureteral stent. The devices allow higher irrigation rates (using a 300mm Hg pressurized system and Wolf semi-rigid miniureteroscope for the US cases) and higher laser power settings to be employed without fear of stone migration. No intra- or post-operative complications were encountered. Survey of operating surgeons revealed a perception of increased ease of performing the procedure and a decrease in overall procedure duration (mean laser time of 8.4 min).

Conclusion: The XenX provides a significant improvement to holmium laser lithotripsy by effectively preventing retrograde stone migration, improving ureteroscopic visualization and kidney drainage, and significantly reducing procedure complexity and apparent operative time. The device may also have application for percutaneous nephrolithotripsy to prevent stone efflux down the ureter.

ABSTRACT 75

THERAPY OF INCIDENTAL PROSTATE CANCER BY HIGH INTENSTIY FOCUSED ULTRASOUND: PROSPECTIVE, LONG-TERM DATA

Chaussy Christian[1,2], Tilki Derya[1,3], Thueroff Stefan[1,4]
[1] Harlachinger Krebshilfe e.V., [2] Dept. of Urology, Univ. Regensburg, Germany, [3] Dept. of Urology, Ludwig-Maximilians-Univ. Muenchen, Germany, [4] Dept. of Urology, Klinikum Muenchen-Harlaching

Introduction: Incidental prostate cancer (PCa) is found in specimens of up to 8% of patients who undergo BPH surgery. There is no consensus about the optimal treatment plan for these patients. We performed a prospective, monocentric study, treating patients with incidental PCa in TURP specimen with high intensity focused ultrasound (HIFU) as a definitive local therapy.

Methods: Since 2000, 65 patients with incidental PCa were treated with robotic HIFU. Median age was 70 (57-87), PSAi was 4.9 (1-32), prostatic volume 39 cc (16-130), and weight of 20 grams (1-95) had been resected by TUR. Histology showed 5% (5-50%) positive chips with a Gleason grade of 5 (3-9). We used robotic Ablatherm® integrated imaging (EDAP-TMS, Lyon) in a single session.

Results: PSA Nadir of 0.07 (0-3.67) after 1.8 (0.7-5.9) months, including 62% <0.1 / 81% <0.5 ng/ml. PSA of 0.13 (0-8.3) equivalent to a PSA velocity of 0.01 ng/ml/year after a mean follow up of 48 months (3-110) was registered. Follow-up showed an incidence of 19% of secondary obstructions caused by necrotic tissue or bladder neck stenosis. Other long-term side effects were mild: intermediate urinary stress incontinence Grade I (11%), and UTI (14%).

Conclusion: PSA Nadir of 0.07 ng/ml as well as the PSA velocity of 0.01 ng/ml/year indicates that HIFU can be used as curative therapy for patients with incidental PCa. The psychological burden of patients who are confronted either with untreated cancer disease in cases of management with active surveillance or with fear of significant side effects in cases of radical surgery or radiation can be avoided by this non-invasive, transrectal, single session therapy.

ABSTRACT 76

THE "CUTANEOUS-PYELO-URETERAL STENT" (C-PU) FOR ROBOTIC-ASSISTED LAPAROSCOPIC PYELOPLASTY (RAL-P)

Pankaj P.Dangle, Mohan S. Gundeti,
University of Chicago Chicago

Introduction: Technique of urinary diversion following dismembered pyeloplasty is debatable, multiple diversion options such as JJ stent (antegrade or retrograde placement), Nephro-ureteral stent Transanastomotic and or transvesical have been used. During robotic pyeloplasty a technique of percutaneous indwelling stent placement via a 14 Fr angiocatheter has been described. All of the above described techniques both necessitate a repeat cystoscopy with its potential cost and repeat anesthesia. And most techniques described have inherent technical challenges especially in small infants with limited applicability with the minimally invasive approach. To overcome these issues we discovered a technique of "Cutaneoous pyeloureteral stent" placement during robotic pyeloplasty.

Methods: After standard port placement, once the posterior anastomosis is completed a Salle stent nephroureteral stent (Cook Medical Inc. Bloomington, IN) is prepared in way that it can be used as CPU stent with our minimal modifications. The distal ureteral end measured so it traverses the anastomosis and into upper ureter and not traversing through the UV junction. The stent is cut obliquely at this point; the guide wire is advanced through the stent and secured externally with a small hemostat. After making skin indentation and visually inspecting the point of entry of the stent to make sure a straight entry into the renal pelvis a 14 Fr angiocath is advanced under vision in percutaneous fashion. With the same angiocath the anterior renal pelvis is punctured in small infants or a small incision is made with the potts scissor. At this point the stent with guide wire is brought into the renal pelvis. The preloaded stent with guide wire is advanced via the cannula of the angiocath, with the help of the robotic needle driver the stent is directed into the ureter. Once the coil is placed in the renal pelvis the stent is stabilized and the wire is withdrawn and rest of the anastomosis is completed. At the end of the procedure the stent is withdrawn under direct vision to lay it straight and is secured to the skin.

Results: We have performed 68 robotic pyeloplasty without any open or laparoscopic conversion, with average age of 8.6 yrs (7weeks-21yrs).The insertion of stent in our experience takes on an average of 4-5 mins. So far we have not observed any complications of the procedure or any urine leak from the puncture site in the renal pelvis after stent removal. In our experience the stent does not cause any additional pain, avoids the bladder spasm and hematuria and are easy to manage once secured well with clear transparent dressing.

Conclusion: In our early experience the technique is feasible, has minimal morbidity, and equivalent success as well as avoids a visit to the operating room for cystoscopy with its additional cost, urethral instrumentation and anesthesia.

Figure: Modified Salle stent for robotic pyeloplasty

ABSTRACT 77

CT CHARACTERIZATION OF DIETARY HYDROXYPROLINE-INDUCED NEPHROLITHIASIS: FURTHER ELUCIDATION OF A PORCINE MODEL OF UROLITHIASIS

Sri Sivalingam, Kristina L Penniston, Tom D Crenshaw, Stephen Y Nakada
University of Wisconsin School of Medicine and Public Health, Dept of Urology, Madison, WI

Introduction: We have shown previously that dietary hydroxyproline (HP) induces renal calcium oxalate crystal formation in the gravid adult pig. As the physiological changes related to pregnancy may positively influence nephrolithiasis in adult pigs, we sought to determine if non-pregnant pigs form stones and to characterize the stones by CT.

Methods: 4 non-gestating pigs were used for this study. They were maintained in the swine research facility near our campus and given 2 weeks to acclimate to limited feeds. Two animals were maintained on a control diet (CD) and 2 were given a HP-enriched diet (10% HP mixed with CD). All animals were euthanized at 21 days, and the kidneys were extracted and flushed with heparinized saline. The *ex vivo* kidneys were then scanned with a GE CT scanner (80kV, 400MA, 1 sec rotation, 0.625mm slices). Kidneys were examined in a blinded manner, for gross appearance and for radiographic evidence of stones.

Results: All treatment group kidneys (4 from 2 gilts) exhibited calculi at or near the papillary tips, and measured up to 1.6 mm in maximal diameter (Figure 1); kidneys from control animals had no identifiable stones. There were no cortical calcifications identified in any of the kidneys. Bivalved kidneys were then examined. The control kidneys appeared normal, with clear corticomedullary boarders, but the treatment kidneys appeared slightly mottled and pale, with a less distinct transition between cortex and medulla. Figure 2 depicts an image of a stone as demonstrated on micro-CT scanning, with identification of the crystal structures as a combination of calcium oxalate monohydrate and dehydrate.

Conclusion: We demonstrated CT characterization of experimentally induced calculi in non-pregnant pigs. Specifically, the stones were at the papillary tips and averaged 1.6 mm. The extracted stone composition was 100% calcium oxalate.

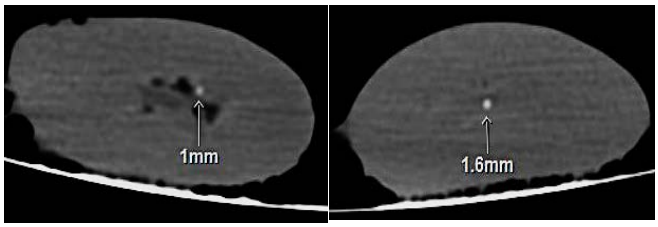

Figure 1: Stones demonstrated on HP-treated pigs at or near the renal papilla measuring up to 1.6mm on CT, standard bone window.

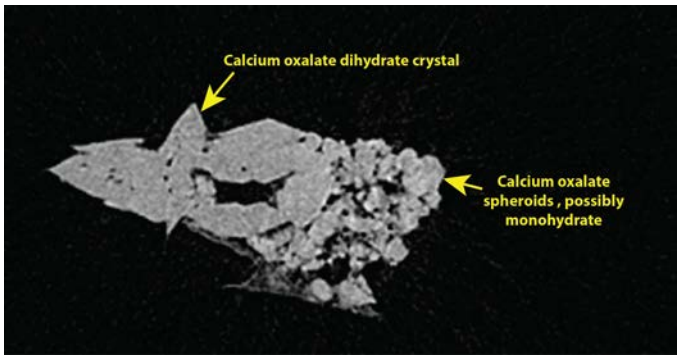

Figure 2: Micro CT demonstration of an extracted stone, confirming a mix of calcium oxalate dihydrate and monohydrate crystals.

ABSTRACT 78

RENAL HEMATOMA AFTER ESWL: INCIDENCE AND RISK FACTORS AFTER 2500 TREATMENTS

Hans-Martin Fritsche, Marco Schnabel, Wolf F. Wieland, Christian G. Chaussy

Department of Urology, Caritas St. Josef Medical Center, University of Regensburg, Germany

Introduction: The aim of this study was to determine the incidence and risk factors for renal hematoma after SWL.

Methods: 1794 patients were included in a prospectively maintained database. We performed 2520 SWL treatments, 1324 procedures were done due to kidney stones in 857 patients, 1196 for ureteral stones in 937 patients. The observation period encompasses the years 2007-2012. All patients underwent an ultrasound control within three days after SWL. Patient with renal hematomas were analyzed and treatment characteristics were compared with the complete population in a non-statistical manner due to the low count of events.

Results: Seven patients developed a renal hematoma after ESWL (0.53%). In four patients the hematoma was asymptomatic, with a size between 0.6x2.6cm and 8x10cm. Three patients developed colicky pain due to the hematoma. One patient with an actively bleeding hematoma sized 17x15cm underwent surgery and received blood transfusion (0.08%). Coagulation status and treatment characteristics in hematoma patients were equal to the control. None of the hematoma patients took low-dose Acetylsalicylic acid.

Conclusion: The overall risk of symptomatic and asymptomatic renal hematoma after SWL treatment of kidney stones is about 0.5%. Clinically relevant or symptomatic hematomas occur in only about 0.25%. Treatment characteristics and low-dose Acetylsalicylic acid do not seem to influence the risk. Older age and vascular comorbidities like hypertension or diabetes seem to be risk factors for development of renal hematoma.

ABSTRACT 79

A SCIENTIFIC CORRELATION BETWEEN ROBOTIC PROSTATE BIOPSY RESULTS WITH POST-RADICAL PROSTATECTOMY WHOLE-MOUNT PATHOLOGY SLIDES

Koh Zong Jie[1], Henry Ho[2], Loh Hwai-Liang[3], Ana R Jara-Lazaro[3], Hong Hong Huang[2], John Yuen[2],Christopher Cheng[1]

[1] Yong Loo Lin School of Medicine, National University of Singapore
[2] Department of Urology, Singapore General Hospital
[3] Department of Pathology, Singapore General Hospital

Introduction: At our institution, the iSR'obot™ Mona Lisa (BiobotSurgicals pte ltd, Singapore) system is used for robot-assisted transperineal prostate biopsy (rTPB) in the detection of prostate cancer (PCa). Intraoperatively, transrectal transverse ultrasound (US) images are reconstructed as a 3-dimensional model of the prostate for core biopsy map planning. A robotic arm guides the urologist in obtaining biopsies at the planned locations. This study aims to correlate the location and Gleason score (GS) of positive rTPB biopsy cores with corresponding tumor foci within whole mount (WM) radical prostatectomy (RP) specimens.

Methods: In this prospective, institutional review board approved clinical trial we performed rTPB for repeat prostate biopsy patients (those with high PSA after previous benign biopsy, PCa on active surveillance, or high grade prostatic intraepithelial neoplasia). Of 292 cases from 2006 through 2011, 64 PCa were diagnosed, of which 27 patients opted for RP; 7 were excluded due to inadequate pathological specimen processing. WM slides were reviewed by 2 pathologists, who demarcated all tumor foci and measured the diameter of the largest focus, defining the index tumor. The slide demonstrating the index tumor in its greatest dimension was selected for correlation with rTPB. As slides are cut at a fixed width of 0.5 mm, the distance from the prostatic apex was determined using the formula: d = [no. of slides from apex x 0.5]. The corresponding rTPB transverse US image could be determined using d. The anteroposterior and transverse diameters of both the WM slide and US image were divided into thirds, forming 9 segments. Location of tumor foci was described by the segments occupied and correlated with biopsy cores within the same segment. The GS was also compared.

Results: The 20 patients had a mean age of 62 years old; their mean PSA was 15.5ng/dL, with a mean prostate volume of 42.3cm^3. 13 patients had GS≤7 on rTPB. rTPB localized 85% of index tumors, with a mean size of 19.6 mm. Remaining 3 undetected cases were located in an anterior segment of the prostate, with a mean size of 9.0 mm. WM pathological GS was accurately predicted in 65% of these cases, with Gleason upgrading in 15%. rTPB detected 60% of all tumor foci. 95% of undetected foci were <5.0mm in largest diameter and located in peripheral segments of the prostate.

Conclusion: rTPB is able to localize most index tumors with 15% risk of Gleason upgrade. Undetected foci on rTPB are clinically insignificant. rTPB has a great role in characterizing PCa for the selection of patients for treatment options such as active surveillance.

ABSTRACT 80

"5-PANG SYSTEM"-Version 2: A MULTIUTILITY SYSTEM FOR PERCUTANEOUS RENAL ACCESS

Rawandale-Patil AV, Patni L G., Patil PA
Institute of Urology Dhule, Maharastra, India 424001

Introduction: We describe and analyzed our innovative 5-PANG (5 Part percutaneous Access Needle With Glidewire) version 2 system for miniPCNL, antegrade ureterorenoscopy, and conventional PCNL.

Methods: The 5-PANG-version 2 system (Figure 1), designed, fabricated, and patented by our institute, consists of 11 parts, allowing puncture and initial tract dilatation for 12 Fr miniPCNL/antegrade ureterorenoscopy or conventional PCNL. The puncture is performed with the first/inner 2 parts. Part 1 is removed and a glide wire advanced to the pelvicalyceal system. Parts 3, 4 & 5 are telescoped over part 2. Part 2, 3 &4 are then removed. A flexible or rigid ureterorenoscope (4.5 Fr) can then be passed through part 5 and a miniPCNL completed. The option of introducing a safety wire exists at this stage. For conventional PCNL, a specially designed dilator rod can be used to continue telescopic dilatation up to the required sheath size (retaining part 5). 73 successive"5-PANG PCNLs" were prospectively evaluated for advantages, disadvantages, safety, and efficacy.

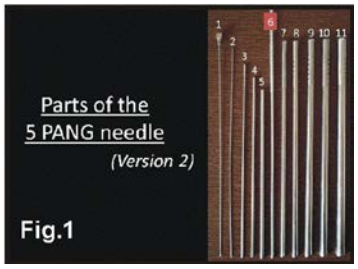

Results: The 5-PANG system reduced exchange of dilators, thus making the tract establishment fast (Table I). Low radiation, conversion to conventional method ,and transfusion rate (due to continuous tract tamponade) were observed. Extrarenal wire kinking/slippage were not seen. It facilitated PCNLs in previously operated kidneys. No failure, limitations, or early or late complications related to the system were observed

Conclusion: The 5-PANG (version 2) is a versatile PCNL system. It makes initial tract dilatation easy, safe, and inexpensive. It prevents extrarenal wire kinking and slippage, straightens curved puncture tracts, avoids extravasation of contrast, and decreases procedure and radiation times. It is fluoroscopy/ultrasound compatible and reusable and can be used for both mini and conventional PCNLs.

TABLE 1 - PATIENT DATA		**5-PANG SYSTEM**
Renal units		73
Mean age in years		35.55 (2-65)
Sex - M:F		1.9:1
History of previous renal surgeries		18 (24.65%)
Time:Puncture to Rod placement (secs)		59.14 (26-453)
Time: Rod placement to sheath placement (secs)		73.13 (35-300)
Radiation Time:Puncture to Rod placement (secs)		2.27 (1-30)
Radiation Time: Rod placement to sheath placement (secs)		5.24 (0.01-17)
Antegrade flexible URS	12Fr	5 (6.84%)
12 Fr Miniperc	12Fr	7 (9.58 %)
Conventional PCNL tract size	20Fr	5 (6.84%)
	22Fr	8 (10.95%)
	24Fr	39 (53.42%)
	26Fr	7 (9.58 %)
	28Fr	2 (2.73%)
Visual clarity	Good	62 (84.93 %)
	Tolerable	8 (10.95 %)
	Poor	3 (4.10 %)
Intra op complications	Minor	2 (2.73 %)
	Major	3 (4.10 %)
Transfusion (patients)		1 (1.36 %)
Post-operative complications		0

SOCIETY OFFICERS:

Presidents
Evangelos Liatsikos
Frank Keeley

Vice-Presidents
Jeff Cadeddu
Koon Ho Rha

Secretary
Jack Vitenson

Treasurer
John Denstedt

Councilor
Louis Kavoussi

Executive Director
Dan Stoianovici

ADVISORY BOARD

Jeffrey Cadeddu

Ralph Clayman

Jean de la Rosette

Misop Han

Thomas Lawson

Pierre Mozer

Stephen Nakada

Jens Rassweiler

Koon Ho Rha

William Roberts

Arthur Smith

Li-Ming Su

Gerald Timm

Hessel Wijkstra

Kevin Zorn

AWARDS:

Best Paper Award:

A NOVEL COMPACT SINGLE INCISION SURGICAL ROBOT WITH CONICAL REMOTE CENTER-OF-MOTION MECHANISM AND ROD ELBOW JOINT

Hyung-joo Kim , Hyun-do Choi, Jun-Won Jang, and Jong-hwa Won
Samsung Advanced Institute of Technology

Top 10 Abstracts:

BEVELED NEEDLE TRAJECTORY CORRECTION. Changhan Jun, Chunwoo Kim, Doyoung Chang, Ryan Decker, Doru Petrisor, Dan Stoianovici; *Johns Hopkins University, Baltimore, MD*

FINE TILT TUNING OF A LAPAROSCOPIC CAMERA BY LOCAL MAGNETIC ACTUATION: TWO-PART LAPAROSCOPIC NEPHRECTOMY EXPERIENCE ON HUMAN CADAVERS. Ryan Pickens, Massimiliano Simi, Arianna Menciassi, Duke Herrell, Pietro Valdastri; Scuola Superiore Sant'Anna, Pisa, Italy; Vanderbilt University, Nashville, TN.

ACTIVE REMOVAL OF BUBBLE SHIELDING IN SWL: AN IN VITRO STUDY. Alexander P Duryea, William W Roberts, Charles A Cain, Hedieh A Tamaddoni, Timothy L Hall; *University of Michigan, Ann Arbor, MI.*

PRE-CLINICAL EVALUATION OF A MRI-SAFE ROBOT FOR ENDORECTAL PROSTATE BIOPSY. Govindarajan Srimathveeravalli, Chunwoo Kim, Doru Petrisor, Jonathan Coleman, Hedvig Hricak, Stephen B Solomon, Dan Stoianovici; *Memorial Sloan-Kettering Cancer Center, New York, NY; Johns Hopkins University, Baltimore, MD.*

IN VITRO COMPARISON OF A NOVEL FACILITATED ULTRASOUND TECHNOLOGY VERSUS STANDARD TECHNIQUE APPROACH FOR PERCUTANEOUS RENAL BIOPSY. Ashleigh Menhadji, Vien Nguyen, Jane Cho, Ringo Chu, Kathy Osann, Philip Bucur, Puja Patel, Achim Lusch, Elspeth McDougall, Jaime Landman; *University of California, Irvine, CA; University of British Columbia, Vancouver, Canada.*

A NOVEL PARABOLOID INTRACORPOREAL LITHOTRIPTOR: CAD ANALYSIS AND IN VITRO COMPARISON WITH HOLMIUM LASER. Rawandale-Patil AV, Patni L G, Mulay A, Patil PA; *Institute of Urology Dhule, Maharastra, India.*

DESIGN OF STEERING MECHANISM AND SURFACE MOSAICS SOFTWARE FOR AUTOMATED BLADDER SURVEILLANCE. Xianming Ye, W. Jong Yoon; *Qatar University, Doha, Qatar.*

IRREVERSIBLE ELECTROPORATION: OUTCOMES IN A MINIMALLY INVASIVE APPROACH TO RENAL TUMORS. Jonathan Melquist, Brian Caldwell, Joseph Caputo, Annie Darves-Bornoz, Jason Kim, Rahuldev Bhalla; *Stony Brook University Medical Center, Stony Brook, NY; Urology Group of New Jersey, Millburn, NJ.*

EVALUATION OF ACCEPTABILITY OF PHYSICAL SIMULATION MODEL FOR TRAINING OF LAPAROSCOPIC PYELOPLASTY. Lauren Poniatowski, Robert Sweet, Troy Reihsen, Francois Sainfort, Sara L. Best, Stephen V. Jackman, Richard E. Link, Wesley A. Mayer, Stephen Y. Nakada, J. Stuart Wolf; *University of Minnesota, Minneapolis, MN; University of Wisconsin, Madison, WI; University of Pittsburgh Medical Center, Pittsburgh, PA; Baylor College of Medicine, Houston, TX; The Methodist Hospital, Houston, TX; University of Michigan, Ann Arbor, MI.*

AWARDS:

Best Reviewer Awards (5 Years):

		2009	2010	2011	2012	2013
Ernesto III	Arada	☼				☼
Riccardo	Autorino		☼		☼	
Thorsten	Bach		☼	☼	☼	
Haixin	Chen					☼
Jean	de la Rosette		☼			
Mahesh	Desai	☼			☼	☼
Brian	Eisner	☼		☼		
Mohamed	Elkoushy			☼	☼	☼
Oscar	Fugita					☼
Arvind	Ganpule				☼	
Petrisor	Geavlete				☼	
Michael	Gong	☼				
Hrishikesh	Joshi	☼				
Wareef	Kabbani		☼			
Avinash	Kambadakone			☼		
Kazumi	Kamoi	☼				
Watid	Karnjanawanichkul			☼		
Louis	Kavoussi					☼
Bodo	Knudsen			☼	☼	
Thomas	Lawson	☼		☼	☼	
Salvatore	Micali		☼			
Kamol	Panumatrassamee				☼	
Sutchin	Patel		☼	☼	☼	☼
Koon Ho	Rha		☼			☼
Mathew	Sorensen					☼
Cristian	Surcel			☼		
Kazuo	Suzuki		☼			
Hessel	Wijkstra			☼		☼
Kevin	Zorn	☼	☼	☼		

REVIEW COMMITTEE:

The review committee has been assembled by e-mail solicitation. Sixty-three reviewers from around the world participated. We gratefully acknowledge their contribution to the success of the meeting and thank them for taking the time to promote the best science.

Naif Al-Hathal
Ernesto Iii Arada
Timothy Averch
Doyoung Chang
Christian Chaussy
Haixin Chen
Antonio Cicione
Jean De La Rosette
Mahesh R. Desai
Mohamed Elkoushy
Mohamed Etafy
Oscar Fugita
Raguram Ganesamoni
Arvind Ganpule
Petrisor Geavlete
Bogdan Geavlete
Dragan Golijanin
Henry Ho
Ryan Hsi
Ana Richelia Jara-Lazaro
Wooju Jeong
Byongchang Jeong
Changhan Jun
Louis Kavoussi
Ali Khalifeh
Hyung-Joo Kim
Joseph Klink
Eugene Kramolowsky
Timur H. Kuru
Jaime Landman
Richard Lee
Seung Bae Lee
Benjamin Lee
Evangelos Liatsikos
Sey Kiat Lim
Giovanni Marchini
Jonathan Melquist
Salvatore Micali
George Mitroi
Vladimir Mouraviev
Craig Niederberger
Gheorghe Nita
Sujeeth Parthiban
Sutchin Patel
Lokesh Patni
Ryan Pickens
Koon Ho Rha
William W Roberts
Georgios Sakas
Simpa Salami
Nelson Salas
Dinesh Samarasekera
Joseph Sewell
Yaniv Shilo
Mathew Sorensen
Govindarajan Srimathveeravalli
Dan Stoianovici
Kae Jack Tay
Hessel Wijkstra
J. Stuart Wolf
Henry Woo
Xianming Ye
Law Zhi Wei

THANKS:

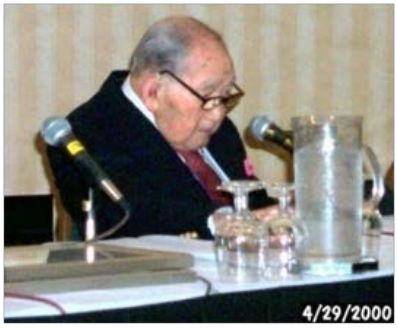

Dr. George Nagamatsu, Engineering and Urology Society Founder

Special thanks to **Dr. Thomas Lawson** for his help formatting this program.

We thank **Michelle Paoli** and **Debra Caridi** for organizing the Annual Meeting.